Perturbative Structure of Reaction Mechanism in Multi-Particle Production Processes

Toshiyuki Morii

College of Liberal Arts, Kobe University, Kobe

Perturbative Structure of Reaction Mechanism in Multi-Particle Production Processes

Toshiyuki Morii

College of Liberal Arts, Kobe University, Kobe

The structure of reaction mechanism in hadronic multi-particle reactions is investigated based on a simplified multi-Regge model and the perturbative picture for the structure of hadron-hadron interaction at high energies is presented. After an introductory sketch on recent historical development, partial cross sections are analyzed by a simplified multi-Regge model. It is clarified that the reaction mechanism in multi-particle production processes is composed of the non-diffractive mechanism and the diffractive one. The model with these mechanisms is formulated and some of the experimental data are analyzed by this model. The structure of effective couplings in a multi-peripheral chain is investigated and it is shown that the dominant reaction mechanism switches over from the non-diffractive mechanism to the diffractive one with increasing energy. Finally, the perturbative picture for the structure of reaction mechanism in multi-particle production processes is discussed based on the results obtained from the above investigation. This paper includes the following contents.

Contents

§1. Introduction

Multi-particle production is one of the most current and attractive problems in the elementary particle physics. In the world of hadrons with strong interactions, the creation and the annihilation of particles are essential at high energies. As the energy goes up in hadron-hadron collisions, multi-particle productions contribute to the main part of the cross section. Furthermore, if we consider that the reaction mechanism of two-body reactions is closely connected with the one of multi-particle production processes through unitarity, it is very important to make clear the dynamical structure of multi-particle production processes in order to clarify the structure of strong interactions.

Recently, many of investigations about multi-particle production phenomena are concentrated mainly in inclusive reactions. Just as the total cross section σ_T for $a + b \to$ anything, the one-particle inclusive cross section $d\sigma/(d^3p_c/E_c)$ for the reaction $a + b \to c +$ anything carries important global information about the production of particle c in ab collisions. The generalization to several-particle inclusive reactions is immediate. The generalized optical theorem relates the one-particle inclusive cross section to a certain discontinuity of an unphysical three-particle to three-particle forward scattering amplitude just as the optical theorem does the total cross section to the elastic forward scattering amplitude, and the discontinuity is parametrized in terms of Regge pole exchanges. Since the inclusive cross section is composed of the summations of the cross sections for individual processes, it is very important to clarify the dynamical structure of reaction mechanism of each channel. In this paper, we investigate the structure of reaction mechanism in multi-particle production processes.

Historically, the investigation of multi-particle production phenomena began with Heisenberg[1] in 1936. Since there are many excellent review articles[2]

of various theories and models until now, we limit the discussion in this section to an introductory sketch on recent development.

On the background of the qualitative success[3] of Regge pole theory[4] in the two-body hadron reactions and the accumulation of abundant experimental data of multi-particle production phenomena in the accelerator energy region [at the Brookhaven AGS and the CERN PS], a multi-Regge pole model*) was proposed in 1967-1968 and investigated in detail by many theorists.[7)~10)] The idea of this model was originally proposed by Amati, Bertocchi, Fubini, Stanghellini and Tonin[11], in 1962, who put forward a multi-peripheral model, so-called the ABFST model from dispersion-theoretical considerations as a natural extention of the one-pion-exchange (OPE) model which had been extensively discussed by Salzman and Salzman[12] and by Dremin, Chernavski and their collaborators[13]. They further developed the model and discussed systematically the characteristic features of multi-particle production phenomena. According to the ABFST model, multi-particle production is assumed to be reduced to the low energy pion-pion scattering. Namely, the multi-particle reaction amplitude in hadron-hadron collisions is assumed to be factorized by many low energy pion-pion scattering amplitudes. The number of vertices increases as the incident energy goes up,but the sub-collision at each vertex remains at low energy. Although this model gives us the Regge pole behaviour of elastic scattering amplitude through unitarity and presents a unified theory of multi-particle production, its quantitative predictions are, unfortunately, not in agreement with experiments. The average multiplicity and the total cross section expected from this model are too small compared with experiments[14]. After that, this model has been abandoned until the revival of it in the multi-Regge

---

*) The first formulation of the multi-Regge model is presented by Ter-Martirosyan[5] and Kibble[6] in 1963.

model in 1967 as mentioned above.

Since 1967-1968, the theoretical and experimental investigation developes vigorously based on the idea of the multi-Regge pole model. As for two-body reactions, experiments have the following important features[15] at high energies;

i) The differential cross sections show forward or backward peaks depending on whether the quantum numbers in the t- or u-channels admit the exchange of a single particle or resonance.

ii) The peaks are roughly of exponential shape of the four momentum transfers t or u.

iii) The cross sections have a power dependence on the energy, $s^{2\alpha-2}$ where α is independent of reaction channels and is characteristic of the exchange quantum numbers, as called as Morrison's rule[16].

We call these features the peripheral properties. These features are in general in agreement with the Regge pole model. It is natural that the qualitative success of the Regge pole model in two-body collisions leads to the generalization of this model to multi-particle production processes. Many of experiment seem to show the propriety of this generalization. The peripheral properties are seen even in multi-particle production processes[17] as analyzed by Hansen et al[18].

Based on the multi-Regge pole model, Chan Hong-Mo et al[7] parametrized the n-particle production amplitude, so-called CLA model, in such a way that:

i) whenever the effective mass of every pair of the final particles is large, the amplitude becomes fully Reggeized;

ii) whenever any group of the final particles forms a cluster with low effective mass, that part of the amplitude which corresponds to interactions within the cluster is replaced by a constant;

and analyzed various distributions of exclusive reactions, for example the c.m. angular distributions and the longitudinal and transverse momentum distributions of

secondaries for varying multiplicity and incoming energy, the average transverse momenta of secondaries as functions of multiplicity, etc., and obtained qualitatively good agreements with experiments. However, the large number of parameters obscure the physical image of the dynamical structure of multiple production.

At about the same time, Van Hove and his collaborators[19] have examined on the basis of typical experimental distributions in exclusive reactions, the fundamental ideas and aspects which are especially interesting in connection with model independent data presentation and analysis. Based on the fact that, in strong interactions, transverse momenta of secondaries are limited to small values and are largely independent of the nature of the particle, the multiplicity n and the c.m. energy $s^{\frac{1}{2}}$, in contrast to the longitudinal momenta of ones, Van Hove et al. proposed a method of the final state classification in longitudinal phase space (LPS) for many-body reactions just as one distinguishes between forward and backward scattering in the case of two-body reactions. Because of the constraints of momentum and energy conservation, all events in LPS fall inside appropriate polyhedrons, for example, a hexagon in three-body final state, a cuboctahedron in four-body final state, etc.. If the reduced longitudinal momenta $x_i = 2p_{\parallel i}^{*} / \sum_{j=1}^{n} |p_{\parallel j}^{*}|$ are used, event points in LPS are classified into some divisions. Since these divisions are connected with the characteristic reaction mechanism based on the multi-Regge model, we can make clear the role of exchange mechanism in exclusive reactions by means of LPS analysis. Van Hove and his collaborators have considered that the events inside each division are produced via production of clusters and have insisted from the analysis of $K^{-}p$ reactions at 10GeV/c that there is a hierarchy of strength of exchanges, i.e.,

$$P > M > S > E,$$

where P stands for pomeron, M for meson, S for strange and E for exotic exchange[20].

LPS analysis is excellent for the classification of the data by the exchange mechanism but does not offer any information about the dynamical structure of clustering.

Furthermore, Namiki et al.[21] have analyzed exclusive reactions by the t_i-cut phase space. They have considered that the dynamical structure of exclusive reactions is effectively due to the universal t_i-cut effect, i.e., $|t_i| \lesssim 1$ (GeV/c)^2 for every t_i in the multi-peripheral chain and shown that the gross features of multiple production at fairly low energies, $P_L \lesssim 30$ GeV/c are understood from this effect. Furthermore, they have clarified that a fireball, i.e., the one of clusters is produced by the t_i-cut mechanism. They have considered the non-diffractive mechanism only and ignored the diffractive one and therfore the behaviour at high energies have not been discussed fully.

Now, another model which stands for the experimental analysis is the fireball model[22], *). This model is obtained phenomenologically by analyzing jet phenomena in cosmic ray energy region. As the first step to clarify the correlation between the multi-Regge pole model with the fireball model, we, formerly, proposed a simple model[25] which contains the Regge-pole hypothesis and the fireball description of experiments. The model is that the fireball is produced by exchanging Regge poles and subsequently decays in flight into secondary mesons. The results of this model are qualitatively in agreement but quantitatively not in agreement with experiments because of too rough simplification of the model.

---

*) The original idea is due to the isobar model by Takagi[23] who improved the statistical model of Fermi[24]. His model has developed to the fireball model, later on and presented a new light to multi-particle production phenomena.

On the other hand, the theoretical investigation of the multi-Regge model has been developed by many theorist. Chew et al.[26] have extended the idea of duality[27] to multiple production and pointed out the justifiability of a rough multi-Regge description with final particles which are stable with respect to strong interactions from threshold to high energies. The factorization and the dominance of small momentum stransfer in each vertex function are assumed in this model, and one obtains the results that the averaged multiplicity shows the ln s behaviour with energy and the multiplicity distribution is Poisson form. Furthermore, by the bootstrap principle[28] the structure of input and output Reggeons and pomeron has been explored in detail. Also, the relation between the multi-Regge model and the original ABFST model has been discussed and a perturbative analysis of the diffractive dissociation mechanism has been presented[29]. The application of this model to the phenomenological analysis for inclusive reactions is qualitatively satisfactory[30].

Feynman[31] and Yang et al.[32] proposed the idea of scaling and limiting fragmentation, respectively at Stony Brook Conference in 1969. These concepts have become very important in the recent inclusive phenomenology and in connection with the parton picture[33] to elementary particles. Meuller[34] has connected these concepts with the Regge concepts through the generalized optical theorem[35] for inclusive processes and made a biginning of the big boom on inclusive reactions.

Over the past two years the maximun beam momentum has increased from 30 GeV/c to 400 GeV/c at NAL and to 3000 GeV/c at the CERN ISR and abundant data have been accumulated. The multi-Regge model in the original form can not account for some of these experiment. For example, the multiplicity distribution[36] is not the Poisson form, except for in the momentum region $P_L \approx 50 \sim 70$ GeV/c, and the correlation parameter f_2[37] is not zero and also the ratio of charged multiplicity (n) to dispersion (D) is constant, i.e., $\frac{\langle n \rangle}{D} \simeq 2$ in costrast to the expectation

from the multi-Regge model.

Meanwhile, it has been insisted that the diffractive excitation model (DEM)*) is important in multiple production, by Hwa[38], Jacob and Slansky et al.[39]. In this model, the averaged multiplicity shows the ln s behaviour with energy but the multiplicity distribution for large multiplicity n is $\sigma_n \sim \frac{1}{n^2}$ which is not in agreement with experiments and the cross sections are not saturated in the low energies by this model[40]. Furthermore, the observation of striking short-range rapidity correlation[41] in inelastic cross sections is contrary to DEM. Since two representative models; the multi-Regge model and the diffractive excitation model, are monistic, they explain only the partial features of experiments and have been faced with difficulties in essential points.

A model which solves these difficulties is so-called two-component model[42], **). The basic idea of two-component model is that two distinct production mechanism -call them multi-prepheral and diffractive- are at work[44]. Phenomenologically, this picture is in agreement with essentially all of the experimental data presently available. However, two-component model cannot be considered a candidate for final theories of particle production, even if it should account for every experimental feature. The two components must be intertwined through the unitarity constraint, since it is artificial to enforce a separation. One interpretation of this model is that two-component model is the first term of a perturbative expansion for the full production amplitude. In fact, recently some attempts[45]

---

*) The essential point of this model is same to the Takagi model[23].

**) This model is proposed originally by Wilson[43] who has considered two component production mechanisms, i.e., the diffractive part which present the almost constant cross sections and small multiplicity, and the pionization one which present the decreasing cross sections at high energies and large multiplicity.

that the full production amplitude is expanded by triple-pomeron coupling perturbatively, are seen. In this paper, from the analyses of exclusive reactions we also, independently, attain the similar picture, i.e., the perturbative picture for the structure of reaction mechanism in multi-particle production processes.

Now, in this paper we consider the structure of reaction mechanisms in multi-particle production processes based on the multi-Regge model. The exchanged objects in the multi-peripheral diagrams are assumed to be two species, i.e., pomeron (P) and meson Reggeon (M), which are assumed effective fixed poles for simplicity and are parametrized as $\alpha_P = 1$ and $\alpha_M = 0$, respectively. We are not concerned with the quantitatively detail discussion of the fitting to the data but the gross feature and the characteristic role of various reaction mechanisms which are produced due to the existence of pomeron and meson Reggeon, and investigate the structure of pomeron and meson Reggeon and the role of them in multi-particle production processes. Pomeron is specified to have a vacuum quantum number and is connected to the almost constant cross section at high energies and it exists in the diffraction mechanism in hadronic interactions, while meson Reggeon is assumed to be responsible to the averaged effect of all secondary Reggeons and is related to the decreasing behaviour of the cross section with increasing energy. The existence of pomeron and meson Reggeon induces two different reaction mechanisms, i.e., the non-diffractive (ND) mechanism and the diffractive (D) one and the D mechanism is composed of many components as discussed in this paper. Present experimental data show the existence of the <u>switch-over</u> mechanism of the dominant reaction mechanism in multi-particle production processes[46),47),48)]. Furthermore, the smallness of the inner pomeron coupling (g^2_{PM}) compared to the inner meson coupling (g^2_{MM}) and the existence of the switch-over mechanism[49)] lead us to a perturbative scheme of the reaction mechanism in multi-particle production processes[50)].

In §2, we briefly outline the multi-Regge model and introduce two sort of exchange objects, i.e., pomeron and meson Reggeon. The partial cross sections are analyzed phenomenologically by this model and it is clarified that the reaction mechanism in exclusive processes is composed of the non-diffractive mechanism and the diffractive one. The model with these mechanisms is formulated in §3 and the structure of the s_i and t_i dependence of the model is investigated. In §4, some of experimental data, in particular, the partial cross sections, the invariant mass spectra, the forward-backward asymmetry and the two-particle distributions are analyzed by assuming that the non-diffractive mechanism (ND) and the single diffractive dissociation one (D_a and / or D_b) are main terms and the double diffractive dissociation one (D_{ab}) and other multi-pomeron exchange ones (D-D, D_a-D, •••) are neglible for reactions with small multiplicity, say several, in the region from threshold to $P_L \simeq 100$ GeV/c. From the analysis of the partial cross sections, it is clarified that the experimental data show the switch-over mechanism of the dominant reaction mechanism from the ND to D mechanism. Also, the importance of the switch-over mechanism is pointed out from all the analyzed physical quantities. Based on the results of the analyses in §4, the gross structure of exclusive reactions is discussed in §5. In §6, we investigate the structure of effective couplings in the multi-peripheral chain, above all the inner couplings in order to make clear the origin of the smallness of the countibutions from D_{ab}, D-D, D_a-D, etc.. It is clarified that the inner pomeron coupling g^2_{PM} is very small compared with the inner meson one g^2_{MM}, i.e., $g^2_{PM}/g^2_{MM} \simeq 0.01$. This result leads to the smallness of the contributions from D_{ab}, D-D, D_a-D, etc., and to a switch-over mechanism of the dominant reaction mechanism with increasing energy as discussed in §7. The perturbative picture of the reaction mechanism in multi-particle production processes is investigated in §8. A new integral equation for production amplitudes is presented and further the duality assumption

is introduced. Finally, the possibility of the non-vanishing adjacent pomeron coupling $g_{PP}{}^2$ is discussed. The production of the multi-fireball and the new particle is included in this scheme in connection with the non-vanishing $g_{PM}{}^2$ and $g_{PP}{}^2$, respectively. Conclusions and discussions are given in §9. We present in appendices (A) Partial cross sections by a simple multi-Regge model in the Chew-Pignotti's approximation and (B) The perturbative expansion of the S-matrix in the formal theory of scattering.

§2. The analyses of partial cross sections by a simplified multi-Regge model

As mentioned in Introduction, we explore the structure of reaction mechanism in multi-particle production processes. The qualitative success of the Regge pole model[3] for high energy reactions with two body final states requires serious attention to the multi-Regge hypothesis[7)~10)] for multiple production.

According to the multi-Regge model, the reaction amplitude (T_n) of the exclusive reaction,

$$a + b \to c_1 + c_2 + \cdots + c_n, \quad ^{*)} \qquad (2\text{-}1)$$

is given at high energies as follows;

$$T_n \sim \gamma_a(t_1)\left(\prod_{i=1}^{n-2}\gamma_i(t_i,t_{i+1},\phi_i)\right)\gamma_b(t_{n-1})\prod_{i=1}^{n-1}\xi_i(t_i)s_i^{\alpha_i(t_i)} + \text{exchange terms}, \qquad (2\text{-}2)$$

where α_i denotes the trajectory of the leading Reggeon exchanged in the i-th subenergy in the multi-peripheral chain as shown in Fig.1. The exchange terms correspond to the diagrams with the different ordering of longitudinal momenta of final particles. In Eq.(2-2), the end vertex factor $\gamma_a(\gamma_b)$ denotes the coupling strength of Reggeon $\alpha_1(\alpha_{n-1})$ to the particles a and c_1(b and c_n) and the inner vertex factor γ_i denotes the one of two Reggeons α_i and α_{i+1} to the particle

---

*) We denote the four momenta of particles a, b and $c_i$as P_a, P_b and q_i, respectively. The energies and masses are ω_a, ω_b and ω_i, and m_a, m_b and m_i, respectively. The number i represents the order from the side of the particle a in a multi-peripheral chain as shown in Fig.1. The invariant variables are defined as

$$s = (P_a + P_b)^2 \ , \ s_i = (q_i + q_{i+1})^2 \text{ and } t_i = (P_a - \sum_{j=1}^{i} q_j)^2 \ .$$

c_{i+1}, ζ_i and ϕ_i denote the signature factor and Toller angle[51], respectively. In the more complicated case, the contribution of secondary Reggeons and / or cuts

Fig. 1

is added to Eq.(2-2) but mostly, these contribution is neglected at high energies. Furthermore, since we can consider that the duality[27] justifies a rough multi-Regge description of high energy multiple production which ignores resonance production and concentrates on those final particles that are stable with respect to strong interactions, we take this model from threshold to high energies.

Mostly, the following assumptions are taken for the practical discussions;

(i) Each vertex part with the signature factor is small except for small value of each momentum transfer t_i and has an exponential behaviour on t_i. We call this the t_i-cut mechanism. From this assumption, the exchange terms of Eq.(2-2) tend to be small and therefore, we neglect these terms, for simplicity.

(ii) Toller angle ϕ_i is able to be neglected[52].

Based on these assumptions, we have the following amplitude;

$$T_n = \sqrt{C_n} \prod_{i=1}^{n-1} e^{a_i t_i} \left(\frac{s_i}{s_0}\right)^{\alpha_i(t_i)} , \qquad (2\text{-}3)$$

where C_n is the normalization factor, a_i denotes the magnitude of the t_i-cut and s_0 is scaling parameter which is taken to be 1 $(GeV)^2$.

The partial cross section (σ_n) is given as follows;

$$\sigma_n = \frac{1}{2\sqrt{\lambda(s,m_a^2,m_b^2)}} \int d\Phi_n \, |T_n|^2 , \qquad (2\text{-}4)$$

$$d\Phi_n = \frac{1}{(2\pi)^{3n-4} C_0^{n-2}} \prod_{i=1}^{n} \frac{d^3q_i}{2\omega_i} \delta^4(P_a + P_b - \sum_{i=1}^{n} q_i), \qquad (2\text{-}5)$$

where $2\sqrt{\lambda(s,m_a^2,m_b^2)}$ denotes the flux factor and $\lambda(x, y, z) = x^2+y^2+z^2-2xy-2yz-2zx$, and $d\Phi_n$ the phase space volume of n-particle final states. C_0 is a scaling parameter and is taken to be 1 $(GeV)^2$. The practical calculation is carried out

by Monte Carlo method which is explained in Ref.87).

Now, we consider the multi-pion production processes in order to clarify the structure of reaction mechanism based on the simplified multi-Regge model.

For simplicity, we assume that the only two sort of Reggeons,i.e., pomeron (P) and effective meson (M) Reggeon are exchanged in the multi-prepheral chain, where pomeron and meson Reggeon are assumed to be the fixed poles and parametrized as $\alpha_P \approx 1$ and $\alpha_M \approx 0$, respectively, and are considered that they are specified only by the internal quantum numbers. The effective meson (M) Reggeon contains the averaged effect of all secondary trajectories. Thus, the reaction mechanism in multi-particle production processes is classified into the non-diffractive (ND) mechanism and the diffractive (D) one. The D and ND mechanism are specified by whether pomeron is exchanged somewhere in a multi-peripheral chain or not, respectively. Phenomenologically, the D mechanism is specified by the almost constant behaviour of its cross section with increasing energy, while the ND mechanism by the rapidly decreasing behaviour of its cross section at high energies. In this section, we investigate the magnitude of the t_i-cut parameter a_i corresponding to pomeron and meson Reggeon exchange mechanism, respectively.

First, we consider the non-diffractive part of reaction mechanism. In this case, pomeron is exchanged nowhere in the multi-peripheral chain and all of the exchanged Reggeons are equally α_M. However, in anticipation of the case of the processes dominated by strange meson exchange and / or baryon exchange, which we consider in analyzing the experimental data of Hansen et al. below, we here write the exchanged Reggeon as $\bar{\alpha}$, in general. In the case of multi-pion production, $\bar{\alpha}$ is assumed to be $\bar{\alpha} = \alpha_M = 0$ as seen in the above discussions. The adequacy of this parameter is discussed below.

Then, the reaction matrix producing n-particle final states is written as follows;

$$|T_n|^2 = \bar{C}_n \ (P_L)^{2\bar{\alpha}} \prod_{i=1}^{n-1} e^{2a_i t_i} \ , \ ^{*)} \qquad (2\text{-}6)$$

where $\bar{C}_n$ is the normalization factor and P_L is the incident laboratory momentum.

From the following analyses of experiments, we obtain the result of $a_i = a = 2\ (\mathrm{GeV/c})^{-2}$ for multi-pion production precesses if we take $\bar{\alpha} = \alpha_M = 0$. We call this mechanism the universal t_i-cut mechanism. Fits by means of this value are shown in Fig.2~4. In Fig.2, we show the energy dependence of the partial cross section σ_n in $\pi^- p \to \pi^- p \pi^0 (\pi^+ \pi^-)^k$, where k = 0, 1 and 2[53]. The normalization factors are arbitrary. The magnitude of t_i-cut of $a_i = 2\ (\mathrm{GeV/c})^{-2}$ explains the gross behaviour of σ_n of the non-diffractive part from threshold to high energies.

Fig. 2

In Fig.3, we show the following quantity;

$$\langle |T_n|^2 \rangle = \frac{\int d\Phi_n \prod_{i=1}^{n-1} e^{2at_i}}{\int d\Phi_n} \propto (P_L)^{-\bar{n}} \ . \qquad (2\text{-}7)$$

---

*) In the multi-Regge limit, we have the following relation;

$$s \simeq s_1 \, s_2 \cdots s_{n-1} \ .$$

Then, the experimental values for n are taken from the analyses of Hofmokl et al.[54),*)].

---

*) The cross section for a given inelastic channel with n particles in the final state may be written as

$$\sigma_n = \langle |T_n|^2 \rangle_{av} \frac{1}{P_{cm}\sqrt{s}} \int d\Phi_n \quad ,$$

where P_{cm} is the c.m. momentum of the primary particles and $1/P_{cm}\sqrt{s}$ is the flux factor. Hofmokl et al. have examined the energy dependence of the average of the square of the transition matrix element:

$$\langle |T_n|^2 \rangle_{av} \propto \sigma^* = \frac{\sigma_n P_{cm}\sqrt{s}}{\int d\Phi_n} \quad ,$$

using available data on cross section for multi-pion production processes of 40 reaction channels with the multiplicity n ranging from 3 to 8 in $\pi^{\pm}p$, $K^{\pm}p$, pp and $\bar{p}p$ inelastic collisions. They find that for all investigated reactions σ^* may be well fitted by a simple power law

$$\sigma^* \propto P_L^{-\bar{n}}$$

where the values of the exponent, $\bar{n}$, increase with the multiplicity n. That the result of Eq.(2-7) and Fig.3 is in agreement with this means that the values of $a_i = 2$ (GeV/c)$^{-2}$ and $\bar{\alpha} = 0$ are good parameters for multi-pion production processes.

As seen in Fig.3, we conclude that the result of Hofmokl et al. is explained by the values of $a_i = 2\ (GeV/c)^{-2}$ and $\bar{\alpha} = 0$. Namely, it is explained by the universal t_i-cut mechanism. Furthermore, it means that the increase of P_L dependendence of the phase space with increasing multiplicity is canceled by the decreases due to the universal t_i-cut mechanism. In Fig.4 we show the multiplicity dependence

Fig. 3

of the incident momentum giving the maximum point (P_n^{max}) of the partial cross section. Experimental values are taken from the analyses of Hansen et al.[18]. When we parametrize as

$$P_n^{max} = An^B \quad , \tag{2-8}$$

we see A is channel-dependent but B is universal for any channels. In the case of $a_i = 2\ (GeV/c)^{-2}$ and $\bar{\alpha} = 0$, results are given in Fig.4 and Table 1 and are in fairly good agreement with experimental values. As seen from the above analyses,

Fig. 4

Table.1

$\bar{\alpha} = 0$ and $a_i = 2\ (GeV/c)^{-2}$ are good parameters for the case of multi-pion production processes.

We consider not only multi-pion production processes but also the processes dominated by strange meson exchange and / or baryon exchange which are investigated by Hansen et al.[18] and study the magnitude of the effective trajectory ($\bar{\alpha}$) in the reaction mechanisms corresponding to these processes.

From Eqs.(2-6) and (2-7), we obtain the following relation;

$$\sigma_n \propto \frac{1}{[Flux]} \cdot (P_L)^{2\bar{\alpha}} \int d\Phi_n \prod_{i=1}^{n-1} e^{2a_i t_i} \quad ,$$

$$\propto \frac{1}{[Flux]} \cdot (P_L)^{2\bar{\alpha}-\bar{n}} \int d\Phi_n \quad . \tag{2-9}$$

When we compare this equation with the analysis of Hansen et al.*) , we get $2\bar{\alpha}-2 \simeq -n_A$ because of $\bar{n} \simeq n-1$ where n_A is a paramater used by Hansen et al.. Therefore we determine the value of $\bar{\alpha}$ from one of n_A as follows;

Exchange	n_A	$\bar{\alpha}$
S = 0 meson	2	0
S = 1 meson	3	-1/2
S = 0 baryon	4	-1

,

where S is the strangeness number. For S = 0 meson exchange, this result is in agreement with our assumption $\bar{\alpha} = 0$. Generally, we can write $\bar{\alpha} = -0.5\ (n_S + 2n_B)$**) where n_S and n_B denote the number of strangeness and baryon number of dominantly exchanged object, respectively. It is noted that the determination of $\bar{\alpha}$ is closely related to the magnitude of a_i. These values of $\bar{\alpha}$ are rather small compared with the one of the leading trajectory estimated mostly from two body reactions. The problem why these exchanged trajectory is lower than the leading trajectory in multi-particle production is still an open question. However, it is not so

---

*) Hansen et al. have examined the energy dependence of σ_A which is defined as $\sigma_n = \sigma_A \times \frac{\int d\Phi_n}{P_L{}^{n-2}}$ and found that experimentally σ_A has the form

$$\sigma_A \propto P_L{}^{-n_A} \quad ,$$

just as in two-body reactions. n_A is a constant independent of multiplicity, but depending on the reaction mechanism in a manner similar to Morrison's rule[16] found for two-body reactions.

**) This equation is same to the relation of effective trajectories to rank numbers[55].

suprising if we notice that in multi-particle production processes, there are many terms contributing to the cross section and many secondary trajectories are allowed to be exchanged and thus, the averaged effect of all secondary trajectories may reduce the intercept of $\bar{\alpha}$, and also the subenergy in the multi-peripheral diagram is not always so large and therefore secondary trajectories may contribute to cross sections largely*).

In summary, we can understand the gross feature of multi-particle production data which are characterized by the non-diffractive mechansim according to the following formula:

(experiment) $\propto$ (exchange effect) $\times$ (t_i-cut effect) $\times$ (phase space factor)

where

experiment ; $\sigma_n(EXP) \sim P_L^{2\bar{\alpha}-2}$,

exchange effect ; $\sigma_n(EXP) \,/\, \sigma_n(t_i\text{-cut}) \sim P_L^{2\bar{\alpha}}$,

t_i-cut effect ; $\sigma_n(t_i\text{-cut}) \,/\, \sigma_n(p\cdot s) \sim P_L^{-(n-1)}$

and phase space factor ; $\sigma_n(p\cdot s) \sim P_L^{n-3}$ **) .

---

*) In general, the exchanged trajectory is lower than the leading trajectory in multi-particle production processes. This tendency is seen in inclusive reactions[56]. Also, it is understood by that in C.L.A model[7] the baryon exchange term contributes largely to the cross section.

**) Here,

$$\sigma_n(t_i\text{-cut}) \propto \frac{1}{[\text{Flux}]} \int_{i=1}^{n-1} e^{2a_i t_i}\, d\Phi_n \quad \text{and}$$

$$\sigma_n(p\cdot s) \propto \frac{1}{[\text{Flux}]} \int d\Phi_n \quad .$$

Next, we investigate the diffractive part of the cross section and determine the structure of its reaction amplitude. The diffractive mechanism is characterized by the existence of pomeron exchange somewhere in the multi-peripheral chain and its cross section is considered to show the constant behaviour at high energies. Based on the multi-Regge model discussed above, we consider the following amplitude as to correspond to the diffractive mechanism for the n-particle production processes:

$$T_n^D = \sqrt{D_n} \cdot \prod_{i=1}^{j-1} e^{a_i t_i} \cdot e^{bt_j} \left(\frac{s_j}{s_0}\right)^{\alpha_P} \cdot \prod_{k=j+1}^{n-1} e^{a_k t_k} \quad , \qquad (2\text{-}10)$$

where D_n is the normalization constant. A pomeron is exchanged in the j-th section in the multi-peripheral chain and is assumed to be a fixed pole whose intercept is 1 as mentioned above. It is assumed that the non-pomeron exchange sections in the multi-peripheral chain are specified by the exchange of $\bar{\alpha}$ which is discussed above, and therefore, by only the universal t_i-cut mechanism ($a_i = 2$ (GeV/c)$^{-2}$) for multi-pion production processes.

In order to check the problem whether the amplitude of Eq.(2-10) gives the constant cross section or not, we consider the reaction $\pi p \to 3\pi p$. Then, we get

$$\sigma_4^D \propto \frac{1}{[\text{Flux}]} \int d\Phi_4 \prod_{i=1}^{2} e^{2a_i t_i} \cdot e^{2bt_3} \left(\frac{s_3}{s_0}\right)^{2\alpha_P} \quad , \qquad (2\text{-}11)$$

where t_3 is the 4-momentum transfer squared from initial to final proton. If we take $a_i = 2$ (GeV/c)$^{-2}$ and $b = 8$ (GeV/c)$^{-2}$, the cross section σ_4^D shows the constant behaviour at high energies, as shown by the solid line in Fig.5. On the other hand, if we take $a_i = 0$ in Eq.(2-11) instead of $a_i = 2$ (GeV/c)$^{-2}$, the cross section does not exhibit the constant behaviour but increases with energy as shown by the broken line in Fig.5. Also, if we take $(s/s_0)^{\alpha_P}$ instead of $(s_3/s_0)^{\alpha_P}$ in Eq.(2-11), we get a result similar to the model of $a_i = 0$ and obtain the dotted line in Fig.5. Thus, it is considered that the amplitude of Eq.(2-10)

is a good description of the diffractive mechanism, when $a_i \simeq 2$ $(GeV/c)^{-2}$ and $b \simeq 8$ $(GeV/c)^{-2}$. These values of parameters are independent of the final multiplicity and the incident momentum.

Fig. 5

Finally, we discuss the role which the non-diffractive (ND) and diffractive (D) mechanism play in the cross section of exclusive reactions. As investigated already, the cross section of the former rises steeply from threshold, reaches a peak and then decreases. On the other hand, the one of the latter rises slowly from threshold and approaches a constant value with increasing energy. As shown in Fig.6 for $\pi^- p \to \pi^-\pi^+\pi^- p$[53], the dominant part in the cross section of the exclusive reaction switches over from the non-diffractive mechanism to the diffractive one. Here, we take ND : D = 2 : 1*) as the relative ratio of coupling of two mechanism.

Fig. 6

If we extend this feature to all inelastic reactions, we would get the gross picture as shown in Fig.7. We believe that when the incident energy is fixed, the non-diffractive and diffractive mechanisms are dominant for higher and lower multiplicity reactions, respectively.

Fig. 7

---

*) This value must not be considered to be so rigorously meaningful because we here consider D_π term only, which produces diffractively a dissociated pion system, as the D mechanism. However, as will be discussed in the following section, the D mechanism for $\pi^- p \to \pi^-\pi^+\pi^- p$ is composed of two terms, i.e., D_π and D_N, though the contribution of D_N is small compared with that of D_π. Also, see the analysis of partial cross sections in §4.

§3. The structure of diffractive and non-diffractive mechanism

In the previous section, it has been clarified that the reaction mechanism in multi-particle production processes is composed of two different reaction mechanism, i.e., the non-diffractive (ND) mechanism and the diffractive (D) one. In this section we formulate the model with these mechanisms more fully and investigate the structure of them.

We consider the reaction of Eq.(2-1). Hereafter we consider only multi-pion production processes. As discussed in the previous section, if we consider the only two sort of Reggeons, i.e., pomeron (P) and effective meson (M) Reggeon, the reaction amplitude for the reaction of Eq.(2-1) is divided into the non-diffractive and diffractive parts. Namely, the amplitude ${}^{ab}T_n$ is written as

$$ {}^{ab}T_n = {}^{ab}T_n{}^{ND} + {}^{ab}T_n{}^{D} \quad , \tag{3-1} $$

where ${}^{ab}T_n{}^{ND}$ and ${}^{ab}T_n{}^{D}$ denote the amplitude of the ND and D mechanism, respectively. We construct the amplitudes ${}^{ab}T_n{}^{ND}$ and ${}^{ab}T_n{}^{D}$ in the following way :

(i) We assume the multi-peripheral diagram as shown in Fig.1.

(ii) The exchange of the meson and pomeron in multi-peripheral chain are parametrized as follows;

(A) $e^{at_i(\frac{s_i}{s_0})^{\alpha_M}}$; $a=2(\mathrm{GeV/c})^{-2}$, $\alpha_M=0$ for meson Reggeon,

(B) $e^{bt_i(\frac{s_i}{s_0})^{\alpha_P}}$; $b=8(\mathrm{GeV/c})^{-2}$, $\alpha_P=1$ for pomeron,

where s_0 is a scaling parameter and is taken to be 1 $(\mathrm{GeV})^2$. These parameters are independent of energy and multiplicity and are assumed to be valid from the threshold to high energies.

(iii) Though there are many multi-peripheral diagrams according to the permutation of the final particles in the multi-peripheral chain, we select only a few diagrams which are considered to play main roles

for each reaction, and construct the amplitude corresponding to them as the effective amplitudes. Also, in the following calculation, these amplitudes are added incoherently*), since we are concerned with the gross structure of the reaction mechanism and with the characteristic features of the ND and the D mechanism.

(iv) The ND mechanism is characterized by such a mechanism that pomeron is exchanged nowhere in multi-peripheral chain as shown in Fig.8(a). We simply parametrize it by only one term (${}^{ab}T_n^{ND}$). On the other hand, the D mechanism is characterized by the existence of pomeron exchange in the multi-peripheral chain and is decomposed as follows;

$$ {}^{ab}T_n^{D} = {}^{ab}T_n^{D_a} + {}^{ab}T_n^{D_b} + {}^{ab}T_n^{D_{ab}} + {}^{ab}T_n^{D\text{-}D} + {}^{ab}T_n^{D_a\text{-}D} + \cdots , \quad (3\text{-}2) $$

where ${}^{ab}T_n^{D_i}$, ${}^{ab}T_n^{D_{ab}}$, ${}^{ab}T_n^{D\text{-}D}$ and ${}^{ab}T_n^{D_a\text{-}D}$ denote the amplitudes of single diffractive dissociation of particle i, the double diffractive dissociation, the double diffraction and the double pomeron exchange with dissociated system of particle a, respectively, and they are specified by the diagrams as shown in Fig.8(b)~(f), respectively.

Fig. 8

Under the above assumptions, each reaction amplitude is parametrized as follows;

$$ {}^{ab}T_n^{\nu} = \sqrt{{}^{ab}C_n^{\nu}} \; R_n^{\nu}(s_i, t_i) , \quad (3\text{-}3) $$

$$ R_n^{\nu}(s_i, t_i) = \prod_{i=1}^{n-1} e^{a_i t_i} \left(\frac{s_i}{s_0}\right)^{\alpha_i} , \quad (3\text{-}4) $$

where ${}^{ab}C_n^{\nu}$ denotes the normalization factor of the ν-type reaction mechanism. If $\alpha_i = \alpha_P$ and α_M, then $a_i = b$ and a, respectively.

---

*) The structure of each reaction mechanism is different from each other and the wave functions have little overlap.

The normalization factor ${}^{ab}C_n^{\nu}$ is given as

$$ {}^{ab}C_n^{\nu} = C_n^{ab}\, \alpha^{\nu}_{ab} \quad , \tag{3-5} $$

where C_n^{ab} is dependent of multiplicity but free from any reaction mechanism and α^{ν}_{ab} is independent of multiplicity but dependent of mechanism. Both C_n^{ab} and α^{ν}_{ab} are independent of the incident momentum.

Next, we consider the following quantity in order to investigate the structure of $R_n^{\nu}(s_i, t_i)$ for the $\pi^- p$ and pp reactions with multiplicity n = 3 and 4;

$$ \bar{\sigma}_n^{\nu} = \frac{1}{2\sqrt{\lambda(s, m_a^2, m_b^2)}} \int d\Phi_n \left| R_n^{\nu}(s_i, t_i) \right|^2 \quad , \tag{3-6} $$

The calculated results from Eq.(3-6) are shown in Fig.9 and summarized as follows:

(i) $\bar{\sigma}_n^{ND}$ rises steeply from threshold, reaches the maximum point and then decreases as $P_L^{-\mu}(\mu \simeq 2)$. On the other hand, $\bar{\sigma}_n^{DN}$ and $\bar{\sigma}_n^{D\pi}$ rise slowly from threshold and approach to a constant with increasing energy. Furthermore, $\bar{\sigma}_n^{D\text{-}D}$ rises slightly faster than D_N and / or D_π *). These properties are common to $\pi^- p$ and pp reactions.

(ii) As for the ND term of $\pi^- p$ and pp reactions with equal multiplicity, we find that the shape of both cross sections ($\bar{\sigma}_n^{ND}$) is similar, but the magnitude of the maximum point of $\bar{\sigma}_n^{ND}$ in $\pi^- p$ reactions is about

---

*) Formerly, we proposed a fireball model with double pomeron exchange corresponding to the D-D mechanism in order to analyze inclusive pp reactions in the accelerator energy region and pointed out the increase of the cross section due to this mechanism with increasing energy[25].

9 times larger than the one in pp reactions*).

(iii) In $\pi^- p$ reaction, $\bar{\sigma}_n^{D_\pi} > \bar{\sigma}_n^{D_N}$ as shown in Fig.9(b). This is due to the relation $s_{p\pi} > s_{\pi\pi}$, where $s_{p\pi}$ ($s_{\pi\pi}$) is the subenergy of pomeron exchange part as shown in Fig.8(b) (Fig.8(c)).

(iv) The relative magnitude of $\bar{\sigma}_n^{D_\pi}$ to $\bar{\sigma}_n^{ND}$ in $\pi^- p$ reactions is nearly equal to that of $\bar{\sigma}_n^{D_N}$ to $\bar{\sigma}_n^{ND}$ in pp reactions when the multiplicity of both channels is same. This comes from the fact that the subenergy of pomeron exchange part of both single-diffractive dissociation mechanisms, i.e., D_π in $\pi^- p$ reactions and D_N in pp reactions, is same $s_{p\pi}$ in both channels.

Fig. 9

---

*) The phase space volume contains the energies of final state particles. If we consider the region of $q_i \simeq 0$, the relative magnitude of the phase space volume of the final state of $\pi^- p \to N + (n-1)\pi$ to the one of $pp \to NN + (n-2)\pi$ is about $\frac{1}{m_\pi} / \frac{1}{m_N} \simeq 7$, which partly accounts for the difference of the magnitude of the maximum point of $\bar{\sigma}_n^{ND}$ between $\pi^- p$ and pp reactions[55].

§4. The analyses of experimental data by the model

Now, we analyze some experimental data by means of the model discussed above. Multi-particle production processes are specified by two variables, i.e., the incident momentum and the final multiplicity. For the present, we pay attention to the reaction mechanism of exclusive reactions with a fixed multiplicity, say several, in the energy region from threshold to $P_L \simeq 100$ GeV/c. Then, it is assumed that the number of pomeron exchanged in the multi-peripheral chain is limited to only one, because the contributions from multi-pomeron exchange mechanism are considered to be small in the energy region below $P_L \simeq 100$ GeV/c. Furthermore, the double diffractive dissociation term D_{ab} is assumed to be small compared with the single diffractive dissociation terms D_a and D_b in this energy region*). The smallness of the contribution from these reaction mechanisms is discussed and clarified in §7. Therefore, we consider only three mechanisms (ND, D_a and D_b) in the first approximation, when we analyze the following experiment. We are not concerned with the quantitatively detail discussion of the fitting to the data but the gross feature and the characteristic role of each mechanism, ND and D.

(1) Partial cross sections

First, we analyze the partial cross section σ_n for the following reactions in order to investigate the energy dependence of cross sections and the role of the ND and D mechanism in each reactions;

$$\pi^- p \to \pi^- \pi^0 p \quad , \tag{4-1-a}$$

$$\pi^- p \to \pi^- \pi^+ \pi^- p \quad , \tag{4-1-b}$$

---

*) Experimentally, the smallness of D_{ab} compared with D_a and / or D_b is seen in the LPS analysis[20]. Also, recent ISR data show the similar results[57].

$$\pi^- p \to \pi^-\pi^+\pi^-\pi^0 p \quad , \tag{4-1-c}$$

$$\pi^- p \to \pi^-\pi^+\pi^-\pi^+\pi^- p \quad , \tag{4-1-d}$$

$$pp \to pp\pi^0 \quad , \tag{4-1-e}$$

$$pp \to pp\pi^+\pi^- \quad . \tag{4-1-f}$$

According to the procedure in the previous section, the amplitude for the above reactions are expressed as follows;

$$\pi p_{T_3} = \pi p_{T_3}^{ND} + \pi p_{T_3}^{D_N} \quad , \tag{4-2-a}$$

$$\pi p_{T_4} = \pi p_{T_4}^{ND} + \pi p_{T_4}^{D_N} + \pi p_{T_4}^{D_\pi} \quad , \tag{4-2-b}$$

$$\pi p_{T_5} = \pi p_{T_5}^{ND} + \pi p_{T_5}^{D_N} \quad , \tag{4-2-c}$$

$$\pi p_{T_6} = \pi p_{T_6}^{ND} + \pi p_{T_6}^{D_N} + \pi p_{T_6}^{D_\pi} \quad , \tag{4-2-d}$$

$$pp_{T_3} = pp_{T_3}^{ND} + pp_{T_3}^{D_N} + pp_{T_3}^{D_N} \quad , \tag{4-2-e}$$

$$pp_{T_4} = pp_{T_4}^{ND} + pp_{T_4}^{D_N} + pp_{T_4}^{D_N} \quad , \tag{4-2-f}$$

where second and third terms in pp reactions denote the single diffractive dissociation amplitude in which pomeron couples to the projectile proton and the target one, respectively. In $\pi^- p$ reactions, the D_π mechanism is forbidden from the conservation law of G-parity when the final multiplicity n is odd and thus we have only two terms, i.e., ND and D_N while we have an additional term D_π for the reactions with even multiplicity. We calculate the energy dependence of the partial cross sections and fit the data[53),58)] which are shown in Fig.10. Experimental data are fitted by using the following relative weights among each mechanism:

$$\alpha^{ND}_{\pi p} : \alpha_{\pi p}{}^{D_N} : \alpha_{\pi p}{}^{D_\pi} = 8 : 2 : 1.1 \quad , \qquad (4\text{-}3\text{-}a)$$

$$\alpha^{ND}_{pp} : \alpha_{pp}{}^{D_N} = 8 : 1.1 \ ^{*)} \quad . \qquad (4\text{-}3\text{-}b)$$

These parameters are taken so as to fit σ_n over all. Also, the normalization factor $C_n{}^{ab}$ is determined so as to fit the experimental data. The total normalization factor of the ND mechanism, ${}^{ab}C_n{}^{ND}$ is taken as follows in the case of three and four final multiplicity-reactions;

$$^{\pi p}C_3{}^{ND} = 1.59 \times 10^2 \quad , \qquad (4\text{-}4\text{-}a)$$

$$^{\pi p}C_4{}^{ND} = 1.61 \times 10^3 \quad , \qquad (4\text{-}4\text{-}b)$$

$$^{pp}C_3{}^{ND} = 0.96 \times 10^3 \quad , \qquad (4\text{-}4\text{-}c)$$

$$^{pp}C_4{}^{ND} = 1.02 \times 10^4 \quad , \qquad (4\text{-}4\text{-}d)$$

where the values of ${}^{ab}C_n{}^{ND}$ are given in dimensionless unit. The fits are shown in Fig.10 and are satisfactory.

Fig. 10

From this analysis the following results can be derived;

(i) In all reactions, the ND mechanism is dominant in the low energy region but it rapidly decreases with increasing energy, while the D mechanism (D_π and / or D_N) approaches to a constant and becomes dominant at high energies. Namely, the dominant reaction mechanism switches over from the ND mechanism to the D mechanism with increasing

---

*) If we assume the factorization and relate ${}^{ab}C_n{}^{\nu}$ to effective couplings as discussed in §6, we can see Eq.(4-3-b) comes from Eq.(4-3-a) automatically. In the word of coupling constants, the ratio of $\alpha_{\pi p}{}^{ND} : \alpha_{\pi p}{}^{D_\pi}$ and the one of $\alpha_{pp}{}^{ND} : \alpha_{pp}{}^{D_N}$ are equally $(f^2_{MN\bar{N}}\, g_{MM}{}^2) : (f^2_{PN\bar{N}}\, g_{PM}{}^2)$.

energy. We call this the switch-over mechanism.

(ii) In πp reactions, the D_π mechanism gives a larger contribution to σ_n than the D_N mechanism despite $\alpha_{\pi p}^{D_N} \simeq \alpha_{\pi p}^{D_\pi}$. This comes mainly from the difference of the structure between $R_n^{D_N}(s_i, t_i)$ and $R_n^{D_\pi}(s_i, t_i)$ as discussed in §3. The D_π part produces the different energy dependence between σ_3 and σ_4 in the $\pi^- p$ reactions.

(iii) Let us consider the contribution to the inelastic total cross section from each channels. If we neglect the partial cross sections with large multiplicities, the following cross sections can be estimated for $\pi^- p$ reactions;

$$\sigma_T^{ND} \simeq \sigma_3^{ND} + \sigma_4^{ND} + \sigma_5^{ND} + \sigma_6^{ND} \quad , \tag{4-5-a}$$

$$\sigma_T^{D} \simeq \sigma_3^{D_N} + \sigma_4^{D_N} + \sigma_5^{D_N} + \sigma_6^{D_N} + \sigma_4^{D_\pi} + \sigma_6^{D_\pi} \quad , \tag{4-5-b}$$

where σ_T^{ND} and σ_T^{D} denote the total contribution from the ND and D mechanism, respectively. The energy dependence of σ_T^{ND} and σ_T^{D} is shown in Fig.11. σ_T^{ND} shows a slowly decreasing behaviour with energy, while σ_T^{D} increases slowly with energy. Therefore, the switch-over mechanism is seen in this case, too. Though only these cross sections do not saturate the inelastic total cross section, it is meaningful to calculate the ratio $\sigma_T^{D} / \sigma_T^{ND}$, which turns out $\simeq \frac{1}{3}$ at $P_L \simeq 16$ GeV/c in our case. Uehara[59] estimated this ratio as $\simeq \frac{1}{2}$ at such an energy, which is not inconsistent with our result. Also, Quigg and Jackson[60] estimated this ratio as $\simeq \frac{1}{3}$.

<Fig. 11

(iv) We estimate in $\pi^- p$ reactions the contribution of D type in σ_n at a fixed s. At three incident momenta, this is presented in Fig.12. At small multiplicities the ratio becomes large as the energy increases but at large multiplicities the ratio is small.

Fig. 12

(2) Invariant mass spectra

The invariant mass spectra of exclusive reactions in $\pi^- p$ collisions are studied here. Since each reaction mechanism exhibits a characteristic distribution in the invariant mass spectra, we can also check the component of the reaction amplitudes. As there are no data of the invariant mass spectra for the reaction considered in (1), we use the one with fixed pion number in the process $\pi^- p \to \pi_f^- (m\pi + N)^+$ for m = 1, 2, 3 and 4[61], where π_f^- is a leading particle.

Experimental data given in the dashed lines in Fig.13 show the following features :

(i) For m = 1, there is a large enhancement for 1.2 GeV < $M(\pi N)$ < 1.7 GeV and a low and nearly flat tail for $M(\pi N)$ > 2 GeV.

(ii) For m = 2, there is a small and broad enhancement around 1.6 GeV, a flat plateau for 2 GeV < $M(2\pi M)$ < 3 GeV and a linear rising for $M(2\pi N)$ > 3 GeV.

(iii) For m = 3, there is a linear rising for $M(3\pi N)$ < 2 GeV and a flat plateau for $M(3\pi N)$ > 2 GeV.

(iv) For m = 4, there is an only linear rising for $M(4\pi M)$ > 2 GeV.

Fig. 13

The process $\pi^- p \to \pi^-_f \ (m\pi + N)^+$ in this experiment contains various channels with one nucleon and m pions and is not same to the reactions considered in Eqs. (4-1-a) ~ (4-1-d). Therefore the normalization factor C_n^{ab} which is determined from the analysis of the partial cross sections in (1) can not be taken for the analysis of invariant mass spectra in this subsections. However, since we are not concerned with the quantitatively detailed discussion of the data fitting but the characteristic role of each mechanism, ND and D, in the invariant mass distributions, we assume that the experimental data in Fig.13 come from effectively the same reaction as considered in Eqs.(4-1-a) ~ (4-1-d) and put the effect of this assumption on the normalization factor of each reaction. In the analysis of the invariant mass distributions, this normalization factor contains some constant factor multiplying on C_n^{ab} which is determind from the analysis in (1) and we take this constant factor commonly for reactions with different value of m. As for the ratio of the relative weight among different reaction mechanisms, we take Eq.(4-3-a).

We calculate the following quantity:

$$\frac{d\sigma_n(s)}{dM(m\pi N)} = \frac{d\sigma_n^{ND}(s)}{dM(c_2 \cdots c_n)} + \frac{d\sigma_n^{D}(s)}{dM(c_2 \cdots c_n)} \qquad (4\text{-}6)$$

where $M(c_2 \cdots c_n) = \sqrt{(\sum_{i=2}^{n} q_i)^2}$. First, we consider the features of each mechanism in the invariant mass spectra. As the typical examples shown in Fig.14 make clear, the results are summarized as follows:

(i) The invariant mass spectrum of the ND mechanism shows the following features : In the energy region near threshold, it shows a sharp peak, and the shape of it crumbles through a dumpling-type to a thin board-type with increasing energy.

(ii) In the case of the D_N mechanism, there is an enhancement near low kinematic boundary, and it becomes bigger with energy. But the

peak position of it does not change largely. This bump corresponds to the so-called cluster of N^*.

(iii) In the case of the D_π mechanism, there is an enhancement near upper kinematic boundary and it also becomes bigger with energy. The peak position of this enhancement moves to the side of large invariant mass as the upper kinematic boundary increases.

(iv) There features are seen commonly for all multiplicity.

Fig. 14

Now, we analyze the experimental data at P_L = 16 GeV/c. We take the value of Eq.(4-3-a) for the relative weights $\alpha_{\pi p}^{ND}$, $\alpha_{\pi p}^{D_N}$ and $\alpha_{\pi p}^{D_\pi}$. The results calculated from our model are shown by the solid lines in Fig.13*) and give a good agreement with data except for the case of m = 3 and are summarized as follows:

(i)' For m = 1, $\sigma_3^{ND} \simeq \sigma_3^{D_N}$. The ND mechanism in the reaction with three body final state has a thin board-type spectrum in the invariant mass distribution and the D mechanism has a large enhancement near $M(\pi N) \simeq 1.4$ GeV, respectively as shown in Fig. 14. Therefore, the large enhancement from 1.2 GeV to 1.7 GeV is explained by the D_N mechanism and the flat tail by the ND one.

(ii)' For m = 2, $\sigma_4^{ND} \simeq \sigma_4^{D_\pi} > \sigma_4^{D_N}$. The ND mechanism has a dumpling-type spectrum at this energy. A nearly flat plateau for 2 GeV < $M(2\pi M)$ < 3 GeV is explained by this mechanism. The D_N mechanism produces a small enhancement near about 1.6 GeV and the D_π one a large enhancement at the large invariant mass region near about 4.5 GeV.

---

*) Here we fix the normalization factor as follows;

1 event / 1 bin = 1.3×10^{-6} mb/GeV

(iii)' For m = 3, $\sigma_5^{ND} > \sigma_5^{D_N}$. In this case, the predicted value in our model is too large compared with the experimental data. Since the discrepancy with the data is seen only in this case, we consider that this experimental data of $\pi^- p \to \pi^-{}_f(3\pi N)^+$ may be wrong*).

(iv) For m = 4, $\sigma_6^{ND} > \sigma_6^{D_\pi} > \sigma_6^{D_N}$. The invariant mass distribution is explained mainly by the ND mechanism at this energy.

It is concluded that at P_L = 16 GeV/c, reactions with small multiplicity are specified mainly by the D mechanism and those with large multiplicity by the ND mechanism, respectively. This result comes from the fact that the threshold energy of reactions with large multiplicity is high compared with that of reactions with small multiplicity. The threshold energy is very important in analyzing the data of exclusive reactions at a fixed energy.

(3) Forward-backward asymmetry

In this subsection, we investigate the connection of the forward-backward (F-B) asymmetry with the reaction mechanism.

We consider the following process:

$$a + b \to \underbrace{c_1 + c_2 + \cdots + c_i}_{n_+} + \underbrace{c_{i+1} + \cdots + c_n}_{n_-}, \qquad (4\text{-}7)$$

where n_+ and n_- denote the number of particles going to the forward and backward direction with respect to the particle a in C. M. S., respectively. The total number (n) of secondary particles is $n_+ + n_-$. If we express the cross section of the above process by $\sigma_n^{(n_+, n_-)}$, we have the following

---

*) Also, the fact that the shape of this experimental data are quite different from the case of m = 2 and m = 4 suggests that this experimental data are doubtful.

relation:

$$\sigma_n = \sum_{n_+=1}^{n-1} \sigma_n^{(n_+,\ n_-)} \quad , \tag{4-8}$$

The F-B asymmetry in collision is characterized by the structure of $\sigma_n^{(n_+,\ n_-)}$. Also, we consider the following asymmetry parameter

$$\bar{\Delta}_n \equiv \sum_{n_+=1}^{n-1} \Delta_n \sigma_n^{(n_+,\ n_-)} \ / \ \sigma_n \quad , \tag{4-9}$$

where $\Delta_n \equiv n_+ - n_- = 2\ (n_+ - \frac{n}{2})$.

The experimental data[62] of $\sigma_n^{(n_+,\ n_-)}$ are shown in Fig.15. It is noted that $\sigma_n^{(n_+,\ n_-)}$ of the reaction $\pi^- p \to \pi^-\pi^+\pi^-\pi^+\pi^- p$ has a peak at $n_+=3$ ($\Delta_n = 0$) and its value increases and then decreases with the incident momentum from P_L=5 GeV/c to 16 GeV/c, while at both side, i.e., at $|\Delta_n| = 4$, it increases monotonically. In the case of pp reactions, $\sigma_n^{(n_+,\ n_-)}$ shows the V-type shape at 28.5 GeV/c and the production of particles in collision is strongly asymmetric.

Fig. 15

In order to understand these experimental features, we consider the connection of this cross section $\sigma_n^{(n_+,\ n_-)}$ to the reaction mechanism discussed above. We show the model calculation of $\sigma_n^{(n_+,\ n_-)}$ for the reaction $\pi^- p \to \pi^-\pi^+\pi^- p$ at 16 GeV/c and 64 GeV/c in Fig.16. Here, we used the model formulated in §3 and the relative weight of Eq.(4-3-a) among each mechanism. The calculated results show the following properties: The ND mechanism has a peak around $|\Delta_n| = 0$, which the D mechanism (D_π and / or D_N) has a peak at $|\Delta_n| = 2$, and a peak at $|\Delta_n| = 0$ decreases with energy but the one at $|\Delta_n| = 2$ increases. Since these characteristic properties by each mechanism (ND and D) can be considered to be seen generally in the reactions with any multiplicity, we can interpret the data of $\pi^- p \to \pi^-\pi^+\pi^-\pi^+\pi^- p$ at 5, 11 and 16 GeV/c as follows: Namely, the

energy dependence of the peak at $\Delta_n = 0$ is specified by the ND mechanism whose cross section increases and then decreases with the incident momentum from P_L = 5 GeV/c to 16 GeV/c as shown in Fig.10 (d), while the increasing behaviour of $\sigma_n^{(n_+, n_-)}$ at both sides is explained by the D mechanism (D_π and D_N) whose cross section increases monotonically in this region. If the energy goes up further, the cross section of ND rapidly decreases and the one of D rises slowly, and therefore the shape of $\sigma_n^{(n_+, n_-)}$ of $\pi^- p \to \pi^-\pi^+\pi^-\pi^+\pi^- p$ will change into the V-type distribution, just as seen in Fig.16. We wish the experimental test about this point. For pp collisions, $\sigma_n^{(n_+, n_-)}$ exhibits the V-type distribution as shown in Fig.15 (b) and this means that the D mechanism dominates even at P_L = 28 GeV/c. The problem why the ratio of the contribution of D to that of ND is large in the case of pp reactions compared with the case of πp reactions is an open question and will be investigated elsewhere.

——————— Fig. 16 ———————

Also, we can estimate the value of the F-B asymmetry parameter for each reaction mechanism from $\sigma_n^{(n_+, n_-)}$. In πp collisions we have

$$\begin{aligned} \bar{\Delta}_n\ (\mathrm{ND}) &\sim \text{small} \quad , \\ \bar{\Delta}_n\ (D_\pi) &\sim + \text{large} \quad , \\ \bar{\Delta}_n\ (D_N) &\sim - \text{large} \quad . \end{aligned} \tag{4-10}$$

The asymmetry parameter is connected with the longitudinal distribution as follows;

$$\bar{\Delta}_n \cdot \sigma_T = \sum_i \left(\int_0^1 \frac{d\sigma_n}{dx_i}\, dx_i - \int_{-1}^0 \frac{d\sigma_n}{dx_i}\, dx_i \right) \quad , \tag{4-11}$$

where $\frac{d\sigma_n}{dx_i}$ denotes the single-particle distribution of the i-th particle in the n-particle production and x_i is the Feynman variable, i.e., $x_i \equiv 2q_{\parallel}^{\,i}/\sqrt{s}$.

The calculated x_i-distribution of $\pi^- p \to \pi^- \pi^+ \pi^- p$ at 27. GeV/c is shown in Fig.17*).

Fig. 17

As discussed above, the quantity $\sigma_n^{(n_+, n_-)}$ and $\bar{\Delta}_n$ are good parameters to make clear what the dominant mechanism is and we expect that these quantities are systematically analyzed experimentally.

(4) Two-particle distribution

Finally, we analyze two-particle distributions in our model. As an example, we consider the reaction $\pi^- p \to \pi^- \pi^+ \pi^- p$ and calculate the longitudenal distribution $\frac{d\sigma_4}{dx_2 dx_3}$ by using the relative weight of Eq.(4-3-a), where x_2 and x_3 denote the Feynman variables of the centrally produced pions on each reaction mechanism. The results are shown in Fig.18 which seem to be consistent with the analysis of the LPS plots for 4-body reactions at 16 GeV/c[20], and summarized as follows:

(i) The contribution from each reaction mechanism to each division, i.e., [A], [B], [C] and [D] which are shown in Fig.18 (a) representatively, are as follows:

$$\text{ND} : [D] > [A] > [C] > [B] ,$$

$$D_\pi : [A] \gg [B], [D], [C] ,$$

$$D_N : [C] \gg [B], [D], [A] .$$

Namely, D_π and D_N seem to produce just as a cluster, while ND spreads

---

*) From the result of Fig.17, we can roughly estimate the value of $\bar{\Delta}_n$ for each reaction mechanism as follows;

$$\frac{\bar{\Delta}_4(\text{ND})}{\sigma_4^{\text{ND}}} \sim + \text{small}, \quad \frac{\bar{\Delta}_4(D_\pi)}{\sigma_4^{D_\pi}} \sim + 2, \quad \frac{\bar{\Delta}_4(D_N)}{\sigma_4^{D_N}} \sim -1.8 .$$

out all divisions.

(ii) The energy dependence is as follows: Namely, ND decreases rapidly in all divisions, while D_π and D_N increase gradually in the divisions [A] and [C], respectively.

Fig.18

On the contrary to Van Hove and his collaborator's insistence[20], it seems to be incorrect to conclude that the D mechanism is completely separated from the ND mechanism at 16 GeV/c, as shown in Fig.18. As the energy goes up, the contribution of ND rapidly decreases and two peaks are produced by D_N and D_π. These circumstances are seen at 64 GeV/c as shown in Fig.18. The energy dependence of the contribution from each mechanism is given at $|x_2| = |x_3| = 0.05$ in each division and shown in Fig.19. Since the relative ratio of D to ND is larger in the divisions [A] and [C] than in the ones [B] and [D], the energy dependence

Fig. 19

is weaker in the former than in the latter. This tendency is supported in the experimental data of $pp \to pp\pi^+\pi^-$ as shown in Fig.20[63].

Fig. 20

The exponent N in $\frac{d^2\sigma_4}{dx_2 dx_3} \propto P_L^{-N}$ for the dependence of two particle distribution on the incident momentum between 16 GeV/c and 64 GeV/c is shown in Fig.21. This result is in qualitatively agreement with the experiment of $\pi^+p \to \pi^+\pi^-\pi^+p$ in the region between 8 GeV/c and 16 GeV/c[64]. The ununiform pattern in Fig.21 is due to the correlation of each mechanism.

Fig. 21

In conclusion, the results of above analyses show that in exclusive reactions there are two different reaction mechanisms, i.e., the non-diffractive (ND) mechanism and the diffractive (D) one, and the dominant reaction mechanism switches over from ND to D with increasing energy. Our model is good in order to grossly understand these characteristic property of exclusive reactions. The structure of the switch-over mechanism is explored in the following sections.

§5. The gross structure of exclusive reactions

As understood from the analyses of the previous section, it has been clarified that the dominant reaction mechanism of exclusive reactions switches over from ND to D with increasing energy. This switch-over mechanism determine the gross structure of exclusive reactions. As shown in Fig. 10, the curve of $\sigma_n(s)$ versus s with fixed multiplicity n is divided into the following three characteristic regions:

Region(I) : The corresponding energy region is from threshold to the point slightly beyond the energy corresponding to the maximum point of $\sigma_n(s)$. In this region, ND dominates; $\sigma_n^{ND} > \sigma_n^{D}$.

Region(II) : Here, $\sigma_n(s)$ is attributed to both ND and D with a comparable order; $\sigma_n^{ND} \sim \sigma_n^{D}$.

Region(III): The high energy region where $\sigma_n(s)$ comes mainly from D; $\sigma_n^{D} > \sigma_n^{ND}$.

We sketch such a feature in Fig.22 on the multiplicity-momentum plane. The regions (I), (II) and (III) construct a band scheme. In the same band region, the structure of the reaction mechanism for different channels is same. If we fix the multiplicity n and increase the incident momentum, the dominant reaction mechanism changes from ND into D. Also, if we fix the incident momentum and increase the multiplicity, the dominant reaction mechanism changes from D to ND as shown in Fig.22. These circumstances are quite different with the case of the C&A model[7].

Fig. 22

We discuss the importance of this viewpoint. As shown in the analysis of §2 and as investigated by Yap Sue-Pin et al.,[21] the empirical formula Eq.(2-8), i.e., $P_n^{max.} = An^B$, which is discovered by Hansen et al.,[18] can be explained qualitatively by the universal t_i-cut mechanism. This fact is understood as follows: The maximum point of $\sigma_n(s)$ belongs to the region (I) and therefore the main part of $\sigma_n(s)$ comes from the ND term, i.e., the universal t_i-cut mechanism for the present case. Also, our analysis of the rank structure[55] of exclusive reactions by the universal t_i-cut mechanism is supported since we were concerned with Region (I), in Ref. 55).

A change of the invariant mass distribution with energy is also specified by the regions (I), (II) and (III). When we fix the momentum at P_L = 16 GeV/c and change the multiplicity, we have already obtained the results of Fig.13. These results are easily understood as follows: The reaction of n =3 belongs to Region (III) at this energy and therefore D_N contributes mainly to the invariant mass distribution. The reaction of n=4 belongs to Region(II) and therefore ND and $D(=D_\pi+D_N)$ contribute comparably. The reactions of n=5 and n=6 belong to Region(I) and therefore ND contributes mainly.

Furthermore we are concerned with the energy dependence of the invariant mass distribution with a fixed multiplicity. As an example, we take the process $\pi^- p \to \pi^- (2\pi N)^+$. At P_L = 16GeV/c which belongs to Region(II) in the present case, $\sigma_4^{ND} \simeq \sigma_4^{D_\pi} > \sigma_4^{D_N}$, but at P_L = 64GeV/c which belongs to Region(III), $\sigma_4^{D_\pi} > \sigma_4^{D_N} > \sigma_4^{ND}$. Therefore a clear enhancement at small invariant mass region which comes from D_N, appears as shown in Fig.23. We wish to await the experimental test about this point. Recent NAL data[65] at 205GeV/c seems to support this tendency.

At low energies near threshold which belong to Region (I), it is expected that the invariant mass distribution is governed mainly by ND.

Fig. 23

Recently, Uehara[59] pointed out that in the reaction $\pi^- p \to \pi_f^- (4\pi N)^+$ at P_L = 16 GeV/c, the linear rising distributions of $M(4\pi N) \gtrsim 2$ GeV comes from $\pi_5^* p$ channel, where π_5^* means a diffractively produced dissociated pion system containing five pions. At this energy, however, the main part of this linear rising is caused by the ND mechanism as discussed above. Hama[66], also, analyzed the same data from the viewpoint of the monistic D mechanism. His analysis seems to be faced with the difficulty in explaining the energy dependence of the partial cross sections and further, the prediction of its model for the invariant mass distribution is in disagreement with the data of $(2\pi N)^+$. It seems to be difficult to fit the various data by the D mechanism only.

Furthermore, the forward-backward asymmetry and the two particle distribution analyzed in the previous section seem to indicate the importance of the band scheme. The experimental data $\sigma_n^{(n_+, n_-)}$ of $\pi^- p \to \pi^-\pi^+\pi^-\pi^+\pi^- p$ at 5, 11 and 16 GeV/c which are shown in Fig.15, are interpreted as follows: Since the momentum region P_L = 5 ~ 16 GeV/c belongs to Region (I) in the present case, $\sigma_n^{(n_+, n_-)}$ is dominanted by ND and its shape is Λ-type distribution. However, if the momentum increases and enters into Region (II) and furthermore into Region (III), the shape of $\sigma_n^{(n_+, n_-)}$ will change from Λ-type into V-type gradually with increasing energy. Also, the two-particle distribution spreads out all divisions on X_i-X_j plane in the Region (I) but will come to be separated into a few divisions with increasing energy as shown in Fig. 18.

As discussed above, the viewpoint of the band scheme is very powerful to understand the gross structure of exclusive reactions. Though we have considered the reactions with several multiplicity and in the region $P_L \lesssim 100$ GeV/c, the problem whether for the reactions with very large multiplicity and in the very high energies, the band sheme exist or not is still an open question. This problem will be investigated elsewhere.

§6. The structure of effective coupling constants

Until now, we have analyzed some experimental data of excluxive reactions and investigated the role of the ND and D mechanism in hadron-hadron collisions based on a simplified multi-Regge model formulated in §3. Then we have assumed that the non-diffractive mechanism (ND) and the single diffractive dissociation one (D_a and / or D_b) are main terms and the double diffractive dissociatiation one (D_{ab}) and other multi-pomeron exchange one (D-D, D_a-D, $\cdots$) are negligible for reactions with small multiplicity, say several, in the region from threshold to $P_L \simeq 100$ GeV/c. However, it has not been clear why the contributions of D_{ab}, D-D and D_a-D, etc. are small. In this section, we investigate the structure of effective couplings in the multi-peripheral chain, above all the inner couplings in order to obtain a clue to solve these problem. The smallness of these terms is discussed in the next section.

Now, the magnitude of the normalization factor ${}^{ab}C_n^{\nu}$ is related to the problem what reaction mechanism ν is dominant. However, it is difficult to estimate the normalization factors of the other reaction mechanisms except for the ND, D_a and D_b mechanism from the prensent experimental data as discussed in §4. However, since ${}^{ab}C_n^{\nu}$ is connected with the effective couplings in the multi-peripheral chain whose magnitudes are able to be estimated using the result of the above analyses as seen in the present section below, we investigate the structure of ${}^{ab}C_n^{\nu}$ by means of rewriting it by the effective couplings.

We assume the factorization and define the effective couplings as follows;

$$ {}^{ab}C_n^{\nu} = f^2_a \left(\prod_{i=1}^{n-2} g^2_i\right) f^2_b \quad , \tag{6-1} $$

where f_a and f_b are the outer coupling constants and g_i is the inner coupling constant*). In πp and pp reactions, there exist four outer couplings ($f_{P\bar{N}N}$, $f_{M\bar{N}N}$, $f_{P\pi\pi}$ and $f_{M\pi\pi}$) and two inner couplings (g_{MM} and g_{PM}), which are defined in Fig.24. The adjacent pomeron coupling g_{PP} defined in Fig.24 (g) is not kinematical forbidden. However, this coupling is dynamically forbidden by the conservation of G-parity and therefore, it is assumed that $g^2_{PP} = 0$, for the present. In §8, the possibility of non-vanishing g^2_{PP} will be discussed. The values of these coupling constants are effective ones because we neglect isospin factor and the permutation factor (1/n!) of same species of particles in the final states. We estimate these values using the results of analyses in §4 and the experimental data of pp total cross section σ_T^{pp} and pp elastic forward peak $\frac{d\sigma_{el}^{pp}}{dt}\Big|_{t=0}$ [67].

Fig. 24

First, we consider $f_{P\bar{N}N}$. The experimental data of σ_T^{pp} and $\frac{d\sigma_{el}^{pp}}{dt}\Big|_{t=0}$ are approximately as follows;

$$\sigma_T^{pp} \simeq 40 \text{ mb} \quad , \tag{6-2}$$

$$\frac{d\sigma_{el}^{pp}}{dt}\Big|_{t=0} \simeq 100 \text{ mb/(GeV/c)}^2 \quad . \tag{6-3}$$

We here assume pomeron dominance in pp elastic reaction at high energies and parametrize as follows;

$$\sigma_T \simeq \frac{1}{s}\beta_{P\bar{N}N}(0)\beta_{P\bar{N}N}(0)\left(\frac{s}{s_0}\right)^{\alpha_P} , \tag{6-4}$$

$$\frac{d\sigma_{el}^{pp}}{dt} \simeq \frac{1}{16\pi s^2}\left|\beta_{P\bar{N}N}(t)\beta_{P\bar{N}N}(t)\xi_P(t)\right|^2\left(\frac{s}{s_0}\right)^{2\alpha_P} , \tag{6-5}$$

where $\beta_{P\bar{N}N}(t) = f_{P\bar{N}N}e^{bt}$, $\xi_P(t)$ denotes the signature factor and $s_o = 1\ (\text{GeV})^2$. Then, we have

$$f^2_{P\bar{N}N} \simeq 107.8 \quad . \tag{6-6}$$

Next, we estimate g^2_{MM}. From Eq.(6-1), we have

$$\frac{ab_{C_4}^{ND}}{ab_{C_3}^{ND}} = \frac{f_a^2 g_{MM}^2 g_{MM}^2 f_b^2}{f_a^2 g_{MM}^2 f_b^2} = g^2_{MM} \quad . \tag{6-7}$$

*) These couplings are all defined in dimensionless, since we introduced the scaling parameter C_0 into the phase space factor as Eq.(2-5).

We get from Eqs.(4-4-a) and (4-4-b)

$$g^2_{MM} \simeq 10 \quad . \tag{6-8}$$

This value may be also estimated from Eqs.(4-4-c) and (4-4-d) , and the same result is obtained.

Further, using the value of ${}^{\pi p}C_3^{ND}$, ${}^{pp}C_3^{ND}$ and g^2_{MM} , we have

$$f^2_{MN\bar{N}} = \sqrt{{}^{pp}C_3^{ND} \,/\, g^2_{MM}} = 9.8 \ , \tag{6-9}$$

$$f^2_{M\pi\pi} = {}^{\pi p}C_3^{ND} \,/\, (g^2_{MM} f^2_{MN\bar{N}}) \simeq 1.63 \ . \tag{6-10}$$

Thirdly, we consider $f^2_{P\pi\pi}$ and g^2_{PM} . We define the following parameters,

$$a^2 = \frac{g^2_{PM}}{g^2_{MM}} \quad , \quad b^2 = \frac{f^2_{P\pi\pi}}{f^2_{M\pi\pi}} \quad , \quad c^2 = \frac{f^2_{PN\bar{N}}}{f^2_{MN\bar{N}}} \quad , \tag{6-11}$$

Then, since in the case of same n but different ν we have generally

$$\frac{{}^{ab}C_n^{\nu}}{{}^{ab}C_n^{\nu'}} = \frac{C_n^{ab}.\alpha^{\nu}_{ab}}{C_n^{ab}.\alpha^{\nu'}_{ab}} = \frac{\alpha^{\nu}_{ab}}{\alpha^{\nu'}_{ab}} \quad , \tag{6-12}$$

the following relations are obtained for $\pi^- p$ reactions, if we replace the leftest side of Eq.(6-12) by the effective couplings using Eq.(6-1);

$$\frac{\alpha_{\pi p}^{ND}}{\alpha_{\pi p}^{D_N}} = \frac{f^2_{M\pi\pi}\, g^2_{MM}}{f^2_{p\pi\pi}\, g^2_{PM}} = \frac{1}{a^2 b^2} \ , \tag{6-13-a}$$

$$\frac{\alpha_{\pi p}^{ND}}{\alpha_{\pi p}^{D_\pi}} = \frac{f^2_{MN\bar{N}}\, g^2_{MM}}{f^2_{PN\bar{N}}\, g^2_{PM}} = \frac{1}{a^2 c^2} \ , \tag{6-13-b}$$

$$\frac{\alpha_{\pi p}^{D_N}}{\alpha_{\pi p}^{D_\pi}} = \frac{f^2_{p\pi\pi}\, f^2_{MN\bar{N}}}{f^2_{M\pi\pi}\, f_{PN\bar{N}}} = \frac{b^2}{c^2} \tag{6-13-c}$$

From Eqs.(6-6), (6-9) and the last equation of Eq.(6-11), we have $c^2 = 11.0$ Using Eq.(6-13-b) and the result of Eq.(4-3-a), i.e., $\alpha_{\pi p}^{ND} : \alpha_{\pi p}^{D_N} : \alpha_{\pi p}^{D_\pi} = 8 : 2 : 1.1$, we have $a^2 = 0.013$ and thus, together with the first equation of

Eq.(6-11) and $g^2_{MM} \simeq 10$, we obtain

$$g^2_{PM} \simeq 0.13 \quad . \tag{6-14}$$

Furthermore, from Eq.(6-13-a), Eq.(4-3-a) and $a^2 = 0.013$, we have $b^2 = 20.0$. Therefore, from the second equation of Eq.(6-11) and Eq.(6-10), we have

$$f^2_{p\pi\pi} \simeq 32.6 \tag{6-15}$$

These results are collected in Table 2. The above results are exhibited in the first column of Table 2. The coupling constants defined as

$$\tilde{g}^2_i \simeq \int g_i^2 \, e^{2a_i t_i} \, dt_i \simeq \frac{g_i^2}{2a_i} \quad , \tag{6-16}$$

which we call the " t_i-cut " coupling constants, are given in the second column. Also, the couplings estimated by Chew and Pignotti[26),*)] are shown in the last column for comparison.

———————— Table 2 ————————

The characteristic properties of these values are summarized as follows:

(1) $\tilde{g}^2_{MM}$ is approximately related to the coefficient of ln(s) term in the averaged multiplicity as follows;

$$\langle n \rangle \simeq \tilde{g}^2_{MM} \ln\left(\frac{s}{s_0}\right) + \text{const.} \quad ,$$

where $\langle n \rangle = \langle n_{\pi^+} \rangle + \langle n_{\pi^-} \rangle + \langle n_{\pi^0} \rangle$. Recent experiment is $\langle n \rangle = 2.26 \ln(s) - 3.04$[68)] and thus, our estimation is not inconsistent with it.

(2) The ratio $f_{PN\bar{N}} / f_{p\pi\pi}$ is about 1.8. This value is near to 3/2 which is estimated from the experimental data of $\sigma_T^{NN} / \sigma_T^{\pi N}$. This fact means

---

*) The couplings estimated by Chew and Pignotti contain the t_i-cut effect.

that the outer pomeron coupling estimated from exclusive cross section is nearly same to the one estimated from inclusive cross section and thus, the channel effect is not so important on the contrary to the case of the outer meson coupling as discussed in (4) below.

(3) There is a hierarchy between the inner couplings g^2_{MM} and g^2_{PM} as $g^2_{MM} \gg g^2_{PM}$, which is not inconsistent with the Chew-Pignotti's result[26] and also Giovannini's estimation[69),*]. This result is very attractive though the reason of this herarchy is as yet unsolved.

(4) The value of $f_{M\pi\pi}$ and $f_{MN\bar{N}}$ are smaller than that of $f_{P\pi\pi}$ and $f_{PN\bar{N}}$, respectively. This result is opposite to the Chew-Pignotti's parameters as shown in the last column of Table 2. The magnitude of their parpmeters is estimated from the charged prong cross section which is an inclusive quantity, while the values of our parameters are estimated from the partial cross section which is an exclusive quantity. In our model we must consider the channel effect in order to analyse the inclusive quantity. As an example, we consider the world of pions and nucleons only. In $\pi^- p$ reaction with three final particles, in addition to the reaction $\pi^- p \to \pi^- \pi^0 p$, the channels of $\pi^- p \to \pi^- \pi^+ n$ and $\pi^- p \to \pi^0 \pi^0 n$ also contribute to the $\pi^- p$ total cross section. The reaction mechanism of these channels are mainly ND. In general, the total cross section has large ND component which comes from the summation of the ND component of various channels with any multiplicity, while the number of channels which have the D component are limited because of the constraint of the conservation of quantum number, for example isospin and G-parity, at the vertex coupled to pomeron. The outer meson coupling is connected to ND, while the outer pomeron coupling is contained in D. Therefore, the outer meson coupling estimated from inclusive cross section contains the effect of these summation of channels and becomes larger than the one estimated directly from exclusive reaction, for example $\pi^- p \to \pi^- \pi^o p$. Thus,

*) The smallness of g^2_{PM} has been emphasized by Chew and Pignotti, firstly. Also, Giovannini pointed out the similar result by discussing the deviation of multiplicity distribution from Poisson form.

roughly speaking, the Chew- Pignotti's parameters and our couplings may not be inconsistent with each other.

§7. The swich-over mechanism of the dominant reaction mechanism

In this section, we consider the results from the previous analyses of the effective couplings.

We consider the reaction of $ab \to ab + (n-2)\pi$ with fixed multiplicity. The partial cross sections from each reaction mechanism, i.e., ND, D_a, D_b, D_{ab}, D-D and D_a-D, etc. are given by multiplying the following normalization factors to $\bar{\sigma}_n^{\nu}$ specified by $R_n^{\nu}(s_i, t_i)$ discussed in §3;

$$ {}^{ab}C_n^{ND} = f^2_{Ma\bar{a}}\, f^2_{Mb\bar{b}}\, [\, g^2_{MM}\,]^{n-2} \quad , \tag{7-1} $$

$$ {}^{ab}C_n^{D_a} = f^2_{Ma\bar{a}}\, f^2_{Pb\bar{b}}\, [\, g^2_{MM}\,]^{n-3}\, [g^2_{PM}\,] \quad , \tag{7-2} $$

$$ {}^{ab}C_n^{D_b} = f^2_{Pa\bar{a}}\, f^2_{Mb\bar{b}}\, [\, g^2_{MM}\,]^{n-3}\, [g^2_{PM}] \quad , \tag{7-3} $$

$$ {}^{ab}C_n^{D_{ab}} = f^2_{Ma\bar{a}}\, f^2_{Mb\bar{b}}\, [\, g^2_{MM}\,]^{n-4}\, [\, g^2_{PM}\,]^2 \quad , \tag{7-4} $$

$$ {}^{ab}C_n^{D\text{-}D} = f^2_{Pa\bar{a}}\, f^2_{Pb\bar{b}}\, [\, g^2_{MM}\,]^{n-4}\, [\, g^2_{PM}\,]^2 \quad , \tag{7-5} $$

$$ {}^{ab}C_n^{D_a\text{-}D} = f^2_{Ma\bar{a}}\, f^2_{Pb\bar{b}}\, [\, g^2_{MM}\,]^{n-5}\, [\, g^2_{PM}]^3 \quad , \tag{7-6} $$

.....

The normalization factor ${}^{ab}C_n^{\nu}$ has a hierarchy because of the smallness of g^2_{PM}. As shown in Eqs.(7-4) and (7-5), both D_{ab} and D-D mechanism are the order of g^4_{PM} while D_a and D_b are the order of g^2_{PM}. If we notice the smallness of g^2_{PM}, we can understand the problem why the contribution of D_{ab} and D-D etc. are small and negligible at low energies compared to ND, D_a and D_b. However, the behaviour of the cross section of each mechanism at high energies is specified by

the structure of $R_n^{\nu}(s_i, t_i)$ as investigated in §3. Thus, we can not conclude that the contribution of D_{ab} and D-D etc. are small at high energies.

The hierarchy of the inner couplings as $g^2_{MM} \gg g^2_{PM}$ specifies the structure of ${}^{ab}C_n^{\nu}$ and leads to the switch-over mechanism of the dominant reaction mechanism when we combine ${}^{ab}C_n^{\nu}$ with $\bar{\sigma}_n^{\nu}$. For example, if we use the effective couplings given in Table 2 and calculate the partial cross section of $pp \to pp\pi^+\pi^-$, we have the result as shown in Fig.25, in which the switch-over mechanism appears with increasing energy as follows;

$$ND \to D_N \to D\text{-}D \to \cdots$$

The contribution from the D_{NN} mechanism is very small because of the smallness of $f_{MN\bar{N}}$ compared with $f_{PN\bar{N}}$.

——————— Fig. 25 ———————

The terms of the multi-pomeron exchange are suppressed by the smallness of g^2_{PM} near the threshold energy, but enhanced by the structure of $R_n^{\nu}(s_i, t_i)$ with increasing energy. Thus, it may be considered that the contribution from the terms of the multi-pomeron exchange becomes larger with increasing energy. This produces the switch-over mechanism.

These circumstances are also understood from the simple model calculation in the high energy limit approximation as discussed in Appendix(A). Namely, for the reaction $ab \to ab + n\pi$, when $\alpha_M = 0$ and $\alpha_P = 1$, we obtain the following partial cross sections in the high energy limit,

$$\sigma_n^{ND} = \tilde{f}^2_{Ma\bar{a}} \cdot \tilde{f}^2_{Mb\bar{b}} \cdot [\tilde{g}^2_{MM}]^n \cdot \frac{(\ln s)^n}{n!} \cdot s^{-2} \quad , \tag{7-7-a}$$

$$\sigma_n^{D}a = \tilde{f}^2_{Ma\bar{a}} \cdot \tilde{f}^2_{Pb\bar{b}} \cdot [\tilde{g}^2_{MM}]^{n-1} \cdot [\tilde{g}^2_{PM}] \cdot [\frac{1}{2^n} - \frac{1}{2(n-1)!} \cdot \frac{(\ln s)^{n-1}}{s^2}] \quad , \tag{7-7-b}$$

$$\sigma_n^{D}b = (\tilde{f}^2_{Pa\bar{a}} \cdot \tilde{f}^2_{Mb\bar{b}} / \tilde{f}^2_{Ma\bar{a}} \cdot \tilde{f}^2_{Pb\bar{b}}) \cdot \sigma_n^{D}a \quad , \tag{7-7-c}$$

$$\sigma_n^{D}ab = \tilde{f}^2_{Ma\bar{a}} \cdot \tilde{f}^2_{Mb\bar{b}} \cdot [\tilde{g}^2_{MM}]^{n-2} \cdot [\tilde{g}^2_{PM}]^2 \cdot [\frac{1}{2^n} - \frac{1}{2(n-1)!} \cdot \frac{(\ln s)^{n-1}}{s^2}] \quad , \tag{7-7-d}$$

$$\sigma_n^{D\text{-}D} = \tilde{f}^2_{Pa\bar{a}} \cdot \tilde{f}^2_{Pb\bar{b}} \cdot [\tilde{g}^2_{MM}]^{n-2} \cdot [\tilde{g}^2_{PM}]^2 \cdot [\frac{\ln s}{2^n} + \frac{1}{8(n-2)!} \cdot \frac{(\ln s)^{n-2}}{s^2}] \quad . \tag{7-7-e}$$

Thus, the partial cross section of ND decreases as $(\ln s)^n/s^2$ at high energies, while D_a, D_b, and D_{ab} increases and approach constants with increasing energy. D-D increases as ln s at high energies. These features produce the switch- over mechanism.

The structure of exclusive reactions having the above features, we next consider the total cross section. The total cross section (σ_T) is given as follows;

$$\sigma_T \simeq \sigma_{el} + \sigma^{ND} + \sigma^{D} \quad , \tag{7-8}$$

where σ_{el} , σ^{ND} , σ^{D} denote the elastic, non-diffractive and diffractive cross section, respectively. Using the discussions by Chew and Pignotti[26], the energy dependence of each cross section is given at high energies as follows;

$$\sigma_{el} \underset{s\to\text{large}}{\sim} s^{2\alpha_P-2} \quad , \tag{7-9-a}$$

$$\sigma^{ND} \underset{s\to\text{large}}{\sim} s^{2\alpha_M-2+\tilde{g}^2_{MM}} \quad , \tag{7-9-b}$$

$$\sigma^{D} \underset{s\to\text{large}}{\sim} s^{\alpha_P+\alpha_M+\frac{1}{2}\tilde{g}^2_{MM}-2+\tilde{g}^2_{PM}} \quad , \tag{7-9-c}$$

where $\tilde{g}^2_{MM}$ and $\tilde{g}^2_{PM}$ contain the t_i-cut effect and correspond to g^2_M and g^2_P of Chew-Pignotti model[26], respectively. If we assume the asymptotic constancy of the total cross section and elastic cross section, we have the following equations;

$$2\alpha_P - 2 \simeq 0 \quad , \tag{7-10-a}$$

$$2\alpha_M - 2 + \tilde{g}^2_{MM} \simeq -2\varepsilon \quad , \tag{7-10-b}$$

$$\alpha_P + \alpha_M + \frac{1}{2}\tilde{g}^2_{MM} - 2 + \tilde{g}^2_{PM} \simeq 0 \quad , \tag{7-10-c}$$

where $\varepsilon > 0$ *).

---

*) When $\varepsilon = 0$, we have $\tilde{g}^2_{PM} \simeq 0$, $\tilde{g}^2_{MM} \simeq 2(1-\alpha_M)$ and $\alpha_P = 1$ as discussed in Ref.26). Then, the inelastic cross section is composed of the non-diffractive cross section only. Therefore, $\varepsilon \neq 0$.

Then we get the following solutions;

$$\alpha_P \simeq 1 \quad , \tag{7-11-a}$$

$$\tilde{g}^2_{MM} \simeq 2(1-\alpha_M)-2\varepsilon \quad , \tag{7-11-b}$$

$$\tilde{g}^2_{PM} \simeq \varepsilon \quad . \tag{7-11-c}$$

The asymptotic constancy of σ_T is due to the cross section of the D mechanism. Thus, we may conclude that the dominant cross section in σ_{inel} switchs over slowly from σ^{ND} to σ^{D} with increasing energy similar to the structure of σ_n as shown in Fig.26. In fact, a dent which comes from the switch-over from σ^{ND} to σ^{D} is experimentally found in $\sigma_T^{K^+p}$ and σ_T^{pp} .

——————— Fig.26 ———————

Such structure of σ_n and σ_T suggests a perturbative picture in powers of pomeron couplings g^2_{PM} for the structure of high energy hadron-hadron interaction.

§8. The perturbative structure of reaction mechanism in hadron-hadron collision

As discussed in the previous section, the hierarchy among the inner couplings ($g^2_{MM} >> g^2_{PM}$) and the switch-over mechanism lead us to the perturbative picture in powers of the pomeron coupling for the structure of reaction mechanisms of multi-particle production processes. The production amplitude is given by the perturbative expansion in powers of the pomeron coupling. In this picture, the Born term is represented by the ND mechanism and the single diffractive mechanism is the first order term. The double diffractive dissociation mechanism and the double diffraction one are the second term. The so-called two component model is the first order approximation in this picture. It is noted that this expansion is formulated not in powers of the number of the pomeron exchanged in a multi-peripheral chain but in

powers of the pomeron coupling as will be discussed below.*) If we identify the dynamical mode of hadron-hadron interaction which is specified by the ND mechanism, to the fireball which is observed in cosmic-ray experiments, this expansion gives us the multi-fireball expansion similar to the models discussed by Chew[70] and also Royzen et al.[71] . At a given energy only a finite number of fireballs is kinematically possible. We formulate a new integral equation for production amplitudes based on the modification of the Chew-Goldberger-Low(CGL) equation[72] and Bethe-Salpeter(BS) equation[71] .

(1) A new integral equation for production amplitudes

In this section, we formulate the integral equation for production amplitudes based on the perturbative picture discussed above.

First, let us consider the ND mechanism of particle a - particle b scattering, pomeron-particle b one and pomeron-pomeron one based on a multi-Regge model. From the CGL equation[72], we have

$$A^0_{ab}(s) = \int d^4q_a \delta^+(q^2_a - m^2_a) G^2_{Ma} R^2 M_b(s') \quad , \tag{8-1-a}$$

$$\tilde{B}^0_b(s) g^2_{PM} = \int d^4q_1 \delta^+(q^2_1 - m^2_1) g^2_{PM} R^2 M_b(s') \quad , \tag{8-1-b}$$

$$M_b(s') = G^2_{Mb} + \int d^4q_2 \delta^+(q^2_2 - m^2_2) g^2_{MM} R^2 M_b(s'') \quad ,$$

and

$$\tilde{C}^0(s) g^2_{PM} = \int d^4q_1 \delta^+(q^2_1 - m^2_1) g^2_{PM} R^2 N(s''') \quad , \tag{8-1-c}$$

$$N(s''') = g^2_{PM} + \int d^4q_2 \delta^+(q^2_2 - m^2_2) g^2_{MM} R^2 N(s'''') \quad ,$$

---

*)Recently, a similar picture for pomeron is discussed by Bishari, Chew and Koplik and Fraser, Snider and Tan, independently.[45] In this picture, two-component model of multi-particle production is taken as a first approximation and higher corrections are generated by repeated pomeron exchange.

where R denotes the Reggeon propagator of the effective meson and G_{Mi} is the external coupling between particle i and meson Reggeon M. $A^0_{ab}(s) = s\sigma_{inel}$. Similarly $\tilde{B}^0_b$ and $\tilde{C}^0$ are proportional to the inelastic cross section of pomeron-particle b scattering and pomeron-pomeron one, respectively. M_b and N denote the inelastic cross sections of Reggeon M-particle b scattering and Reggeon M- Reggeon M one, respectively. It is noted that the pomeron exchange part of the elastic scattering is not included in Eq.(8-1-a) but its non-pomeron exchange part is included in it.

Next, we include the D mechanism in production amplitudes as suggested by switch-over mechanism. From the analogy of the BS equation discussed by Royzen et al.[71] . We have the following equations;

$$A_{ab}(s) = A^0_{ab}(s) + \int d^4q_a \delta^+(q^2_a - m^2_a) G^2_{Pa} D^2 g^2_{PM} \tilde{B}_b(s') + \int d^4k \tilde{B}^0_a(s_1) g^2_{PM} D^2 g^2_{PM} \tilde{B}_b(s_2) \quad , \tag{8-2-a}$$

$$\tilde{B}_b(s') = G^2_{Pb} \cdot g^{-2}_{PM} + \tilde{B}^0_b(s') + \int d^4q_b \delta^+(q^2_b - m^2_b) G^2_{Pb} D^2 \tilde{C}(s'') + \int d^4k \tilde{B}^0_b(s_3) g^2_{PM} D^2 \tilde{C}(s_4) \quad , \tag{8-2-b}$$

$$\tilde{C}(s'') = \tilde{C}^0(s'') + \int d^4k \tilde{C}^0(s_5) g^2_{PM} D^2 \tilde{C}(s_6) \quad , \tag{8-2-c}$$

where D denotes pomeron propagator and G_{Pi} is external coupling between particle i and pomeron. $A_{ab}(s) \approx s\sigma_T(s)$ and similarly $\tilde{B}_b$ and $\tilde{C}$ are proportional to the total cross section of pomeron-particle b scattering and pomeron-pomeron one, respectively. A graphical representation of Eqs.(8-2) is shown in Fig.27, where the kinematical variables are defined.

Fig. 27

We must note the following properties of Eqs.(8-2);

(i) The contribution from the pomeron exchange part of elastic amplitude is included in $A_{ab}(s)$.

(ii) Each ND mechanisms, i.e., A^0_{ab}, $\tilde{B}^0_b$ and $\tilde{C}^0$, are the Born term of Eqs.(8-2-a),

(8-2-b) and (8-2-c), respectively. If $g^2_{PM} = 0$, then Eqs.(8-2) is reduced to Eqs.(8-1).

(iii) $A_{ab}(s)$ is represented by a perturbative expantion in powers of the pomeron coupling g^2_{PM} . Namely, the zeroth approximation is composed of the ND mechanism and the elastic scattering. The single diffractive dissosiation is the first order approximation. The double diffractive dissosiation mechanism and the double diffraction one are the second order term. We note that this approximation is characterized not by the powers of the number of the pomeron exchange in the multi-peripheral chain, but by powers of the inner pomeron coupling.

(iv) As suggested by the switch-over mechanism, the order of the approximation in Eqs.(8-2) is considered to be specified by the magnitude of the incident momentum. For example, in pp collision we have phenomenologically

$$P_L^{\text{eff.}} \simeq 5\times(10)^n \text{ GeV/c}$$

where $P_L^{\text{eff.}}$ denotes the incident momentum. From this expression it is implied that the term of the n-th order belongs to contribute effectively to the total cross section.

When we want to consider the gross structure of production amplitude, Eqs.(8-2) are useful. Thus, we can consider that Eqs.(8-2) are the basic dynamical equations for production amplitudes.

The graphical representation of the iterative expansion of Eqs.(8-2) is given in Fig.28(a). Each term of this perturvative expansion is grouped into the four series, i.e., D_a-series, D_b-series, D_{ab}-series and D-D-series as discussed in appendix(B). The wavy lines in Fig.28 represent pomerons. If we square the amplitudes, integrate final states, we assume the ND cross section to be given by one leading Regge pole*), (and sum over the appropriate final states,) to be referred as an inelastic pomeron (α) . The inelastic pomeron

---

*) It is of course a nontrivial assumption that an absorptive part with the ND mechanism in the intermediate state is given approximately by Regge pole alone and that cuts are unimportant.[73]

is different with the pomeron ($\alpha_p \simeq 1$) (we call it the elastic pomeron), and is specified from Eq.(7-9-b) as follows;

$$s^{2\alpha_M - 2 + \tilde{g}^2_{MM}} \propto s^{\alpha - 1} \quad , \tag{8-3}$$

where α is the trajectory of the inelastic pomeron. Furthermore, from Eq.(7-10-b) we have

$$\alpha \simeq 1 - 2\varepsilon \quad . \tag{8-4}$$

Therefore, the intercept of this pole is lower than that of pomeron, $\alpha_p > \alpha$. Such a constraint follows because only a subset of the intermediate states which contribute to the total cross section and thus to the elastic pomeron (P), are allowed to contribute to be the <u>inelastic</u> pomeron (P_{in}).[74]

Applying the same procedure to the other processes shown in Fig.28(a) leads to Fig.28(b) in which each component of the absorptive part is expanded by the triple-Reggeon couplings $f_{PP\alpha}$—— pomeron-pomeron-inelastic pomeron coupling.

——————— Fig.28 ———————

In the zeroth approximation, we have the following equations;

$$\sigma_T \simeq \sigma_{el} + \sigma^{ND} \quad , \tag{8-5}$$

$$\mathrm{Im}\, P \simeq s\sigma_{el} + \mathrm{Im}\, P_{in} \quad , \tag{8-6}$$

where P and P_{in} denote pomeron amplitude and inelastic pomeron one, respectively.

Finally, if the adjacent pomeron coupling is admitted and thus $g^2_{PP} \neq 0$, we must modify Eq.(8-2-c) as follows;

$$\tilde{C}(s'') = g^2_{PP} \cdot g^{-2}_{PM} + \tilde{C}^0(s'') + \int d^4q_1 \delta^+(q^2_1 - m^2_1) g^2_{PP} D^2 \tilde{C}(s''') + \int d^4k \tilde{C}^0(s_5) g^2_{PM} D^2 \tilde{C}(s_6) \quad . \tag{8-7}$$

Then, we may obtain terms of adjacent multi-pomeron exchange. We will discuss

about this point in (3) of this section.

(2) The introduction of duality

Until now, we have considered the simplified model and not discussed the duality problem. In this subsection, we consider the model with duality.[75),76)]

We consider the structure of the Born term of Eqs.(8-2) by introducing the duality. Then, the ND term is divided into the $\bar{X}$- and $\bar{H}$-type component taking the urbaryon rearrengement diagram (URD) into account.[76),*)] The $\bar{X}$- and $\bar{H}$-components are corresponding to the non-resonant and resonant part, respectively. For example, we consider the lowest state of pomeron-pomeron scattering. We have two mechanisms, i.e., $\bar{H}$- and $\bar{X}$-type which are characterized by URD as in Fig.29.

Fig.29

Thus, we have

$$A^0_{ab}(s) = A^0_{ab}(\bar{X}) + A^0_{ab}(\bar{H}) \quad , \tag{8-8}$$

where $A^0_{ab}(\bar{X})$ and $A^0_{ab}(\bar{H})$ denote the contribution from the $\bar{X}$- and $\bar{H}$-type mechanism, respectively. Furtermore, from the duality constraint we have

$$A^0_{ab}(\bar{X}) \simeq \mathrm{Im}\, P_{in} \quad , \tag{8-9}$$

$$A^0_{ab}(\bar{H}) \simeq \mathrm{Im}\, R \quad , \tag{8-10}$$

where R denotes the Regge amplitude of the ordinary leading reggeon with $\alpha_R \simeq \frac{1}{2}$.

This two component structure of the ND mechanism introduces two pomeron couplings (g^2_{PX} and g^2_{PH}) and two triple-Reggeon couplings ($f_{PP\alpha}$ and f_{PPR}) as shown in Fig.30 to the perturbative expansion of production amplitudes and absorptive part, respectively.

---

*) For example, the $\bar{X}$-type URD is characterized by the connected diagrams in which neither pair of urbaryon lines in a and b annihilates and the $\bar{H}$-type URD by the connected diagrams in which at least one pair of urbaryons in a and b annihilates in the collision of the particle a and b as shown in Fig.29.

Also this leads to two sorts of fireball with large and small mass, respectively. It is mainly due to the difference of the intercept of each trajectories, i.e., $\alpha \simeq 1-2\varepsilon$ and $\alpha_R \simeq \frac{1}{2}$. Thus, we have the following relations;

(i) $\bar{X}$-type mechanism $\longleftrightarrow$ non-resonant part $\longleftrightarrow$ fireball with large mass,

(ii) $\bar{H}$-type mechanism $\longleftrightarrow$ resonant part $\longleftrightarrow$ fireball with small mass.

Also, it is noted that the other contributions which are characterized by the triple-Reggeon couplings $f_{RR\alpha}$ and f_{RRR} are included in the Born terms ($A^0_{ab}(\bar{X})$ and $A^0_{ab}(\bar{H})$).

Fig.30

(3) The possibility of non-vanishing g^2_{PP}

In this subsection, we discuss the possibility of non-vanishing g^2_{PP} . Let us begin with the assumption of the existence of such a particle that is stable for strong interaction and has the quantum numbers of P = + , C = + and I = 0 where P,C and I denote parity, charge conjugation parity and isospin, respectively. Then, the coupling g^2_{PP} is not kinematically forbidden. However, this coupling is dynamically forbidden by the Iizuka rule[77] that the creation of a urbaryon pair which becomes constituents of a single hadron is strongly suppressed. If such a particle exists and $g^2_{PP} \neq 0$, then the Iizuka rule is breakdown.

Recently, Niu et al.[78] found a new particle with long life-time in cosmic-ray experiment and Ogawa et al.[79] pointed out that this new particle may be composed of the p' urbaryon which was introduced in the modified Nagoya model[80]. It seems to be stable for strong interaction and decays by weak interaction or another new interaction. This particle may belong to the same multiplet as the new particle assumed here. Then, we have the following relation;

$$2\alpha_p - 2 + \tilde{g}^2_{PP} \approx 0 \quad . \tag{8-11}$$

From Eqs.(7-10-b), (7-10-c) and (8-11), we obtain the following solutions;

$$\alpha_p \approx 1-\delta \quad , \tag{8-12-a}$$

$$\tilde{g}^2_{MM} \approx 2(1-\alpha_M) - 2\varepsilon \quad , \tag{8-12-b}$$

$$\tilde{g}^2_{PM} \approx \varepsilon + \delta \quad , \tag{8-12-c}$$

$$\tilde{g}^2_{PP} \approx 2\delta \quad , \tag{8-12-d}$$

where $\delta < \varepsilon$. Here, we assumed only the asymptotic constancy of the total cross section. We obtain the result that in this case the intercept of pomeron is smaller than one. The solutions of Eqs.(8-12) is reduced to the solutions of Eqs.(7-11) when $\delta \to 0$.

It may be considered that the new particle is produced by the adjacent pomeron exchange, which seems to develop so as to give the considerable contribution to the total cross section at super high energies. Also, the production probability of this particle is proportional to the coupling g^2_{PP}, which seems to be very small. For example, we show this production mechanism in Fig.31.

Fig.31

§9 Conclusions and discussions

1. We have investigated the structure of reaction mechanism in hadronic multi-particle production reactions based on a simplified multi- Regge model and clarified that (1) the reaction mechanism in multi-particle production processes is composed of two different reaction mechanism, i.e., the non-diffractive(ND) and diffractive (D) one, and (2) the dominant reaction mechanism switches over from ND to D with increasing energy, and (3) this switch-over mechanism produces the perturbative picture of production amplitudes.

2. From the phenomenological analyses of exclusive reactions with several multiplicity and in the region $P_L \lesssim 100$ GeV/c, the existence of the band scheme has been pointed out. Namely, the domain of the reaction is divided into the following characteristic regions in the multiplicity-momentum plane:

Region(I): Non-diffractive mechanism dominates,

Region(II): Non-diffractive and diffractive mechanisms are comparable to each other,

Region(III): Diffractive mechanism dominates.

In the same region, the gross structure of reaction mechanism is same.

3. From the analysis of partial cross sections of $\pi^- p$ and pp reactons, it was clarified that the inner pomeron coupling g^2_{PM} is very small compared with the inner meson coupling g^2_{MM}, i.e., $g^2_{PM}/g^2_{MM} \simeq 0.01$*). The existence of this hierarchy specifies the structure of ${}^{ab}C_n^{\nu}$ and furthermore, produces a switch-over mechanism of the dominant reaction mechanism if we combine ${}^{ab}C_n^{\nu}$ with the structure of $R_n^{\nu}(s_i,t_i)$. Namely, the following two features have been clarified;

(i) The hierarchy among the inner couplings as follows;

$$g^2_{MM} >> g^2_{PM} >> g^2_{PP} \quad ,^{**)}$$

(ii) The switch-over mechanism of the dominant reaction mechanism in multi-particle production processes.

According to this hierarchy, we have considered the following three worlds;

(I) The world with $\tilde{g}^2_{MM} = 2$, $\tilde{g}^2_{PM} = 0$ and $\tilde{g}^2_{PP} = 0$,

(II) The world with $\tilde{g}^2_{MM} = 2\text{-}2\varepsilon$, $\tilde{g}^2_{PM} = \varepsilon$ and $\tilde{g}^2_{PP} = 0$,

(III) The world with $\tilde{g}^2_{MM} = 2\text{-}2\varepsilon$, $\tilde{g}^2_{PM} = \varepsilon + \delta$ and $\tilde{g}^2_{PP} = 2\delta$.

In (I), $\alpha \approx 1$ and $\alpha_P \approx 1$, in (II) $\alpha \approx 1\text{-}2\varepsilon$ and $\alpha_P \approx 1$ and in (III) $\alpha \approx 1\text{-}2\varepsilon$ and $\alpha_P \approx 1\text{-}\delta$. The realistic world develops from (I) to (III) with increasing energy. The order of the approximation in Eqs.(8-2) is dependent on the magnitude of the incident momentum. Also, we included the production of the multi-fireball and the new particle in the scheme in connection with the non-vanishing of g^2_{PM} and g^2_{PP}, respectively.

---

*) The ratio g^2_{PP}/g^2_{MM} is related to the one f_{PPP}/f_{RRP} where f_{PPP} and f_{RRP} denote the triple-pomeron coupling and the Reggeon-Reggeon-pomeron one, respectively. The recent analysis[81] is given as follows; $f_{PPP}/f_{RRP} \simeq 0.01$. This result is consistent with our estimation of g^2_{PM}/g^2_{MM}.

**) Here, the very smallness of g^2_{PP} is assumed and this assumption is believed to be reasonable.

4. In §8, we assumed the asymtotic constancy of the total cross section. This assumption is very important and specified the dynamics of hadron-hadron interaction.

In (II), we have

$$\sigma_T^{ab} \xrightarrow[s\to\infty]{} \sigma_{el}^{ab}\left[\frac{(1+\gamma_a)(1+\gamma_b)}{2}\right] , \tag{9-1}$$

where $\gamma_i \equiv G^2_{Mi}/G^2_{Pi}$ [26]. On the other hand, by the optical model[82] we have

$$\frac{\sigma_T^{ab}}{\sigma_{el}^{ab}} = \frac{2}{1-\eta} , \tag{9-2}$$

where $(1-\eta)$ is the opacity. From Eqs.(9-1) and (9-2), we obtain the following relation at asymptotic energies;

$$1-\eta = \frac{4}{(1+\gamma_a)(1+\gamma_b)} . \tag{9-3}$$

When we consider pp scattering, the equality of the external couplings G_{MN} and G_{PN} leads to the results of $\eta = 0$. Phenomenologically, we have $\eta > 0$ because $\gamma_i > 1$. These relations are very interesting since they seem to suggest the solution of the problem what specifies the magnitude of γ_i.

5. The model for pomeron discussed by Carlitz, Green and Zee[83], is equivalent to the model that the Born term is composed of only the $\bar{H}$-type mechanism and the higher order expansion is given by only the D_{ab}-series in our scheme discussed in §8. Also, the model discussed by Silverman, Ting and Yesian[84] is the one that the Born term is composed of only the $\bar{H}$-type mechanism and the higher order expansion is given by the D_a-series, D_b-series and D_{ab}-series. However, they limited the discussion to the first order approximation. The integral equation investigated in this paper includes these models. Thus, it is the basic and fundamental equation for the production amplitudes.

6. Recent NAL data[85] of the partial cross section of $pp \to pp\pi^+\pi^-$ seem to support the existence of the switch-over mechanism as shown in Fig.10(f). If the experiment

is performed in the more high energy region, the existence of the switch-over mechanism may be confirmed more certainly and the existence of the D-D mechanism will be clarified.

Also, the switch-over mechanism appears in the total cross section. Recently, it was discussed by Kagiyama[86] that the switch-over mechanism from ND to D is important in order to explain the increasing behaviour of the correlation parameter f_3^-. This result supports our scheme for reaction mechanism.

7. For both $\pi^- p$ and pp reactions, the relative weight of D to ND becomes large gradually as the multiplicity increases, as shown in Fig.10. This fact is also seen from Eqs.(7-7). For example, at fixed energies, ND decreases faster than D_a (or D_b) with multiplicity n because the factor 1/n! in ND decreases faster than the factor $1/2^n$ in D_a (or D_b) for large n. Therefore, for the large multiplicity-reactions, the ND mechanism may not be dominant even in the low energy and the D may be dominant. If it is right, a band scheme discussed in the reaction with several multiplicity, is broken down. It is very interesting how this property influences to the physical quantity. This problem shall be investigated elsewhere.

Appendices

(A) Partial cross section by a simle multi-Regge model in the Chew-Pignotti's approximation

We discuss the partial cross sections of each reaction mechanism (ND, D_a, D_b, D_{ab}, D-D, $\cdots$) based on a simple multi-Regge model by assuming the multiperipheral amplitude of the Chew-Pignotti type[26]. We consider the reaction $a + b \to a + b + n\pi$. Exchanged objects are pomeron ($\alpha_P = 1$) and effective meson Reggeon ($\alpha_M = 0$) as discussed in the text.

First, let us consider the ND mechanism. Then, all of the exchanged objects in the multi-peripheral chain are effective meson Reggeons and therefore the partial cross section (σ_n^{ND}) of ND is given as follows in the Chew-Pignotti approximation;

$$\sigma_n^{ND} = \tilde{f}^2_{Ma\bar{a}}\ \tilde{f}^2_{Mb\bar{b}}\ [\tilde{g}^2_{MM}]^n \int \exp\{2(\alpha_M \sum_{i=1}^{n+1} x_i - X_0)\} \prod_{i=1}^{n+1} dx_i \delta(\sum_{i=1}^{n+1} x_i - X_0) \quad , \tag{A-1}$$

where $\tilde{f}^2_i$ and $\tilde{g}^2_j$ are the outer and inner couplings, respectively, which contain the t_i-cut effect as seen in Eq.(6-16) ,and $x_i = \ln(s_i / s_0)$ and $X_0 = \ln(s / s_0)$.
Using the equation

$$\int_0^\infty dx_1 dx_2 \cdots dx_n\ \delta(\sum_{i=1}^{n} x_i - X_0) = \frac{X_0^{n-1}}{(n-1)!} \quad , \tag{A-2}$$

we can get the following result;

$$\sigma_n^{ND} = \tilde{f}^2_{Ma\bar{a}}\ \tilde{f}^2_{Mb\bar{b}}\ [\tilde{g}^2_{MM}]^n \frac{X_0^n}{n!}\ e^{2(\alpha_M - 2)\cdot X_0} \quad , \tag{A-3}$$

which gives the Poisson distribution with respect to multiplicity n. And $\alpha_M = 0$ leads to

$$\sigma_n^{ND} = \tilde{f}^2_{Ma\bar{a}}\ \tilde{f}^2_{Mb\bar{b}}\ [\ \tilde{g}^2_{MM}\ ]^n \frac{(\ln s)^n}{n!}\ s^{-2} \quad , \tag{A-4}$$

which is Eq.(7-7-a).

In the D_a mechanism, one pomeron couples to particle b and thus,

$$\sigma_n^{D_a} = \tilde{f}^2_{Ma\bar{a}}\ \tilde{f}^2_{Pb\bar{b}}\ [\tilde{g}^2_{MM}]^{n-1}\ \tilde{g}^2_{PM} \int \exp\{2\alpha_M \sum_{i=1}^{n} x_i + 2\alpha_P x_{n+1} - X_0\}$$
$$\times \prod_{i=1}^{n+1} dx_i\ \delta(\sum_{i=1}^{n+1} x_i - X_0) \quad . \tag{A-5}$$

This equation becomes easily as

$$\sigma_n^{D_a} = \tilde{f}^2_{Ma\bar{a}}\ \tilde{f}^2_{Pb\bar{b}}\ [\tilde{g}^2_{MM}]^{n-1}\ \tilde{g}^2_{PM}\ e^{(2\alpha_M - 2)X_0} \int_0^{X_0} dz\ \frac{(X_0 - z)^{n-1}}{(n-1)!}\ e^{-2(\alpha_M - \alpha_P)z}$$
$$= \tilde{f}^2_{Ma\bar{a}}\ \tilde{f}^2_{Pb\bar{b}}\ [\tilde{g}^2_{MM}]^{n-1}\ \tilde{g}^2_{PM} \frac{(\ln s)^n}{n!}\ s^{(2\alpha_M - 2)}\ {}_1F_1(1,\ n+1;\ -2(\alpha_M - \alpha_P)\ln s), \tag{A-6}$$

where ${}_1F_1(\alpha, \gamma\ ;\ z)$ is the confluent hypergeometric function.
Using the following approximation for very large $|z|$;

$$F(\alpha,\ \gamma;\ z)\sim\frac{\Gamma(\gamma)}{\Gamma(\gamma-\alpha)}\ (-z)^{-\alpha}\ \sum_{n=0}^{\infty}\ (-1)^n\ \frac{(\alpha)_n(\alpha-\gamma+1)_n}{n!\ z^n}$$

$$+\frac{\Gamma(\gamma)}{\Gamma(\gamma)}\ e^z z^{\alpha-\gamma}\ \sum_{n=0}^{\infty}\ \frac{(1-\alpha)_n(\gamma-\alpha)_n}{n!\ z^n}\quad , \qquad \text{(A-7)}$$

$$\sim\frac{\Gamma(\gamma)}{\Gamma(\gamma-\alpha)}(-z)^{-\alpha}+\frac{\Gamma(\gamma)}{\Gamma(\alpha)}\ e^z z^{\alpha-\gamma}\quad , \qquad \text{(A-8)}$$

we obtain the following partial cross section for the D_a mechanism;

$$\sigma_n^{D_a}=\tilde{f}^2_{Ma\bar{a}}\ \tilde{f}^2_{Pb\bar{b}}\ [\tilde{g}^2_{MM}]^{n-1}\ \tilde{g}^2_{PM}\ [\frac{1}{2^n}-\frac{1}{2\cdot(n-1)!}\cdot\frac{(\ln s)^{n-1}}{s^2}\ ]\ , \qquad \text{(A-9)}$$

where $\alpha_M=0$ and $\alpha_P=1$ are taken into account in this equation.

This is Eq.(7-7-b). Similarly $\sigma_n^{D_b}$ and $\sigma_n^{D_{ab}}$ can be calculated and become Eqs. (7-7-c) and (7-7-d).

Futhermore, the partial cross section of D-D is as follows;

$$\sigma_n^{D\text{-}D}=\tilde{f}^2_{Pa\bar{a}}\ \tilde{f}^2_{Pb\bar{b}}\ [\tilde{g}^2_{MM}]^{n-2}\ [\tilde{g}^2_{PM}]^2\int\exp\ \{\ 2\alpha_M\sum_{i=2}^{n}x_i+2\alpha_P(x_1+x_{n+1})-X_0\}$$

$$\times\ \prod_{i=1}^{n+1}\ dx_i\ \delta\ (\sum_{i=1}^{n+1}\ x_i-X_0)$$

$$=\tilde{f}^2_{Pa\bar{a}}\ \tilde{f}^2_{Pb\bar{b}}\ [\tilde{g}^2_{MM}]^{n-2}\ [\tilde{g}^2_{PM}]^2\ e^{(2\alpha_M-2)X_0}\int_0^{X_0}\int_0^{X_0-x}\ dxdy$$

$$\times\ e^{-2(\alpha_M-\alpha_P)(x+y)}\ \frac{(X_0-x-y)^{n-2}}{(n-2)!}\quad . \qquad \text{(A-10)}$$

Following transformation of variables,

$$x+y=t,\quad xy=s\quad ,$$

leads to

$$\sigma_n^{D\text{-}D}=\tilde{f}^2_{Pa\bar{a}}\ \tilde{f}^2_{Pb\bar{b}}[\tilde{g}^2_{MM}]^{n-2}\ [\tilde{g}^2_{PM}]^2\ \frac{(\ln s)^n}{2n!}\ s^{(2\alpha_M-2)}\cdot{}_1F_1(2,n+1;-2(\alpha_M-\alpha_P)\ln s)\ .$$

(A-11)

Using the above approximation for the confluent hypergeometric function ${}_1F_1(2,n+1;-2(\alpha_M-\alpha_P)\ln s)$, we can obtain similarly

$$\sigma_n^{D-D} = \tilde{f}^2_{Pa\bar{a}} \tilde{f}^2_{Pb\bar{b}} [\tilde{g}^2_{MM}]^{n-2} [\tilde{g}^2_{PM}] [\frac{\ln s}{2^n} + \frac{1}{8\cdot(n-2)!} \cdot \frac{(\ln s)^{n-2}}{s^2}], \quad (A\text{-}12)$$

which is Eq.(7-7-e).

(B) The perturbative expansion of the S-matrix

We discuss the perturbative expansion of the S-matrix in the formal theory of scattering. Unitarity is $SS^+=S^+S=1$. As usual we define the T-matrix by $S=1+iT$. Then we get unitarity for T is the form:

$$i(T^+ - T) = TT^+ \quad . \quad (B\text{-}1)$$

We define the Lorentz invariant and δ-function free scattering amplitudes as follows;

$$\langle k' |T| k\rangle = (2\pi)^4 \delta^4(k-k') \langle k' |F| k\rangle \quad . \quad (B\text{-}2)$$

Unitarity for F is easily found to read:

$$i \langle k |F^+-F| k\rangle = (2\pi)^4 \sum_n \langle k |F^+| n\rangle \langle n |F| k\rangle \delta^4 (k-k_n) \quad , \quad (B\text{-}3)$$

where the sum over n denotes the sum over intermediate states and the integration over allowed phase-space.

Symbolically, from the integral equation of Eqs.(8-2) in §8, F is given as follows:

$$\begin{aligned} F &= F^0_{ab} + (aD + \tilde{F}^0_b D)\, \tilde{F}_b \quad , \\ \tilde{F}_b &= b + \tilde{F}^0_b + \tilde{C}\,(Db + D\tilde{F}^0_b), \\ \tilde{C} &= \tilde{C}^0 + \tilde{C}^0 D \tilde{C} \quad , \end{aligned} \quad (B\text{-}4)$$

where F, $\tilde{F}_b$ and $\tilde{C}$ corresponds to particle a-particle b, pomeron-particle b and pomeron-pomeron reaction amplitude, respectively. F^0_{ab}, $\tilde{F}^0_b$ and $\tilde{C}^0$ are the Born term of each reaction amplitude. D is pomeron propagator and a and b are couplings of particle a and b to pomeron, respectively.

From the last equation of Eq.(B-4), we have $\tilde{C}=\frac{\tilde{C}^0}{1-\tilde{C}^0 D}$.

Therefore we obtain

$$F = F^0_{ab} + (aD + \tilde{F}^0_a D)\ [b + \tilde{F}^0_b + \frac{\tilde{C}^0}{1-\tilde{C}^0 D}(Db + D\tilde{F}^0_b)]$$

$$= F^0_{ab} + aDb + aD\frac{\tilde{C}^0}{1-\tilde{C}^0 D}Db + aD(1 + \frac{\tilde{C}^0}{1-\tilde{C}^0 D}D)\ \tilde{F}^0_b$$

$$+ \tilde{F}^0_a D(1 + \frac{\tilde{C}^0}{1-\tilde{C}^0 D}D)b + F^0_a D(1 + \frac{\tilde{C}^0}{1-\tilde{C}^0 D}D)\ \tilde{F}^0_b \quad . \qquad \text{(B-5)}$$

This gives us the perturbative expansion of the S-matrix. The third-, forth-, fifth- and sixth-term correspond to the D-D-, D_b-, D_a- and D_{ab}-series because the factor

$\frac{1}{1-\tilde{C}^0 D}$ is expanded as follows;

$$\frac{1}{1-\tilde{C}^0 D} = 1 + \tilde{C}^0 D + \tilde{C}^0 D\tilde{C}^0 D + \cdots \quad . \qquad \text{(B-6)}$$

Also, in the case of the model with duality, the structure of the Born term is given in the forms;

$$F^0_{ab} = \bar{X}^0 + \bar{H}^0,\ \tilde{F}^0_i = \tilde{X}^0_i + \tilde{H}^0_i,\ \tilde{C}^0 = \tilde{\bar{X}}^0_i + \tilde{\bar{H}}^0_i \quad , \qquad \text{(B-7)}$$

where the first and second terms in the right hand side of Eq.(B-7) denote the non-resonant and resonant interaction in the ND mechanism.

Acknowledgement

The auther is most grateful to Professor S. Takagi and members of Department of Applied Mathematics, Faculty of Engineering Science, Osaka University, and Professor M. Kawaguchi of National Laboratory of High Energy Physics, Tsukuba, for many lively discussion and kind hospitalty. He would like to thank Professor K. Kobayakawa of College of Liberal Arts, Kobe University, for useful discussion and continuous encouragement.

Also, he thanks members of the research group "Multi-Particle Production" organized by Research Institute for Fundamental Physics, Kyoto University, in 1972 and 1973, for helpful discussion. Above all, he wishes to express his gratitude to Dr. H. Noda of Department of Physics, Ibaraki University, for valuable discussion in the course of this work.

Furthermore, he thanks Professor S. Takagi for carefully reading through the manuscript.

The numerical calculations were carried out with FACOM 230-60 at Computer Center, Kyoto University.

Finally, he thanks Miss S. Nagai for typing the manuscript.

Table 1

Values for A and B in the expression $P_n^{max} = An^B$ for πp, Kp and pp reactions, respectively.

Initial Particles	A(GeV/c)		B	
	Theor.	Exp.*)	Theor.	Exp.*)
πp	0.030	0.067 ± 0.025	2.9	2.5 ± 0.2
Kp	0.065	0.11 ± 0.08	2.9	2.4 ± 0.5
pp	0.095	0.13 ± 0.05	2.9	2.6 ± 0.2

*) Experimental values are taken from Ref.18).

Table 2

Summary of coupling constants

effective coupling	t_i-cut coupling	Chew-Pignotti's coupling
$g^2_{MM} \simeq 10$	$\tilde{g}^2_{MM} \simeq 2.5$	$g^2_M \simeq 1$
$g^2_{PM} \simeq 0.13$	$\tilde{g}^2_{PM} \simeq 0.008$	$g^2_P \simeq 0.02$
$f^2_{PN\bar{N}} \simeq 107.8$	$\tilde{f}^2_{PN\bar{N}} \simeq 6.7$	$\tilde{f}^2_{PN\bar{N}} \simeq 5.1$*)
$f^2_{MN\bar{N}} \simeq 9.8$	$\tilde{f}^2_{MN\bar{N}} \simeq 2.5$	$\tilde{f}^2_{MN\bar{N}} \simeq 8.8$*)
$f^2_{P\pi\pi} \simeq 32.6$	$\tilde{f}^2_{P\pi\pi} \simeq 2.0$	
$f^2_{M\pi\pi} \simeq 1.63$	$\tilde{f}^2_{M\pi\pi} \simeq 0.41$	

*) This coupling is estimated by us using Chew-Pignotti model[26].

References

1) W. Heizenberg, Z. Phys. 101 (1936), 533.

2) For example, see Z. Koba and S. Takagi, Fortschritte der Physik 7 (1959), 1;
Z. Koba, Fortshritte der Physik 11 (1963), 118;
T. Kobayashi and M. Namiki, Suppl. of Theor. Phys. 33 (1965), 1.

3) For example, see V. D. Barger and D.B.Cline, Phenomenological Theories of High Energy Scattering (W.A.Benjamin, Inc., New York, 1969).

4) For example, see E.J.Squires, Complex Angular Momenta and Particle Physics (W.A.Benjamin, Inc., New York, 1963).

5) K.A.Ter-Martirosyan, Sov. Phys. JETP, 17 (1963), 223.

6) T.W.B.Kibble, Phys.Rev. 131 (1963), 2282.

7) Chan Hong- Mo, K.Kajantie and G.Ranft, Nuovo Cim. 49A (1967), 159;
Chan Hong-Mo, K.Kajantie, G.Ranft, W.Beusch and E.Flaminio, Nuovo Cim. 51A (1967), 696;
Chan Hong- Mo, J.Łoskiewicz and W.W.M.Allison, Nuovo Cim. 57A (1968), 93.

8) N.F.Bali, G.F.Chew and A.Pignotti, Phys. Rev. Letters 19 (1967), 614;
G.F.Chew and A.Pignotti, Phys. Rev. 176 (1968), 2112.

9) F.Zachariazen and G.Zweig, Phys.Rev. 160 (1967), 1322,1326.

10) J.Finkelstein and K.Kajantie, Nuovo Cim. 56 (1968), 659.

11) D.Amati, S.Fubini, A.Stanghellini and M.Tonin, Nuovo Cim. 22 (1961), 569;
D.Amati, S.Fubini and A.Stanghellini, Nuovo Cim. 26 (1962), 896;
L.Bertocchi, S.Fubini, and M.Tonin, Nuovo Cim. 25 (1962), 626.

12) F.Salzman and G.Salzman, Phys. Rev. Letters 5 (1960), 377; Phys. Rev. 121 (1961), 1541 ; 125 (1962), 1703.

13) I. M. Dremin, JETP 41 (1961), 821;
I. M. Dremin and D. S. Chernavsky, JETP 43 (1962), 551.

14) Z.Koba and A.Krzywicki, Nucl. Phys. 46 (1963), 471, 485.

Also, afterwards, it has been pointed out that the ABFST model does not saturate the total cross sections of NN and πN reactions and the cross section of the annihilation channel of $\bar{N}\bar{N}$ reaction. See, D.M.Tow, Phys. Rev. D2 (1970), 154; O.Miyamura, T.Morii, S.Sato and I.Yotsuyanagi, Soryusiron Kenkyu, 44 (1972),433.

15) L.Van Hove, Proceedings of the 13th International Coference on High-Energy Physics, Berkeley, 1966;
B.Belletini, Proceedings of the 14th International Conference on High-Energy Physics, Vienna, 1968;
J.D.Jackson, Proceedings of the Lund International Conference of Elementary Particles, Lund, 1969.

16) D.R.O.Morrison, Phys. Rev. 165 (1968), 1966.

17) T.Morii, Soryusiron Kenkyu 45 (1972), C29.

18) J.D.Hansen, W.Kittel and D.R.O.Morrison, Nucl.Phys. B25 (1971), 605.

19) L.Van Hore, Phys. Letters 28B (1969), 429; Nucl. Phys. B9 (1969), 331.

20) L.Van Hove, Phys. Reports 1C (1971), 347;
W.Kittel, Proceedings of the 1972 CERN School of Physics, CERN 72-17, (1972), P.227.

21) M.Namiki, I.Ohba and Yap Sue-Pin, Prog. Theor. Phys. 47 (1972), 1247.

22) G.Cocconi, Phys. Rev. 111 (1958), 1966;
K.Niu, Nuovo Cim. 10 (1958), 994;
P.Ciok, T.Coghen, J.Gierula, R. Holynski, A.Jurak, M.Miesowicz, T.Saniewska, O.Stanisz and J.Pernegr, Nuovo Cim. 10 (1958), 741.
Also, recent development is seen in R.Hagedron and J.Ranft, Suppl. Nuovo Cim. 6 (1968), 169.

23) S.Takagi, Prog. Theor. Phys. 7 (1952), 123.

24) E.Fermi, Prog. Theor. Phys. 5 (1950), 570; Phys. Rev. 81 (1951), 683.

25) T.Morii, Prog. Theor. Phys. 43 (1970), 731; Soryusiron Kenkyu 44 (1971), 131.

26) G.F.Chew and A.Pignotti, Phys. Rev. 176 (1968), 2112.

27) R.Dolen, D.Horn and C.Schmid, Phys. Rev. 166 (1968), 1768;
G.F.Chew and A.Pignotti, Phys. Rev. Letters 20 (1968), 1078.

28) L.Caneschi and A.Pignotti, Phys. Rev. 180 (1969), 1525; 184 (1969), 1915.
I.G.Halliday and L.M.Saunders, Nuovo Cim. 60 (1969), 494.

29) G.F.Chew, T.Rogers and D.R. Snider, Phys. Rev. D2 (1970), 765;
G.F.Chew, D. R. Snider, Phys. Rev. D1 (1970), 3453.

30) L.Caneschi and A.Pignotti, Phys. Rev. Letters 22 (1969), 1219.

31) R.P.Feynman, Phys. Rev. Letters 23 (1969), 1415.

32) J.Benecke, T.T.Chou, C.N.Yang and E. Yen, Phys. Rev. 188 (1969), 2159.

33) J.Kogut and L.Susskind, Physics Reports 8C (1973), 75.

34) A.H.Mueller, Phys. Rev. D2 (1970), 2963.

35) M.Toller, Nuove Cim. 37 (1965), 631.

36) G.Charlton et al., Phys. Rev. Letters 29 (1972), 515;
E.L.Berger, B.Y.Oh and G.A.Smith, Phys. Rev. Letters 29 (1972), 675;
E.L.Berger, Phys. Rev. Letters 29 (1972), 887.

37) For example, see M.Jacob, XVI International Coference of High Energy Physics, Chicago- Batavia, 1972.

38) R.C.Hwa, Phys. Rev. Letters 26 (1971);
R.C.Hwa and C.S.Lam, Phys. Rev. Letters, 27 (1971), 1098.

39) M.Jacob and R.Slansky, Phys. Letters 37B (1971), 408; Phys. Rev. D5 (1972), 1874.

40) K.Gottfried and O.Kofoed-Hansen, Phys. Letters 41B (1972), 195.

41) C.Quigg, Berkeley Meeting of the Division of Particles and Fields, A.P.S. (1973).

42) For example, see C.Quigg, "Two-component Models for Particle Production", Stony Brook preprint ITP-SB-73-42 (1973).

43) K.G.Wilson, Cornell preprint CLNS-131 (1970).

44) T.Morii and H.Noda, Prog. Theor. Phys. 49 (1973), 2141, 2143;
S.Kagiyama, Prog. Theor. Phys. 49 (1973), 2031;
H.Harari and E.Rabinovici, Phys. Letters 43B (1973), 49;
K.Fialkowski and H.T.Miettinen, Phys. Letters 43B (1973), 61;
A.Kobayashi, T.Matsuoka, K.Ninomiya and S.Sawada, Prog. Theor. Phys. 45 (1971), 403;
H.Noda and K.Kinoshita, Prog. Theor. Phys. 48 (1972), 877.

45) M.Bishari, G.F.Chew and J.Koplik, LBL preprint LBL-2129;
M.Bishari and J.Koplik, Phys. Letters 44B (1973), 179;
W.R.Frazer, D.R.Snider and C-I. Tan, preprint UCSD-10P10-127;
D.Amati, L.Caneschi and M.Ciafaloni, Nucl. Phys. B62 (1973), 173.

46) T.Morii and H.Noda, Prog. Theor. Phys. 51 (1974), NO.2.

47) T.Morii and H.Noda, Prog. Theor. Phys. 51 (1974), NO.3.

48) T.Morii, Kobe preprint (Kobe University) NULA-HP-73-3 (unpublished);
H.Noda, Invited talk at Summer School, National Laboratory of High Energy Physics, Tsukuba, 1973.

49) T.Morii and H.Noda, Kobe preprint (Kobe University) KULA-HP-74-4.

50) T.Morii and H.Noda, Kobe preprint (Kobe University) KULA-HP-74-5.

51) Chang Hong-Mo, K.Kajantie and G.Ranft, loc. cit. in Ref. 7).

52) For example, see E.L.Berger, Phys. Rev. 179 (1969), 1567.

53) R.Honecker et al., Nucl. Phys. B13 (1969), 571;
High-Energy Reactions Analysis Group, "Compilation of Cross Sections I-π^- and π^+ Induced Reactions", CERN/HERA 72-1, May 1972;

54) T.Hofmokl and A.Wroblewski, Phys.Letters 31B (1970), 391.

55) T.Morii and H.Noda, Prog. Theor. Phys. 50 (1973), 626.

56) M.S.Chen, L.L.Wang and T.F.Wong, Phys. Rev. D5 (1972), 1667;
Chang Hong-Mo, H.I.Miettinen and R.G.Robert, Nucl. Phys. B54 (1973), 411;
I.Ohba and T.Tamama, Prog. Theor. Phys. 48 (1972), 2301;
H.Nowak and H.J.Schreiber, Lettre AL Nuovo Cim. 8 (1973), 21.

57) L.Foa, Rapporteur's talk at the Second Aix-en-Prorence International Conference on Elementary Particles, Aix-en-Provence, Sept. 1973.

58) Particle Data Group, "$\bar{N}N$ and $\bar{N}D$ Interactions [Above 0.5 GeV/c]-A Compilation", UCLA-20000 $\bar{N}N$, August 1970.

59) M.Uehara, Prog. Theor. Phys. 49 (1973), 227.

60) C.Quigg and J.D.Jackson, NAL report NAL-THY-93 (October, 1972).

61) D.R.O.Morrison, Rapporteur's talk at the XV th International Conference on High Energy Physics, Kiev, 1970.
D.R.O.Morrison, CERN Report NO. CERN/D. Ph. II/PHYS 71-10 (unpublished);
W.Kittel, Proceedings of the Colloquium on Multi-particle Dynamics, University of Helsinki, 1971.

62) M.Deutschmann et al., Nucl. Phys. B50 (1972), 61;
W.Burdett et al., Nucl. Phys. B48 (1972), 13.

63) N.K.Yamdagni and M.Gavrilas, "Longitudinal Phase Space Analysis of the Reaction $pp \to pp\pi^+\pi^-$ between 4 and 25 GeV/c", paper presented at the Amsterdam International Conference on Elementary Particles (1971).

64) J.V.Beaupre et al., CERN preprint CERN/D.Ph.II/PHYS 72-1 (1972).

65) G.S.Abrams, et al., LBL preprint, LBL-2112;
F.C.Winkelmann, et al., LBL preprint, LBL-2113;
D.W.G.S.Leith, SLAC preprint SLAC-PUB-1330.

66) Y.Hama, Phys. Rev. D6 (1972), 3306.

67) F.Zachariazen, Physics Reports 2C (1971), 1.

68) G.R.Charlton and G.H.Thomas, Phys. Letters 40B (1972), 378.

69) A. Giovannini, Nuovo Cim. 10A (1972), 713.

70) G.F.Chew, Phys. Rev. D7 (1973), 934.

71) V.N.Akimov, D.S.Chernavskii, I.M.Dremin and I.I.Royzen, Nucl. Phys. B14 (1969),285.

72) G.F.Chew, M.L.Goldberger and F.E. Low, Phys. Rev. Letters, 22 (1969), 208.

73) H.D.I.Abarbanel, Phys. Rev. D6 (1972), 2788.

74) J.Koplik, Phys. Rev. D7 (1973), 558.

75) H.Lee, Phys. Rev. Letters 30 (1973), 719;
G.Veneziano, Phys. Letters 43B (1973), 413.

76) H.Noda and K.Kinoshita, Prog. Theor. Phys. 48 (1972), 877.

77) J.Iizuka, K.Okada and O.Shito, Prog. Theor. Phys. 35 (1966), 1061.

78) K.Niu, E.Mikumo and Y.Maeda, Prog. Theor. Phys. 46 (1971), 1644.

79) T.Hayashi, E.Kawai, M.Matsuda, S.Ogawa and S.Shige-eda, Prog. Theor. Phys. 47 (1972), 280.

80) Z.Maki, M.Nakagawa and S.Sakata, Prog. Theor. Phys. 28 (1962), 870.

81) T.Kawabe, private communication.
K.Abe et al., Phys. Rev. Letters 31 (1973), 1530.

82) M.Bando et al. Suppl. Prog. Theor. Phys. 41 & 42 (1967), 347.

83) R.Carlitz, M.B.Green and A.Zee, Phys. Rev. D4 (1971), 3439.

84) D.Silverman, P.D.Ting and H.J.Yesian, Phys. Letters 35B (1971), 427.

85) M.Derrick et al., ANL preprint ANL/HEP 7534 (1973).

86) S.Kagiyama, Fukuoka preprint (Fukuoka University) FUKUOKA-EP-73-3.

87) E.Byckling and K.Kajantie, Nucl. Phys. B9 (1969), 568;
E.Byckling et al., Journal of Computational Physics 4 (1969), 521.

Figure Captions

Fig. 1 Multi-peripheral diagram corresponding to the first term of Eq.(2-2).

Fig. 2 The energy dependence of n-paeticle production cross sections.

Fig. 3 The multiplicity dependence of the value $\bar{n}$ in Eq.(2-7).

Fig. 4 The multiplicity dependence of the momentum giving the maximum point of the partial cross section.

Fig. 5 The energy dependence of the cross section for the reaction $\pi p \to 3\pi p$.

Fig. 6 The role which the non-diffractive mechanism (N.D.M.) and the diffractive one (D.M.) play in the cross section of $\pi^- p \to \pi^-\pi^+\pi^- p$. Experimental data are taken from Ref.53).

Fig. 7 The illustration of the dominant region of each mechanism (the non-diffractive and diffractive one) on the multiplicity-energy plain.

Fig. 8 Multi-peripheral diagrams which characterize the ND and D mechanism. The wavy and dashed lines represent pomeron and meson exchange, respectively.

Fig. 9 The energy dependence of $\bar{\sigma}_n^{\nu}$. (a) $\pi^- p \to \pi^-\pi^0 p$, (b) $\pi^- p \to \pi^-\pi^+\pi^- p$, (c) $pp \to pp\pi^0$ and (d) $pp \to pp\pi^+\pi^-$.

Fig.10 The partial cross sections of $\pi^- p$ and pp collision. (a) $\pi^- p \to \pi^-\pi^0 p$, (b) $\pi^- p \to \pi^-\pi^+\pi^- p$, (c) $\pi^- p \to \pi^+\pi^-\pi^+\pi^0 p$, (d) $\pi^- p \to \pi^+\pi^-\pi^+\pi^-\pi^+ p$, (e) $pp \to pp\pi^0$ and (f) $pp \to pp\pi^+\pi^-$.
The solid lines represent the contribution from each mechanism and the dashed lines represent the total sum of these contribution in each reaction. The experimental data are taken from Ref.53) and Ref.58). Also, recent NAL data at 205 GeV/c which is taken from Ref.85) are shown in (f).

Fig.11 (a) The partial cross sections of the ND mechanism and σ_T^{ND} which are shown in the solid lines and the dott-dashed line, respectively.
(b) The partial cross sections of the D mechanism and σ_T^{D}.
The solid lines represent σ_n^{DN}, the dashed lines $\sigma_n^{D\pi}$ and the dott-dashed line σ_T^{D}.

Fig.12 The contribution of the D mechanism in σ_n for varying multiplicity. The shaded regions come from the D mechanism.

Fig.13 The invariant mass distributions of $\pi^- p \to \pi^-_f (m\pi+N)^+$ at P_L= 16 GeV/c for m=1,2,3 and 4. The experimental data are taken from Ref.61) and are shown in the dotted lines. The solid lines represent the results calculated in our model by Monte Carlo method, and show the total sum of the contributions from all mechanisms, ND and D.

Fig.14 The typical examples for the energy dependence of the invariant mass distribution of each mechanism. (A) The ND mechanism in $\pi^- p \to \pi^-_f (\pi N)^+$, (B) The D_N mechanism in $\pi^- p \to \pi^-_f (\pi N)^+$ and (C) The D_π mechanism in $\pi^- p \to \pi^-_f (4\pi N)^+$. In all cases, the unit of the ordinate-axis is arbitrary.

Fig.15 The experimental data of $\sigma_n^{(n_+,n_-)}$. (a) $\pi^- p \to \pi^-\pi^+\pi^-\pi^+\pi^- p$ and (b) $pp \to pp\pi^+\pi^-$, $pp \to pp\pi^+\pi^-\pi^+\pi^-$.

Fig.16 The results from the model calculation by our model for $\sigma_n^{(n_+,n_-)}$ of $\pi^- p \to \pi^-\pi^+\pi^- p$ at 16 GeV/c and 64 GeV/c.

These results contain the relative weight of Eq.(4-3-a) among each mechanism.

Fig.17 The model calculation for $\frac{d\sigma_4}{dx_i}$ of $\pi^- p \to \pi^-_f \pi^+_3 \pi^-_2 p$ at 27 GeV/c from each mechanism. (a) ND, (b) D_π and (c) D_N .

Fig.18 The model calculation for $\frac{d^2\sigma_4}{dx_2 dx_3}$ of $\pi^- p \to \pi^-_f \pi^+_3 \pi^-_2 p$ at 16 GeV/c and 64 GeV/c from each mechanism, (a) ND, (b) D_π and (c) D_N. (d) The total sum of each contribution. The results contain the relative weight of Eq.(4-3-a).

Fig.19 The momentum dependence of $\frac{d^2\sigma_n}{dx_2 dx_3}$ predicted from our model in each division ($|x_2| = |x_3| = 0.05$) for $\pi^- p \to \pi^-_f \pi^+_3 \pi^-_2 p$.

Fig.20 Weighted cross sections for $pp \to pp\pi^+\pi^-$ in the indicated LPS regions as functions of the incident laboratory momentum.

Fig.21 Exponent N in $\frac{d^2\sigma_4}{dx_2 dx_3} \propto P_L^{-N}$ for the dependence of two particle distribution on the incident momentum between 16 GeV/c and 64 GeV/c, in the scale given in the upper left.

Fig.22 The illustration of the band scheme on the multiplicity-momentum plane.

Fig.23 The invariant mass distrbution of $\pi^- p \to \pi^- {}_f(2\pi N)^+$ at P_L= 16 GeV/c and 64 GeV/c in our model. The contributions from each mechanism at P_L= 16 GeV/c and 64 GeV/c are shown in the solid lines and the dotted lines, respectively.

Fig.24 Effective coupling constants. Outer couplings are (a) $f_{PN\bar{N}}$, (b) $f_{MN\bar{N}}$, (c) $f_{P\pi\pi}$ and (d) $f_{M\pi\pi}$, and inner couplings are (e) g_{MM}, (f) g_{PM} and (g) g_{PP}. The adjacent pomeron coupling g_{PP} is forbidden dynamically by the conservation of G-parity.

Fig.25 The switch-over mechanism in the reaction $pp \to pp\pi^+\pi^-$. The solid lines represent the contribution from each mechanism and the dashed line represents the total sum of these contributions.

Fig.26 The illustration of the switch-over mechanism of (a) the n-particle production cross section and (b) the inelastic cross section.

Fig.27 A graphical representation of Eqs.(8-2).

Fig.28 A graphical representation of the iterative expantion of (a) production amplitudes and (b) an absorptive part.

Fig.29 The illustration of the lowest state of pomeron-pomeron scattering in terms of URD. (a) $\bar{H}$-type mechanism and (b) $\bar{X}$-type mechanism.

Fig.30 The illustration of the structure of the Born terms A^0_{ab}, $\tilde{B}^0_b$ and $\tilde{C}^0$ in terms of URD. They are characterized by the two component structure of the ND mechanism, i.e., $\bar{H}$- and $\bar{X}$- mechanism.

Fig.31 The production mechanism of the new particle by the adjacent pomeron exchange.

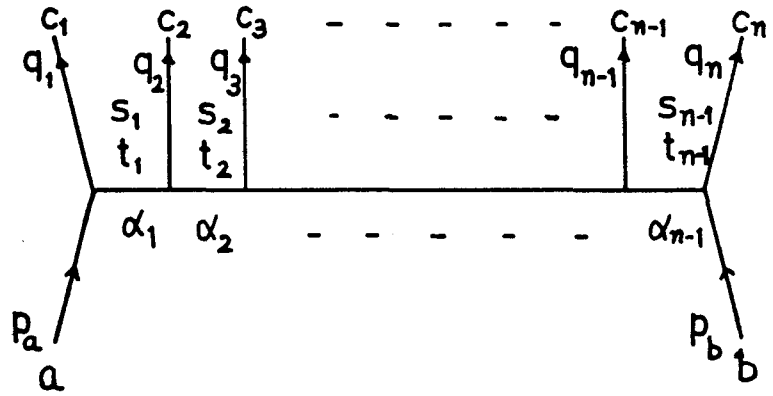

Fig. 1

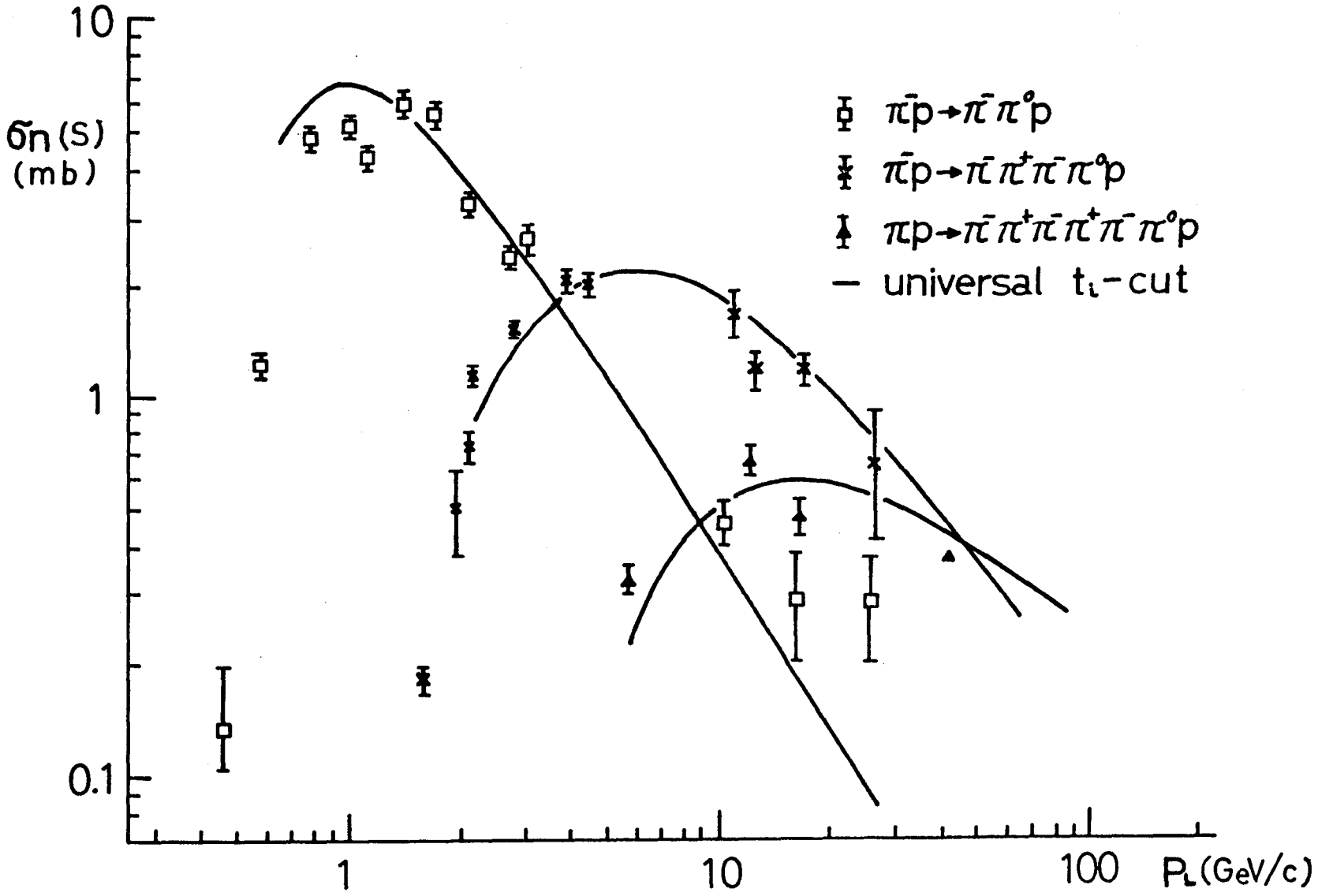
10
1
0.1
σn(S)
(mb)
1
10
100
PL(GeV/c)
π⁻p→π⁻π°p
π⁻p→π⁻π⁺π⁻π°p
πp→π⁻π⁺π⁻π⁺π⁻π°p
— universal tL-cut

Fig. 2

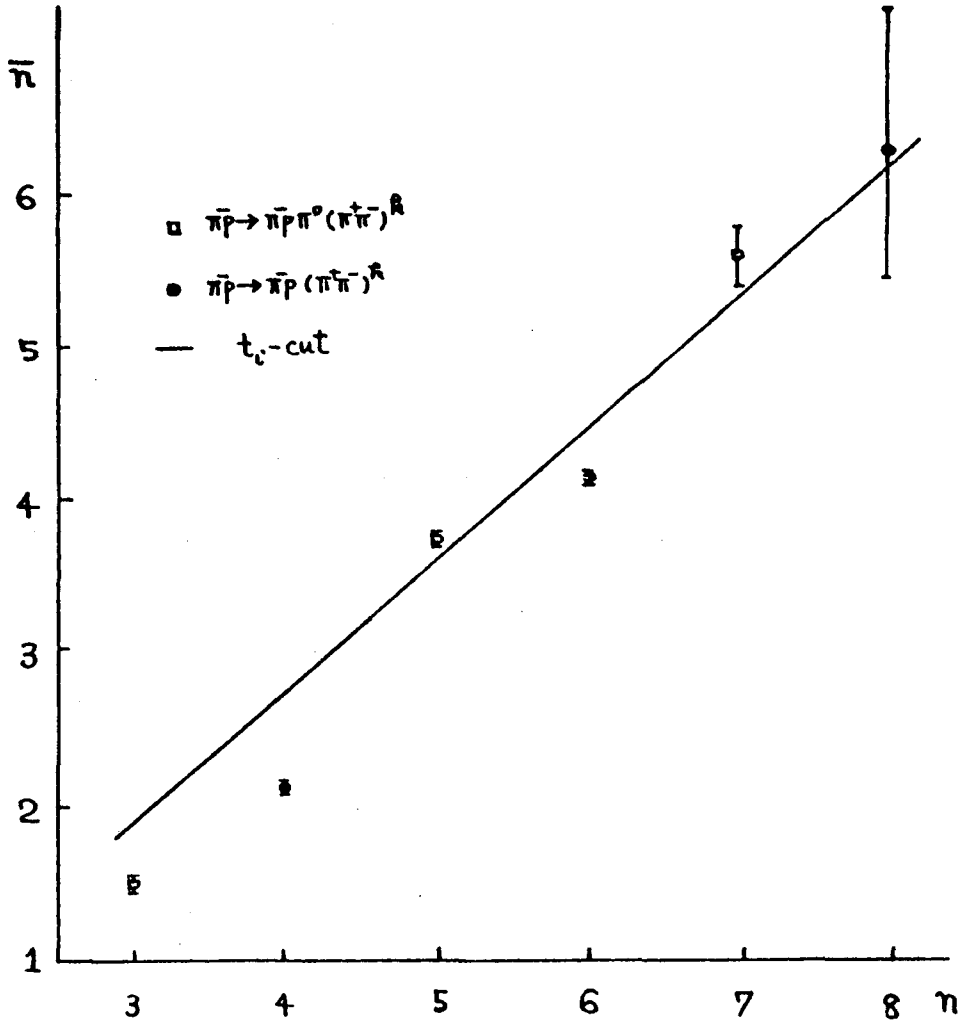
$\bar{n}$
6
5
4
3
2
1
$\bar{p}p \to p\bar{p}\pi^0(\pi^+\pi^-)^n$
$\bar{p}p \to p\bar{p}(\pi^+\pi^-)^n$
t_i-cut
3
4
5
6
7
8
n

Fig.3

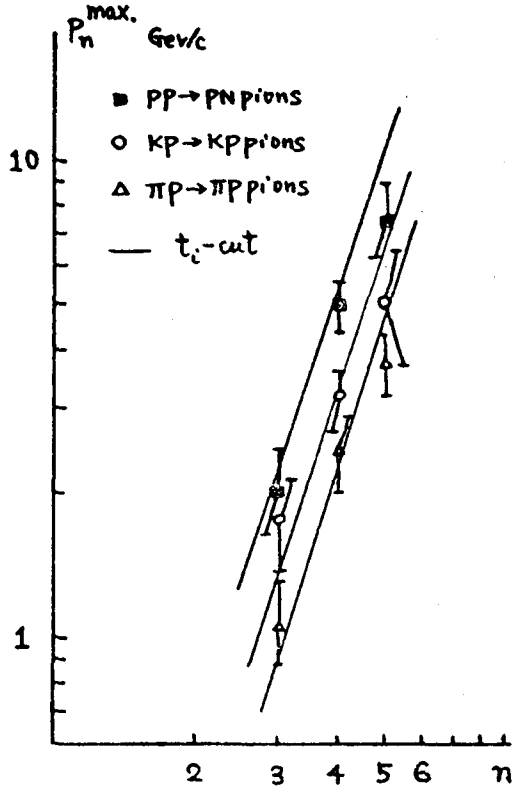
$P_n^{max.}$ Gev/c
pp → pN pions
Kp → Kp pions
πp → πp pions
t_i-cut
10
1
2
3
4
5
6
n

Fig.4

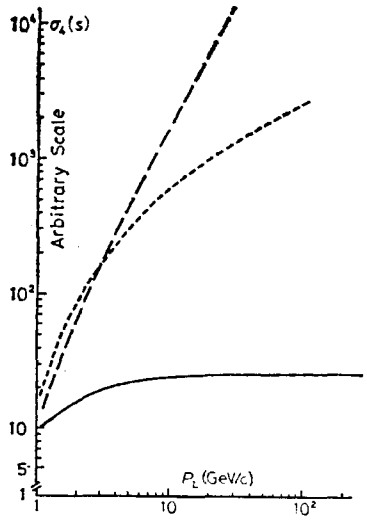

Fig. 5

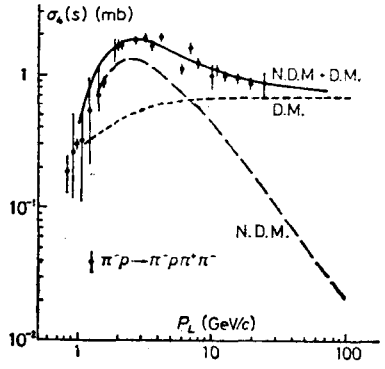

Fig. 6

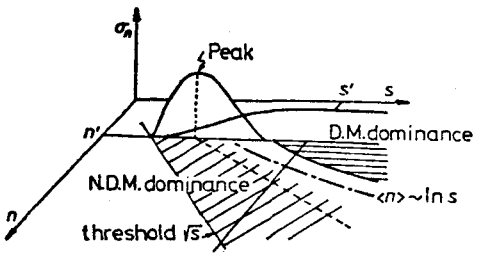

Fig. 7

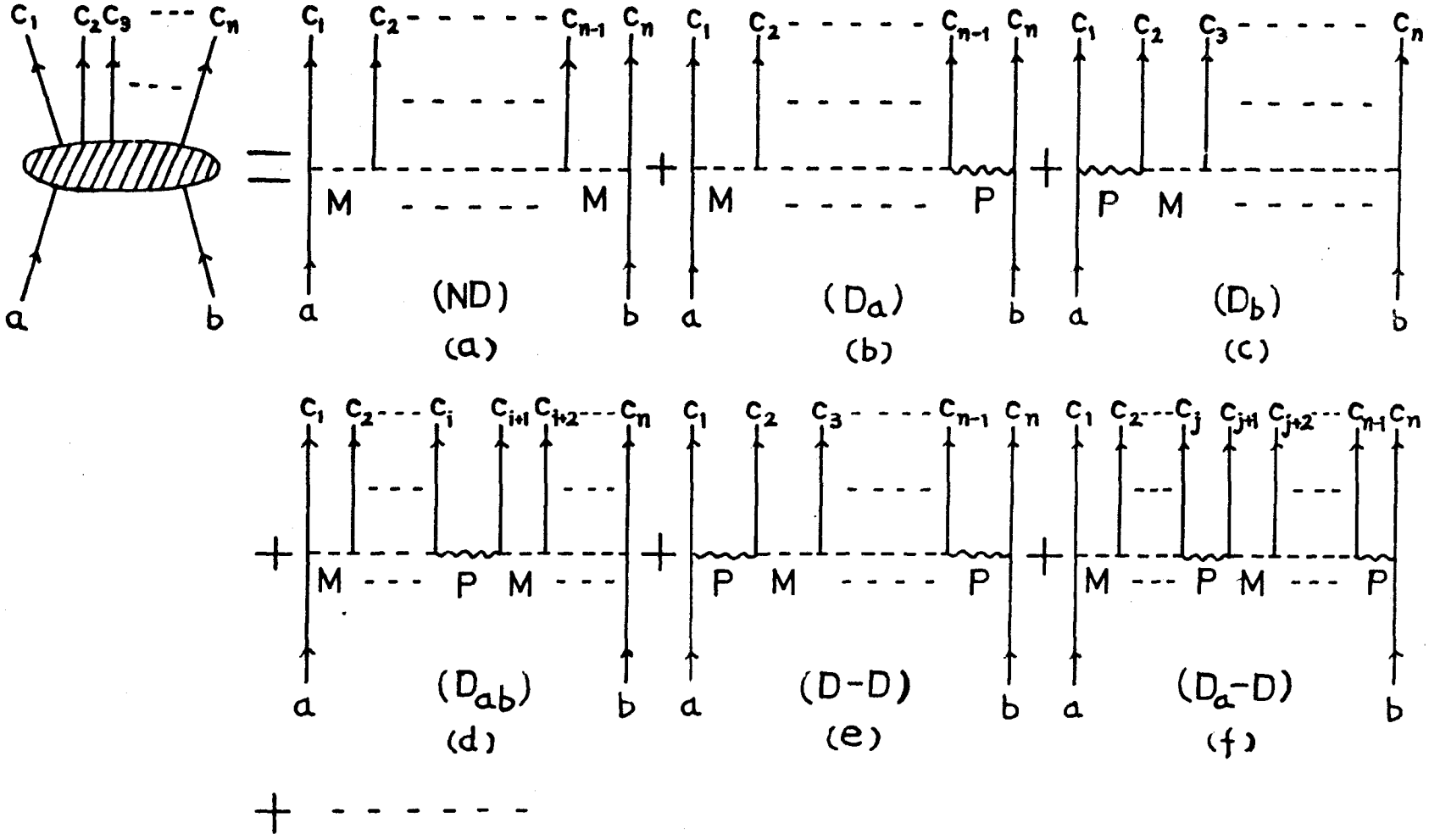

Fig.8

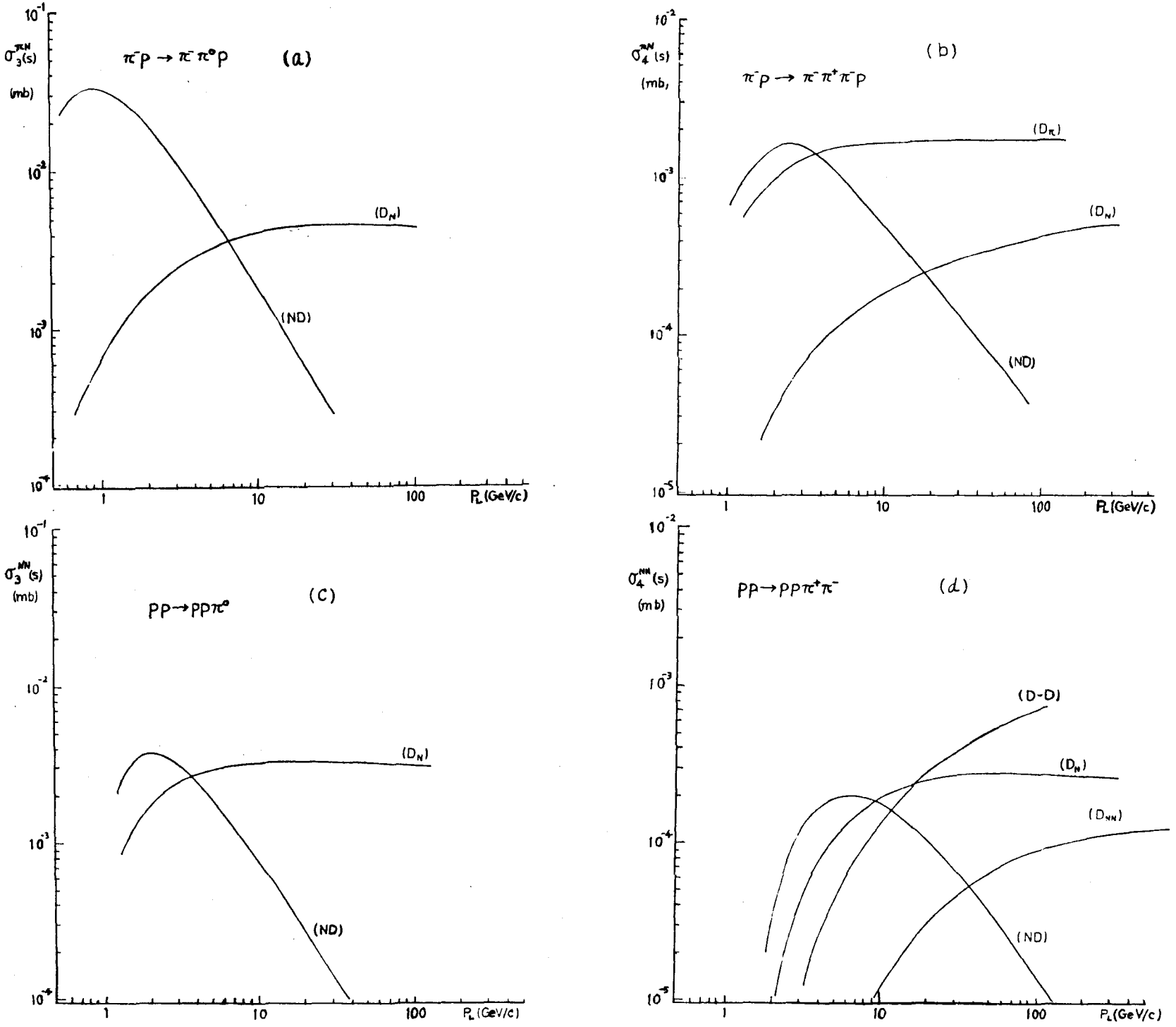
$\sigma_3^{\pi N}(s)$ (mb)
$\pi^- p \to \pi^- \pi^0 p$
(a)
(D_N)
(ND)
P_L (GeV/c)
$\sigma_4^{\pi N}(s)$ (mb)
$\pi^- p \to \pi^- \pi^+ \pi^- p$
(b)
(D_π)
(D_N)
(ND)
P_L (GeV/c)
$\sigma_3^{NN}(s)$ (mb)
$pp \to pp\pi^0$
(C)
(D_N)
(ND)
P_L (GeV/c)
$\sigma_4^{NN}(s)$ (mb)
$pp \to pp\pi^+\pi^-$
(d)
(D-D)
(D_N)
(D_{NN})
(ND)
P_L (GeV/c)

Fig.9

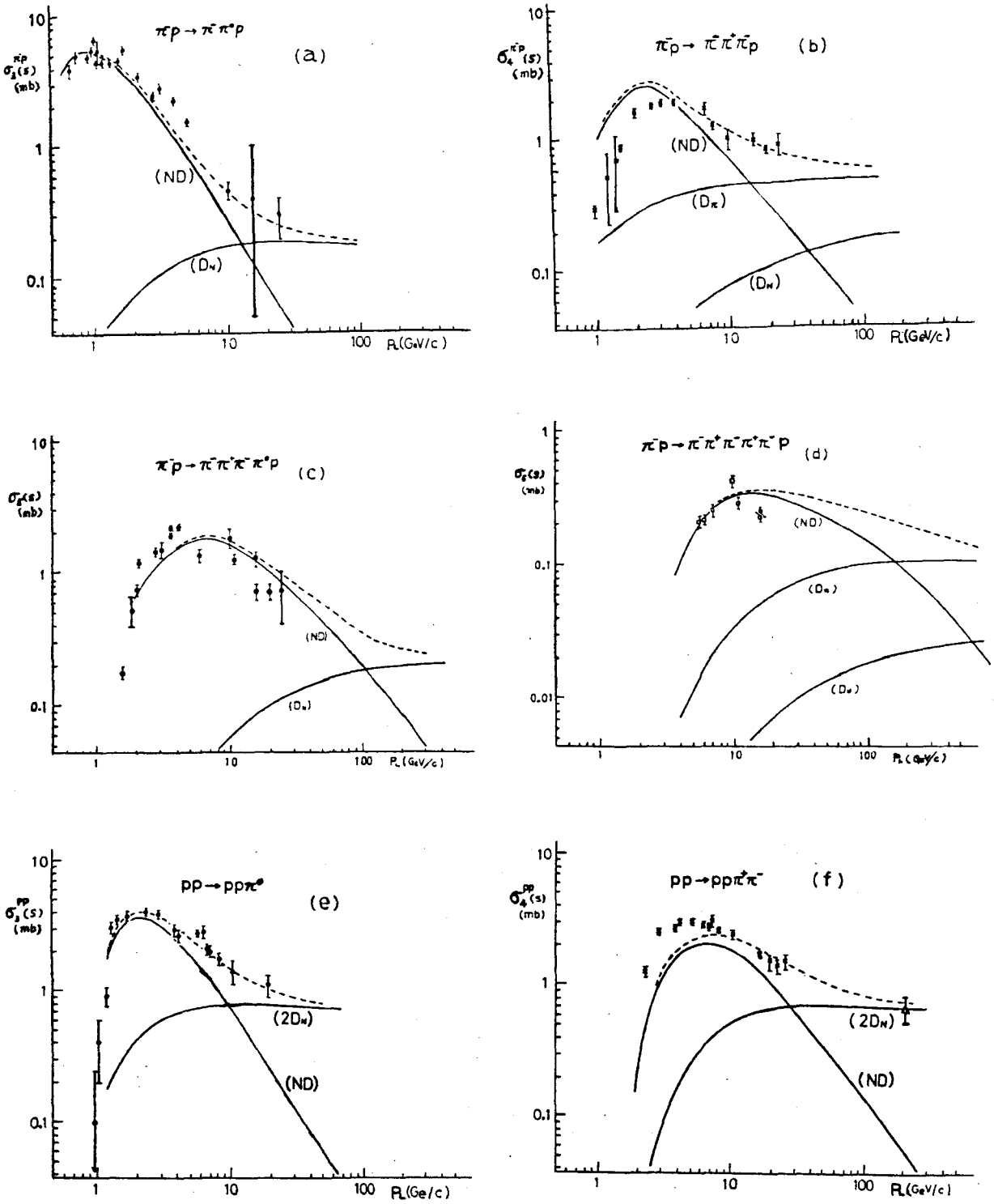
$\pi^- p \to \pi^- \pi^0 p$
(a)
(ND)
(D_N)
P_L(GeV/c)
$\pi^- p \to \pi^- \pi^+ \pi^- p$ (b)
(ND)
(D_π)
(D_N)
P_L(GeV/c)
$\pi^- p \to \pi^- \pi^+ \pi^- \pi^0 p$ (c)
(ND)
(D_π)
P_L(GeV/c)
$\pi^- p \to \pi^- \pi^+ \pi^- \pi^+ \pi^- p$ (d)
(ND)
(D_π)
(D_ρ)
P_L(GeV/c)
$pp \to pp\pi^0$
(e)
$(2D_N)$
(ND)
P_L(Ge/c)
$pp \to pp\pi^+\pi^-$ (f)
$(2D_N)$
(ND)
P_L(GeV/c)

Fig.10

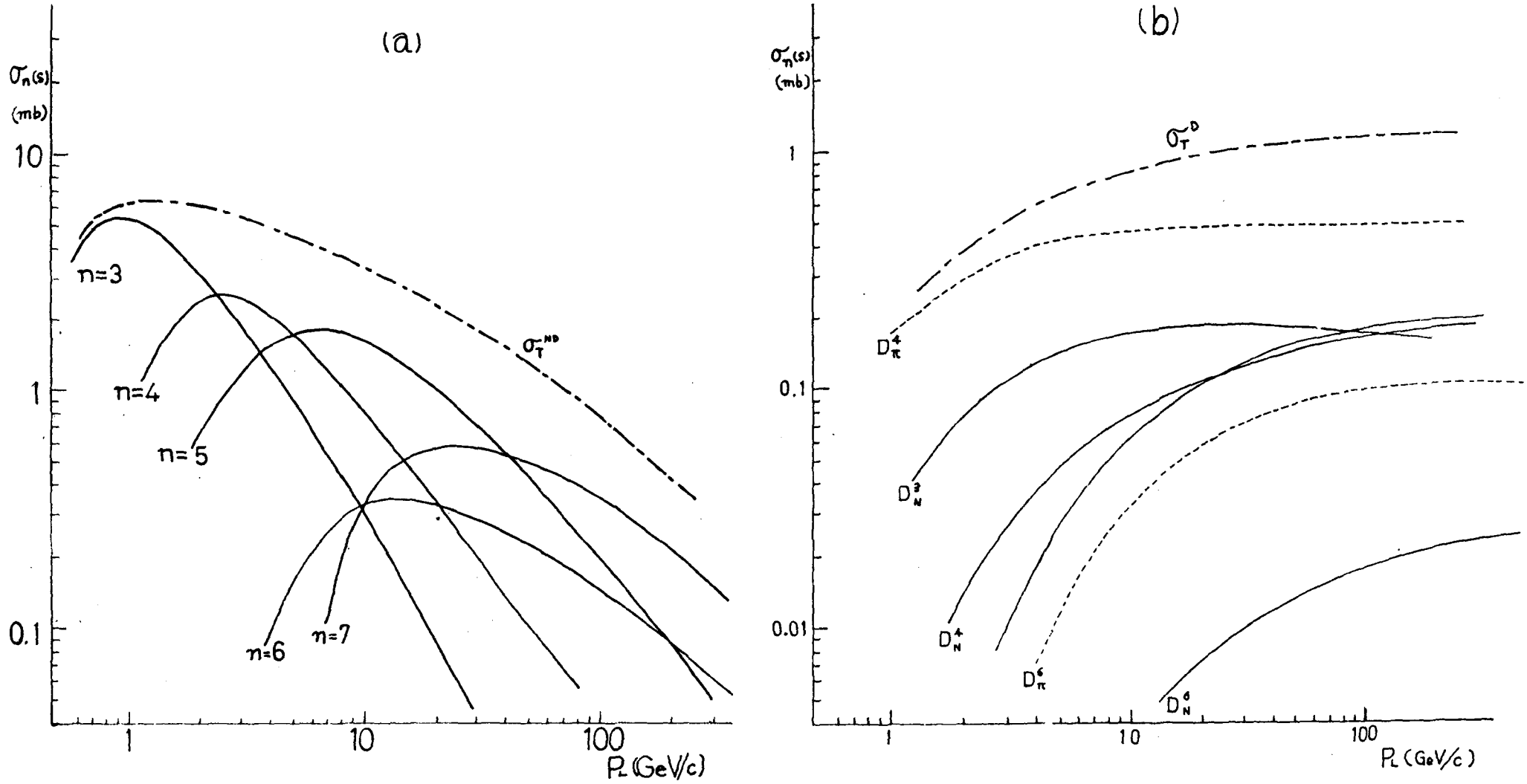
(a)
$\sigma_{n(s)}$
(mb)
10
1
0.1
n=3
n=4
n=5
n=6
n=7
σ_T^{ND}
1
10
100
P_L (GeV/c)
(b)
$\sigma_{n(s)}$
(mb)
1
0.1
0.01
σ_T^D
D_π^4
D_N^3
D_N^4
D_π^6
D_N^6
1
10
100
P_L (GeV/c)

Fig.11

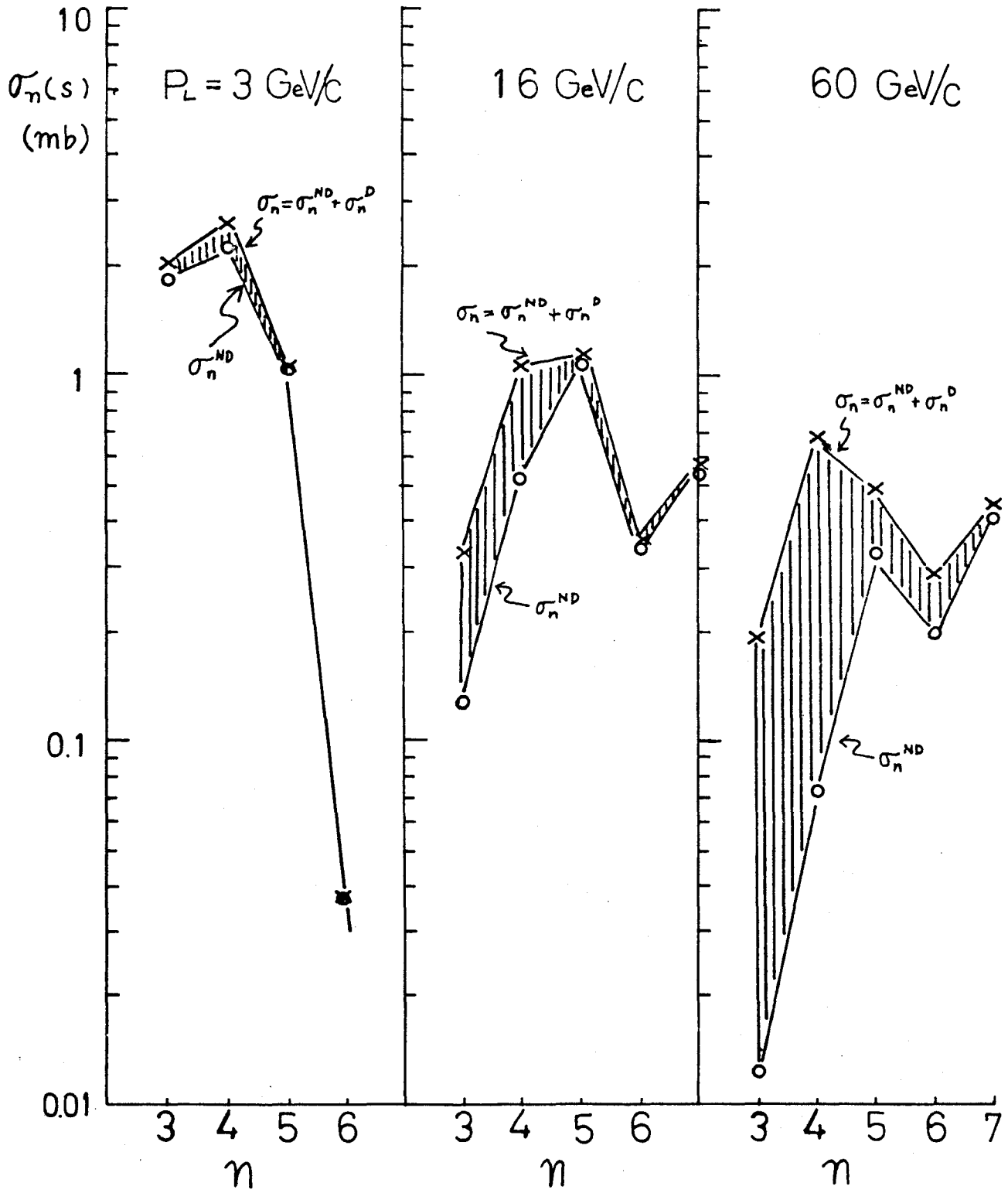
10
1
0.1
0.01
$\sigma_n(s)$
(mb)
P_L = 3 GeV/c
16 GeV/c
60 GeV/c
$\sigma_n = \sigma_n^{ND} + \sigma_n^D$
σ_n^{ND}
3 4 5 6
3 4 5 6
3 4 5 6 7
n
n
n

Fig. 12

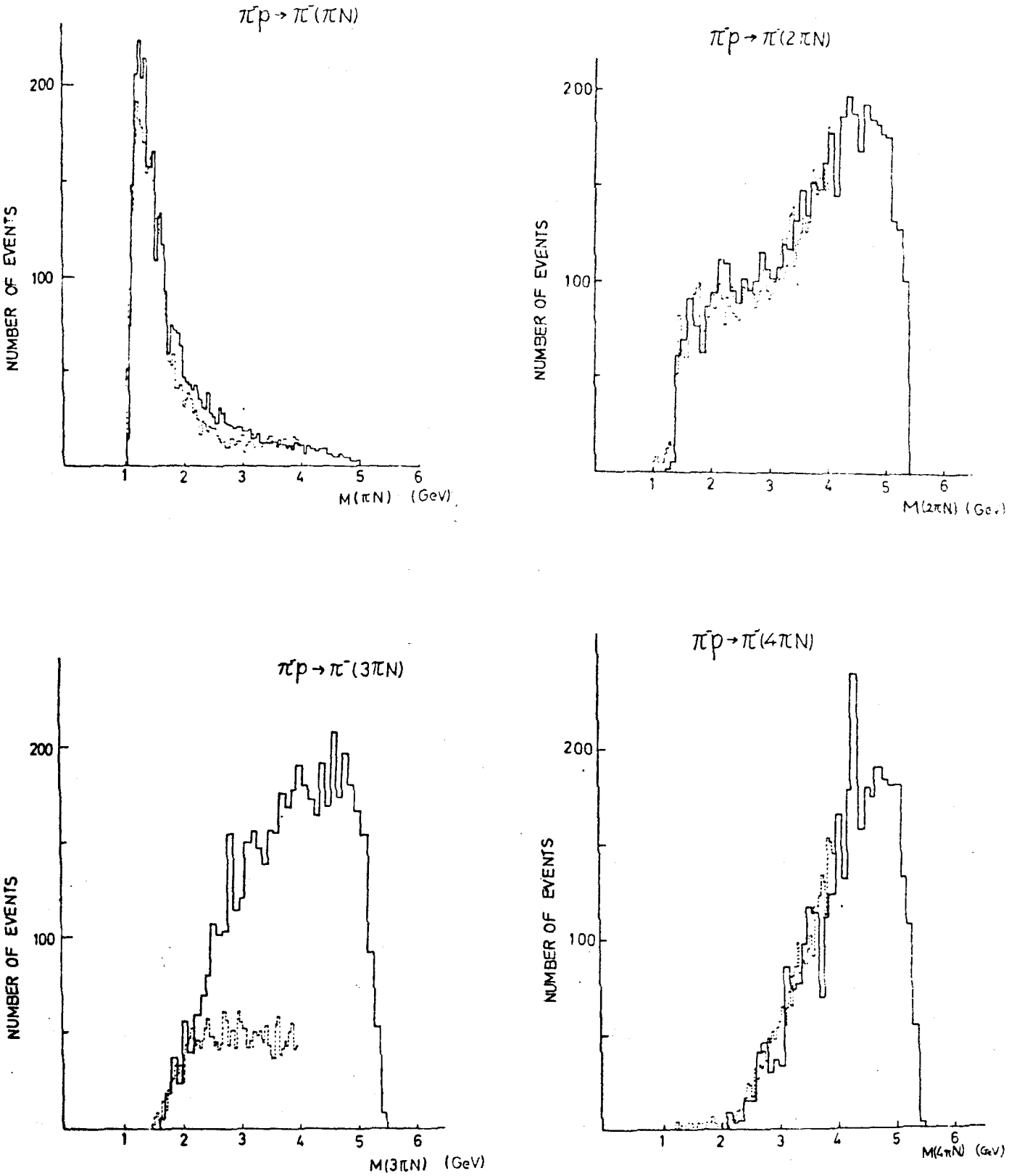
$\pi^- p \to \pi^- (\pi N)$
NUMBER OF EVENTS
200
100
1
2
3
4
5
6
M(πN) (GeV)
$\pi^- p \to \pi^- (2\pi N)$
NUMBER OF EVENTS
200
100
1
2
3
4
5
6
M(2πN) (GeV)
$\pi^- p \to \pi^- (3\pi N)$
NUMBER OF EVENTS
200
100
1
2
3
4
5
6
M(3πN) (GeV)
$\pi^- p \to \pi^- (4\pi N)$
NUMBER OF EVENTS
200
100
1
2
3
4
5
6
M(4πN) (GeV)

Fig.13

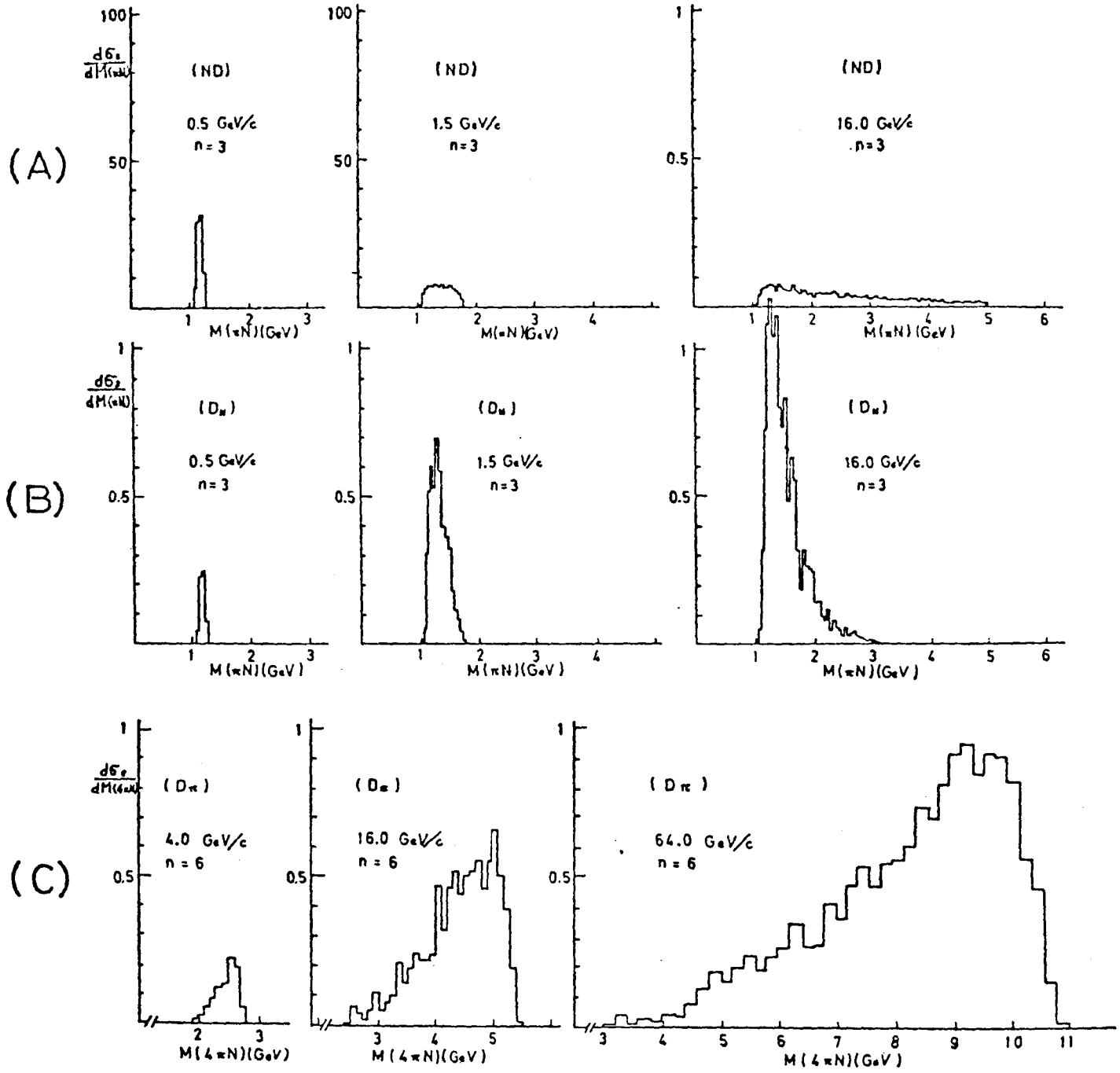
(A)
(ND)
0.5 GeV/c
n = 3
1.5 GeV/c
n = 3
16.0 GeV/c
n = 3
M(πN)(GeV)
(B)
(Dπ)
0.5 GeV/c
n = 3
1.5 GeV/c
n = 3
16.0 GeV/c
n = 3
M(πN)(GeV)
(C)
(Dπ)
4.0 GeV/c
n = 6
16.0 GeV/c
n = 6
64.0 GeV/c
n = 6
M(4πN)(GeV)

Fig.14

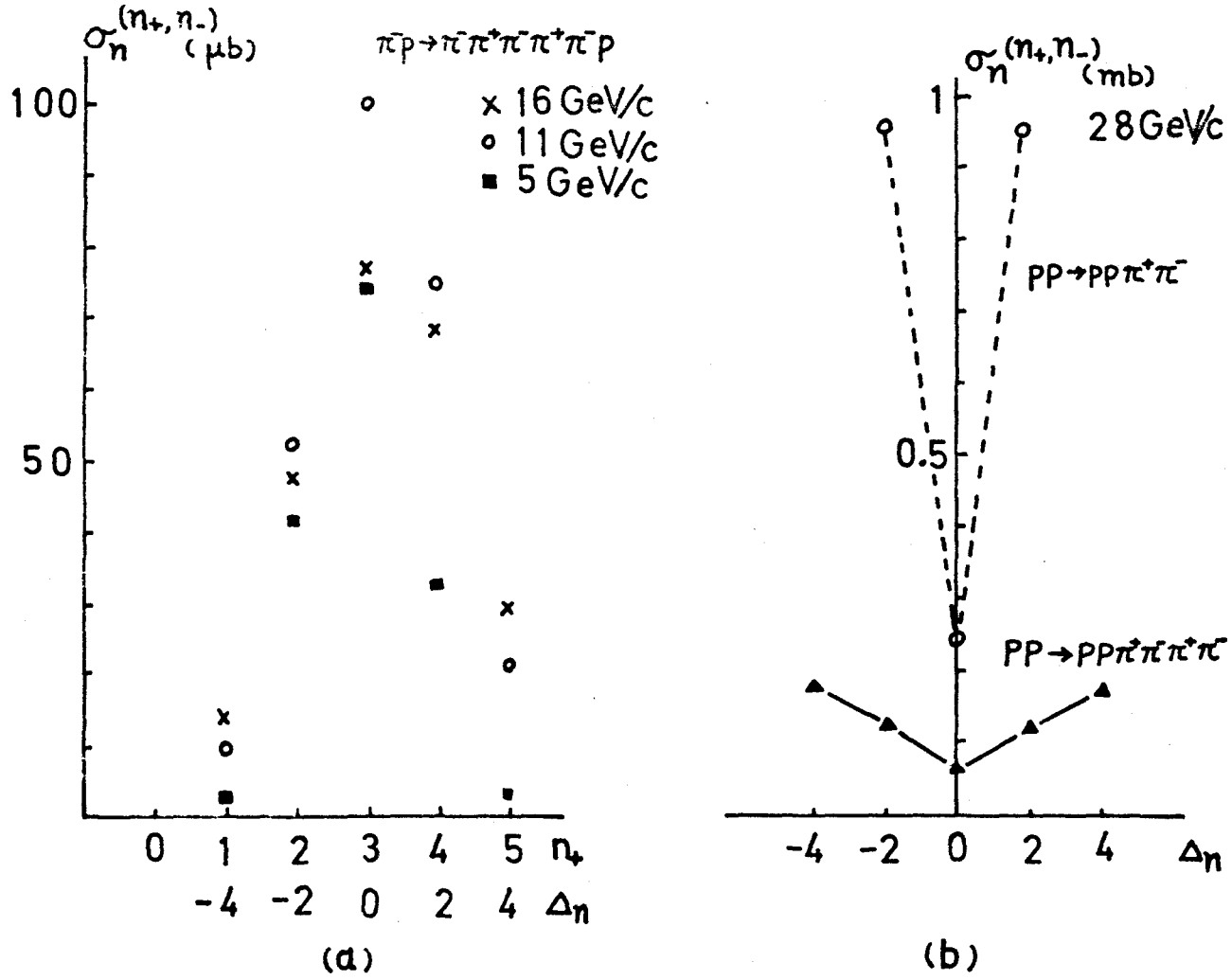
$\sigma_n^{(n_+,n_-)}$ (μb)
$\pi^-p \to \pi^-\pi^+\pi^-\pi^+\pi^-p$
× 16 GeV/c
○ 11 GeV/c
■ 5 GeV/c
100
50
0 1 2 3 4 5 n_+
-4 -2 0 2 4 Δn
(a)
$\sigma_n^{(n_+,n_-)}$ (mb)
1
0.5
28 GeV/c
$PP \to PP\pi^+\pi^-$
$PP \to PP\pi^+\pi^-\pi^+\pi^-$
-4 -2 0 2 4 Δn
(b)

Fig.15

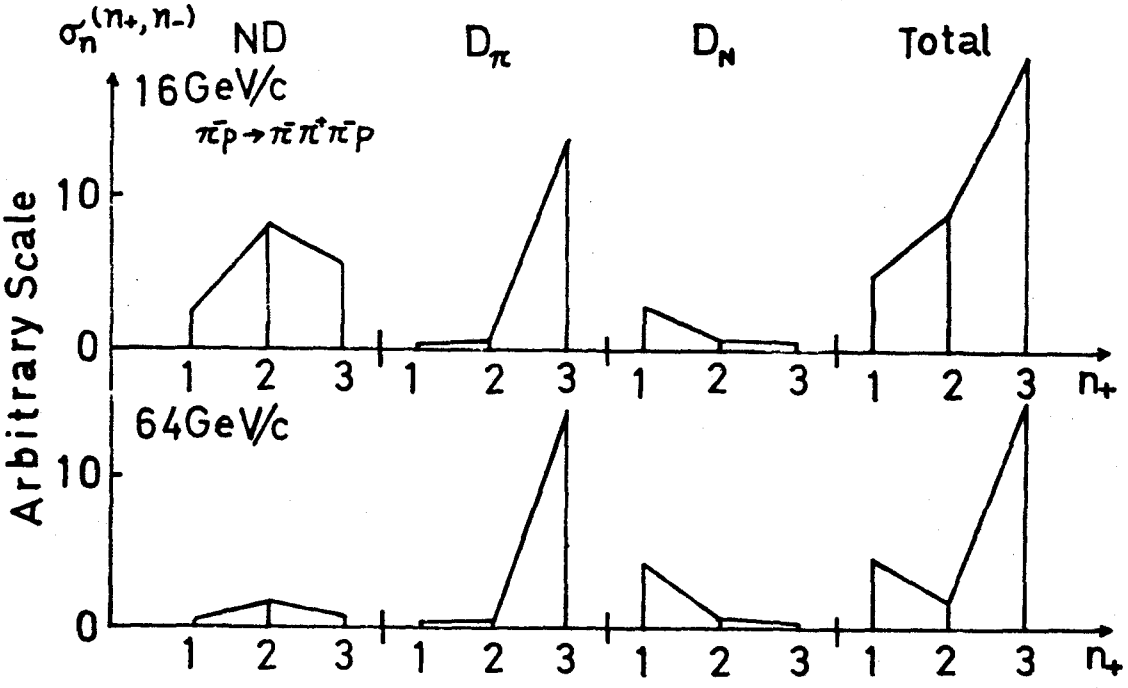
$\sigma_n^{(n_+,n_-)}$
ND
D_π
D_N
Total
16 GeV/c
$\pi^-p \to \pi^-\pi^+\pi^-p$
Arbitrary Scale
10
0
1 2 3 1 2 3 1 2 3 1 2 3 n_+
64 GeV/c
10
0
1 2 3 1 2 3 1 2 3 1 2 3 n_+

Fig.16

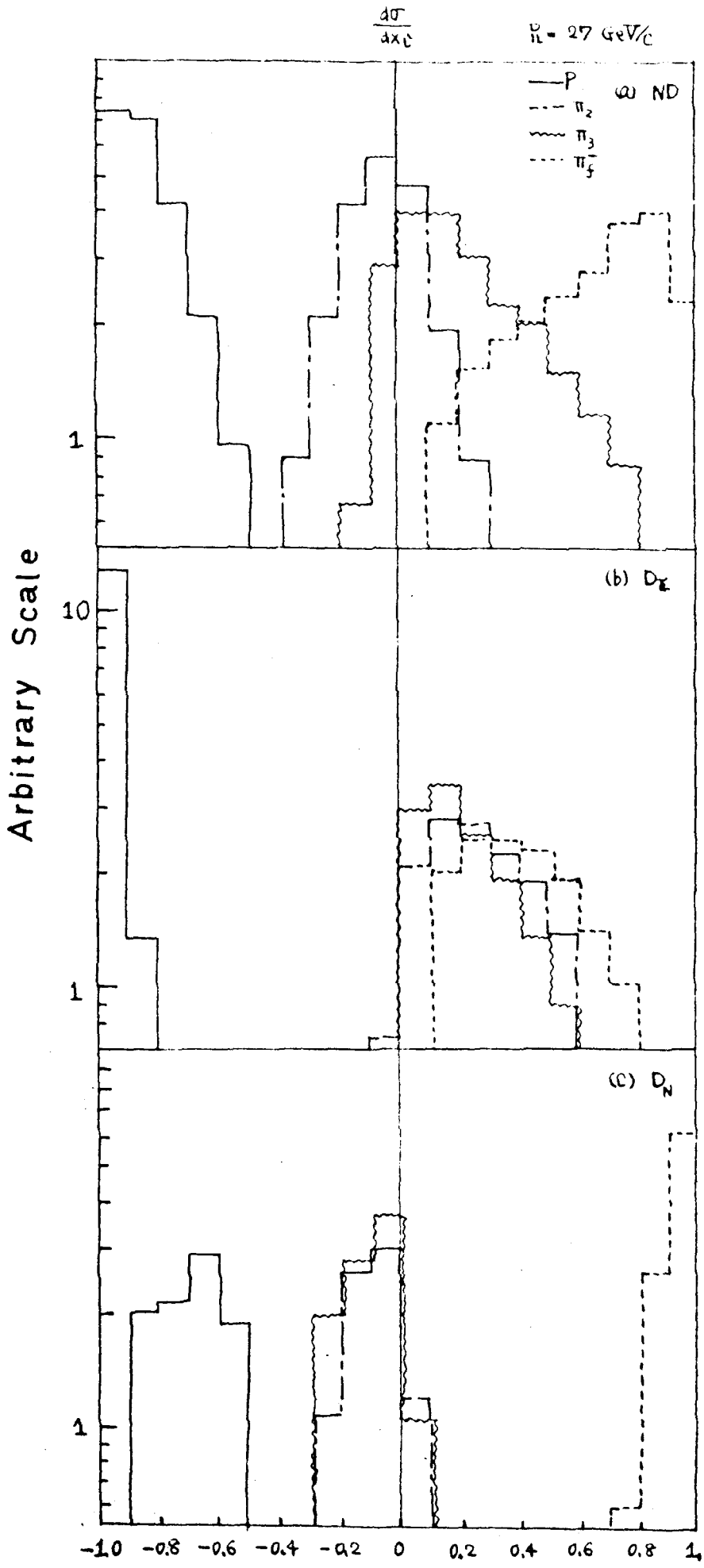
$\frac{d\sigma}{dx_L}$
p_L = 27 GeV/c
P
π_2
π_3
π_f^-
(a) ND
(b) D_E
(c) D_N
Arbitrary Scale
1
10
1
1
-1.0
-0.8
-0.6
-0.4
-0.2
0
0.2
0.4
0.6
0.8
1.0
x_L

Fig.17

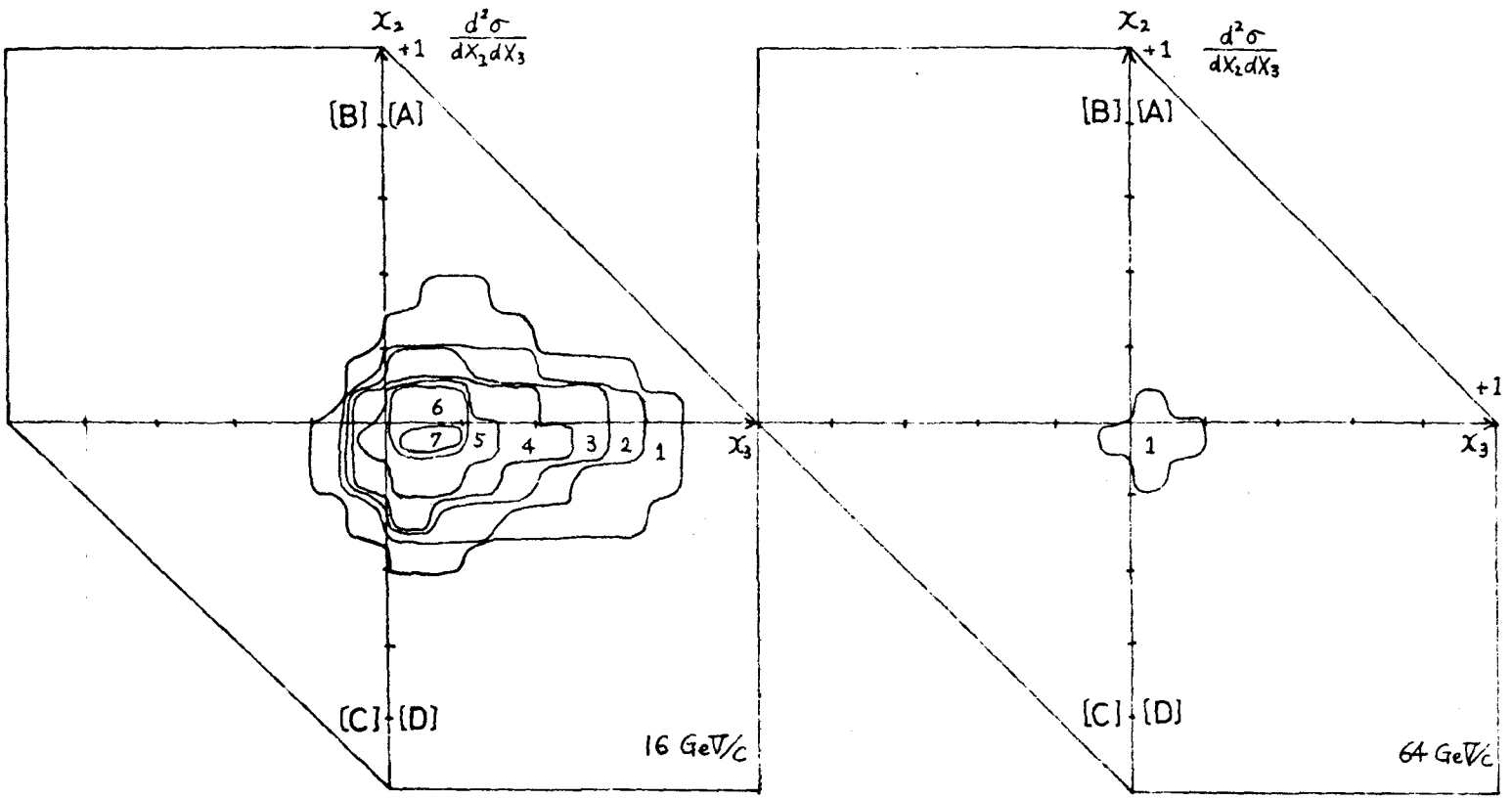

(a) ND

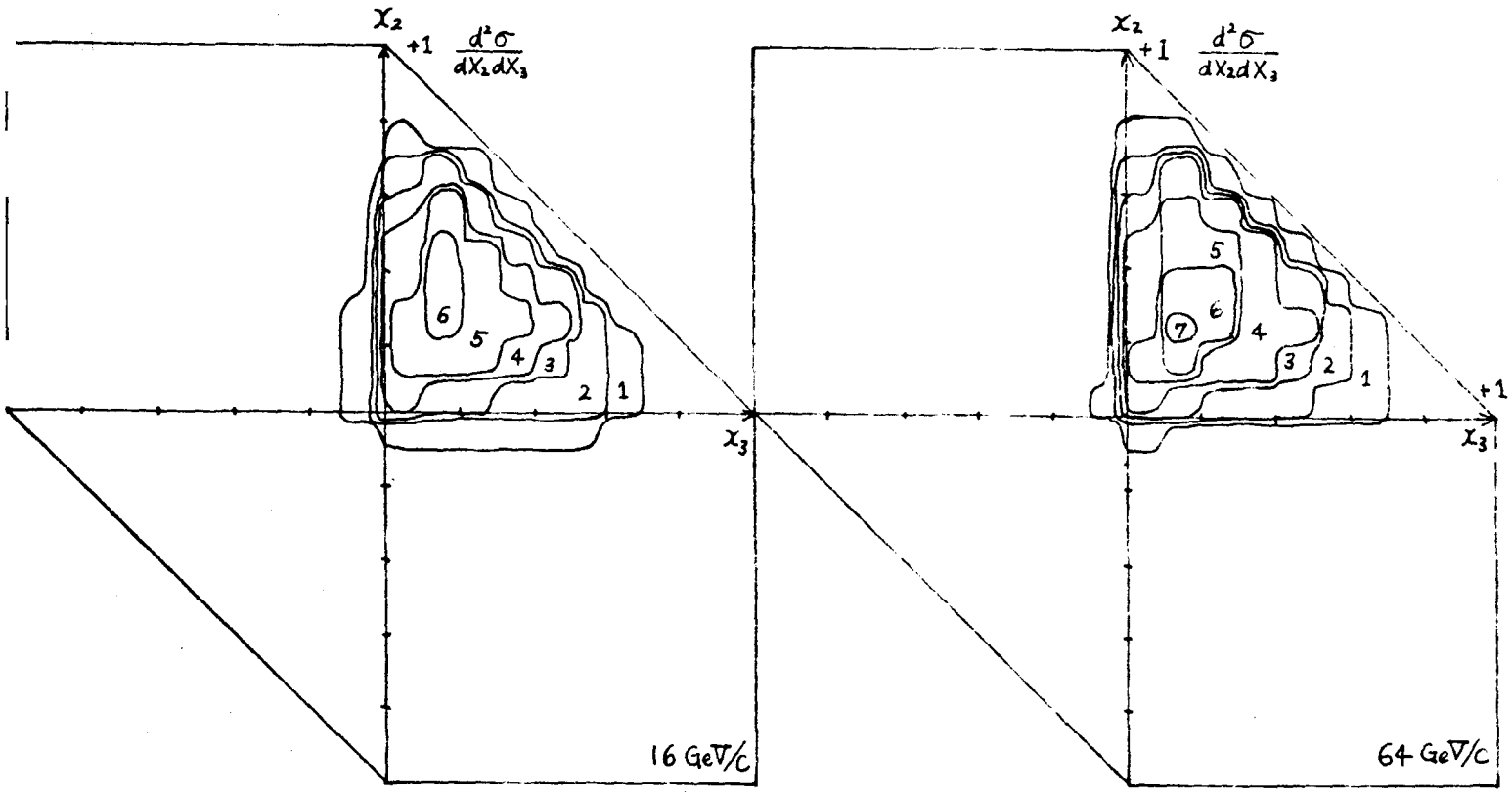

(b) D_π

Fig. 18

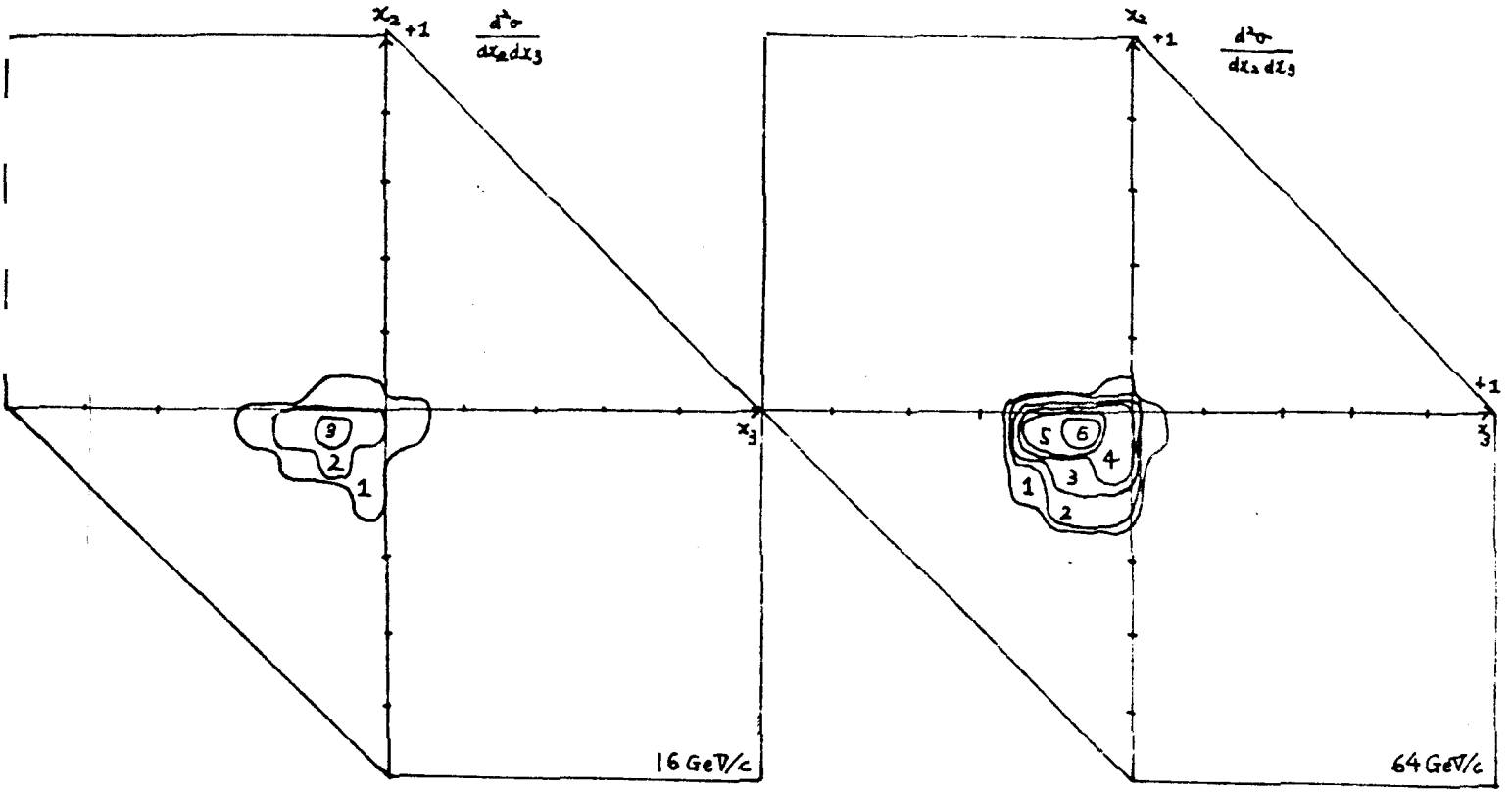

(c) D_N

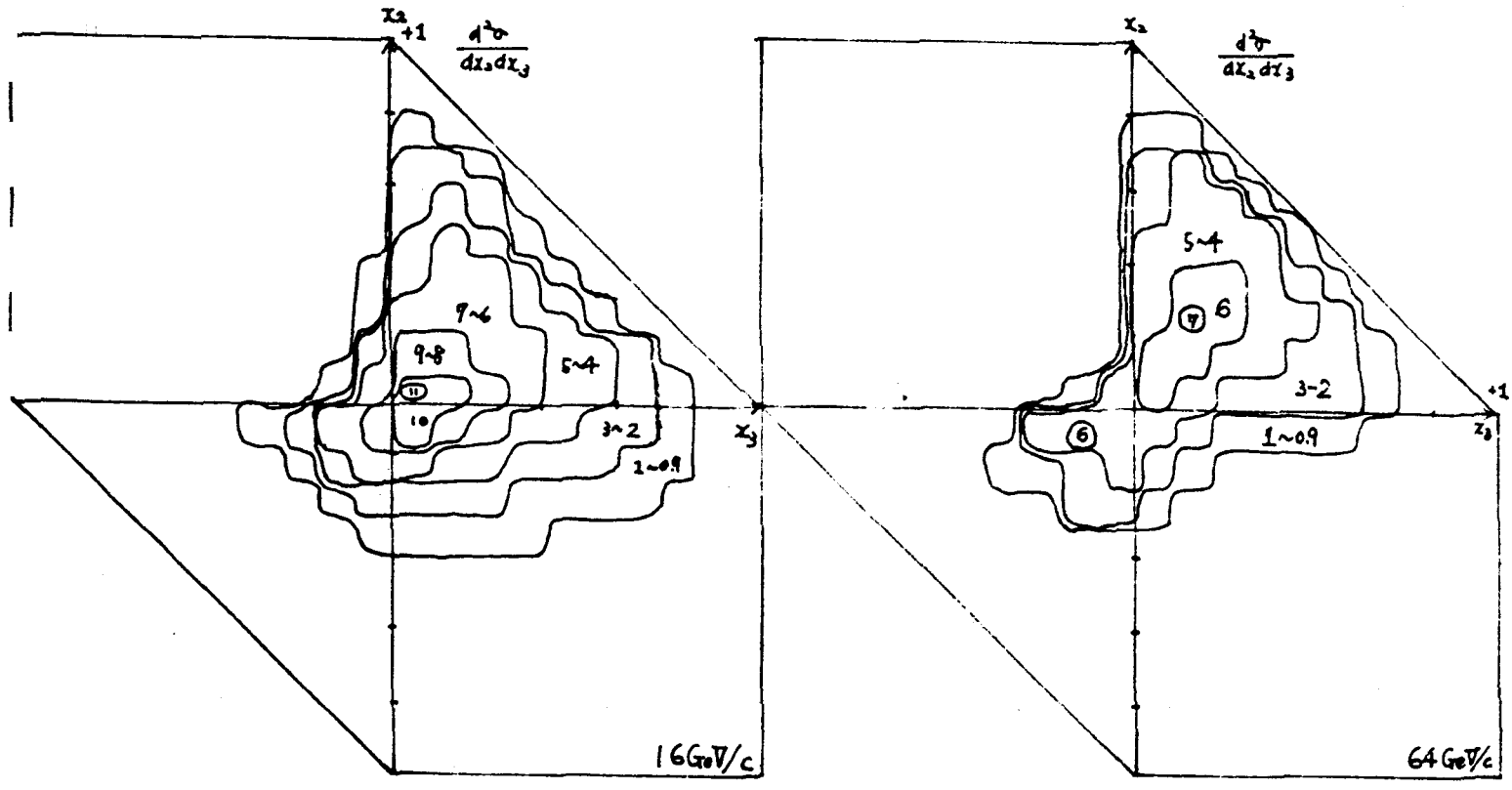

(d) Total

Fig. 18

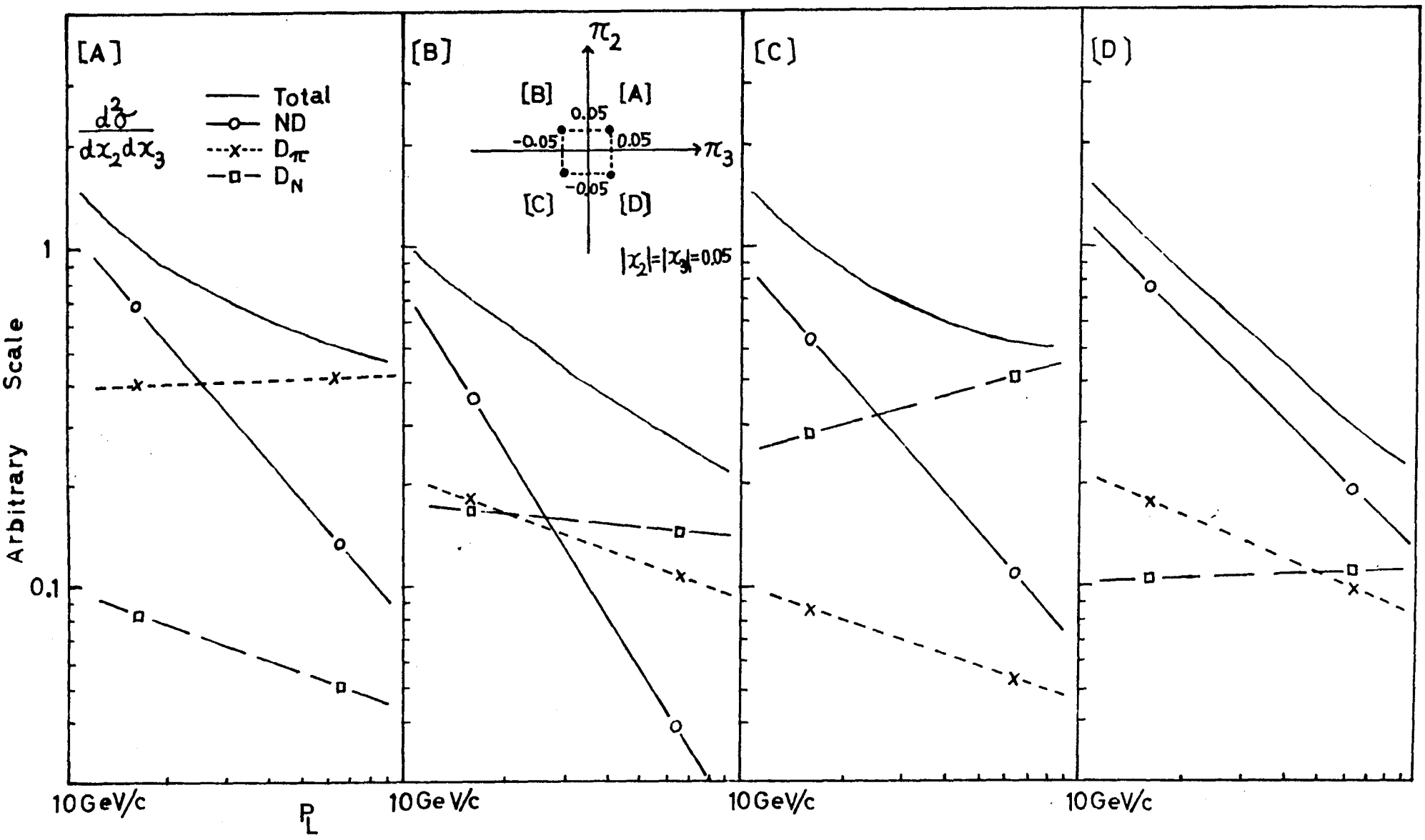
[A]
[B]
[C]
[D]
Total
ND
D_π
D_N
$\frac{d^2\sigma}{dx_2 dx_3}$
π_2
π_3
0.05
-0.05
$|x_2|=|x_3|=0.05$
Arbitrary Scale
1
0.1
10GeV/c
P_L

Fig.19

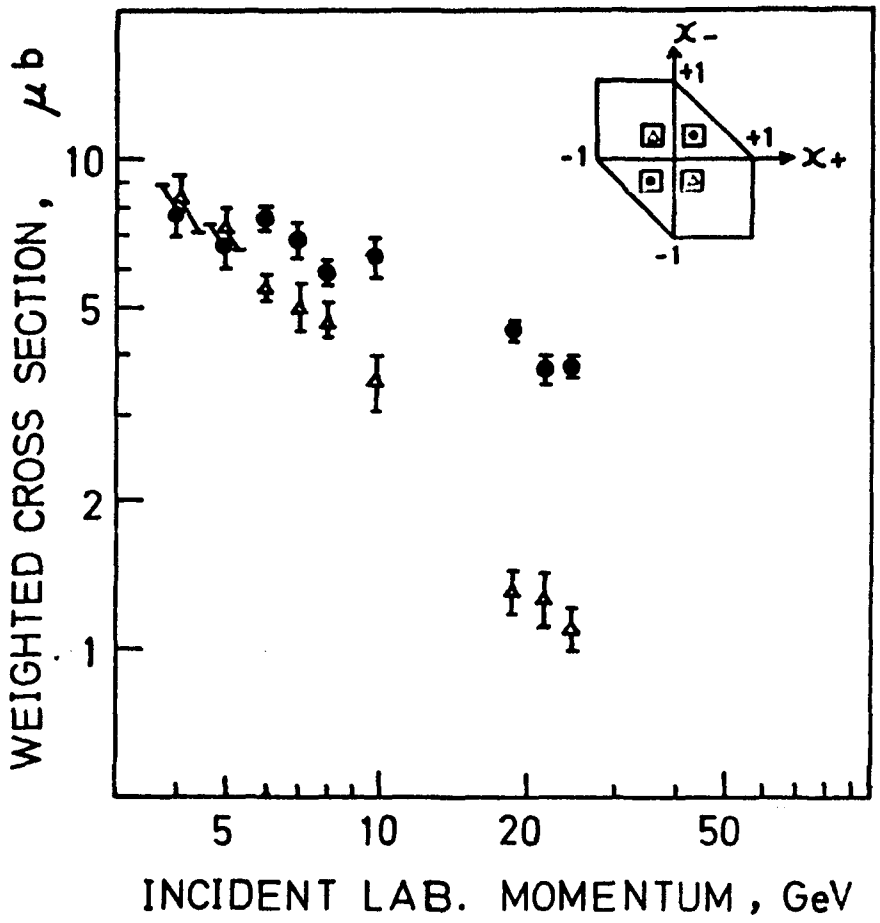
WEIGHTED CROSS SECTION, μb
10
5
2
1
5
10
20
50
INCIDENT LAB. MOMENTUM, GeV
X-
+1
-1
+1
X+
-1

Fig.20

EXPONENT N

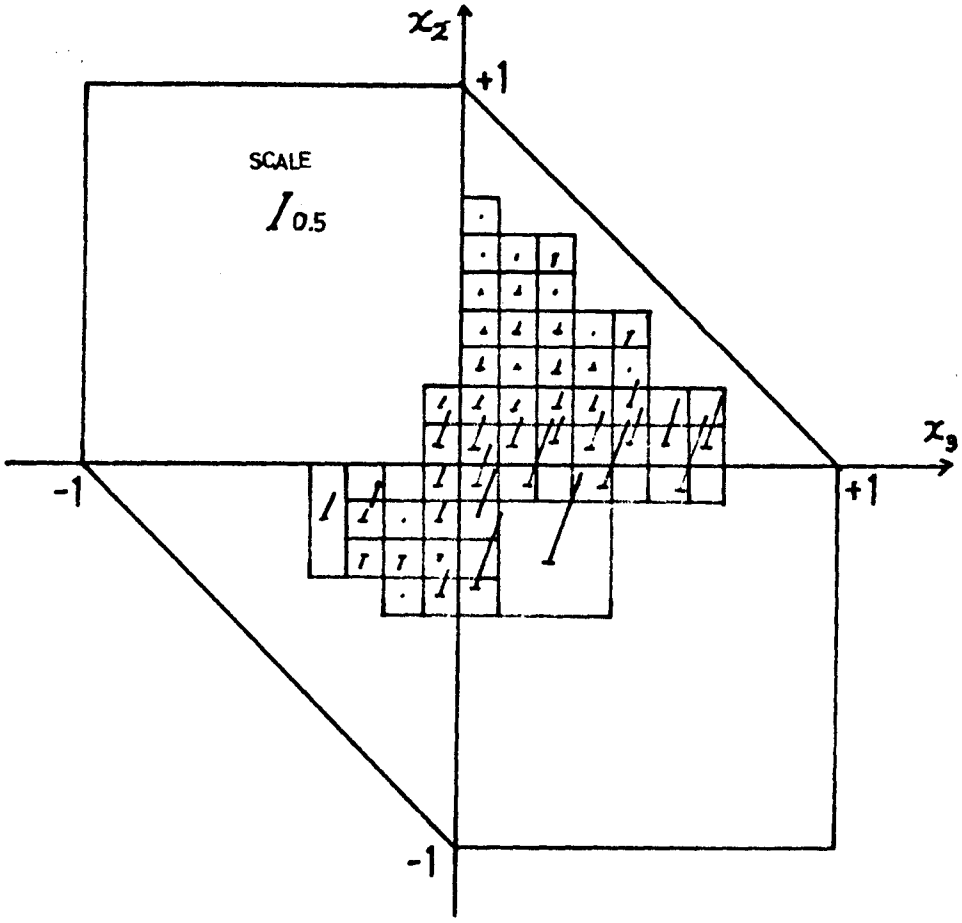

Fig. 21

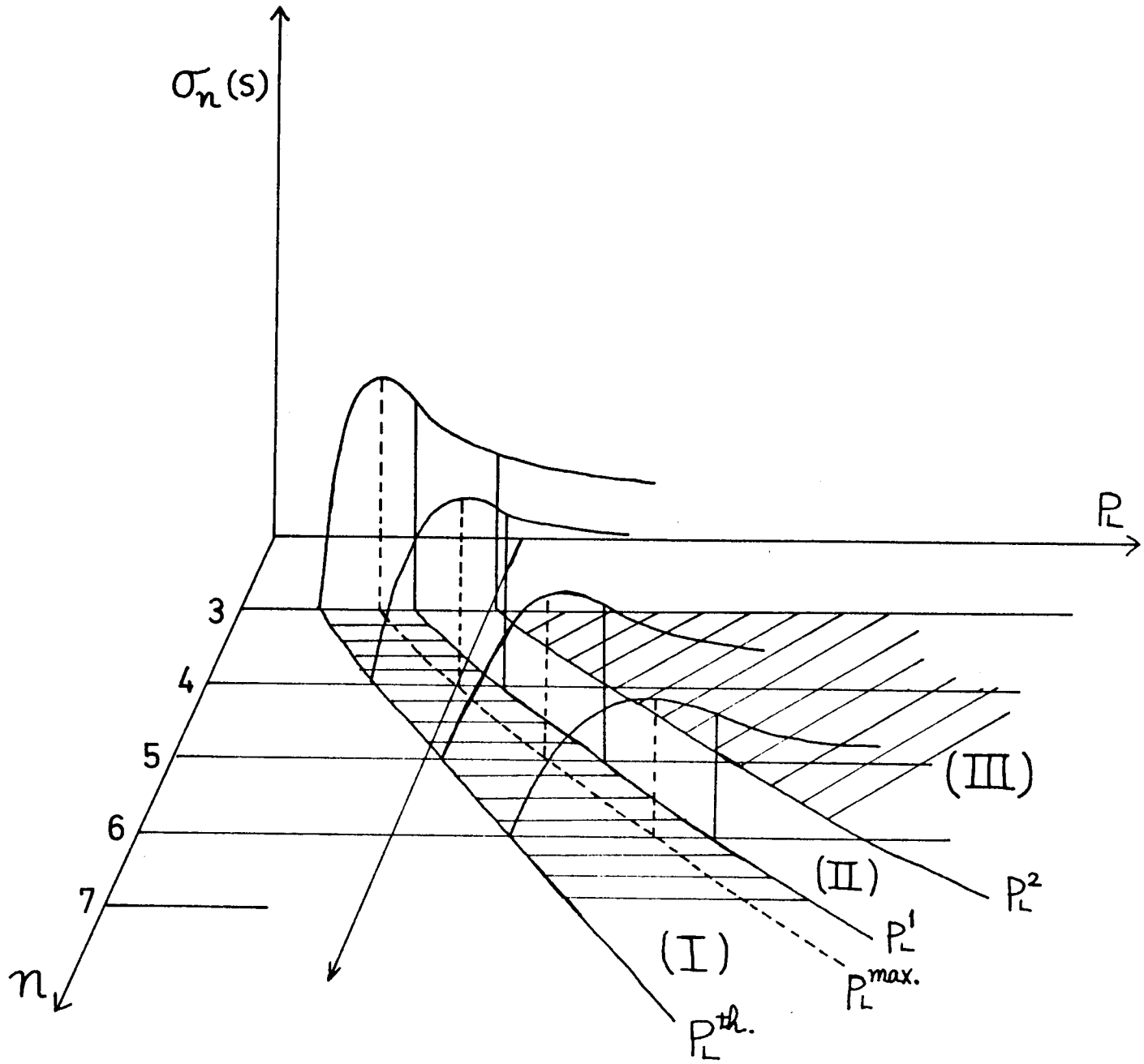

Fig. 22

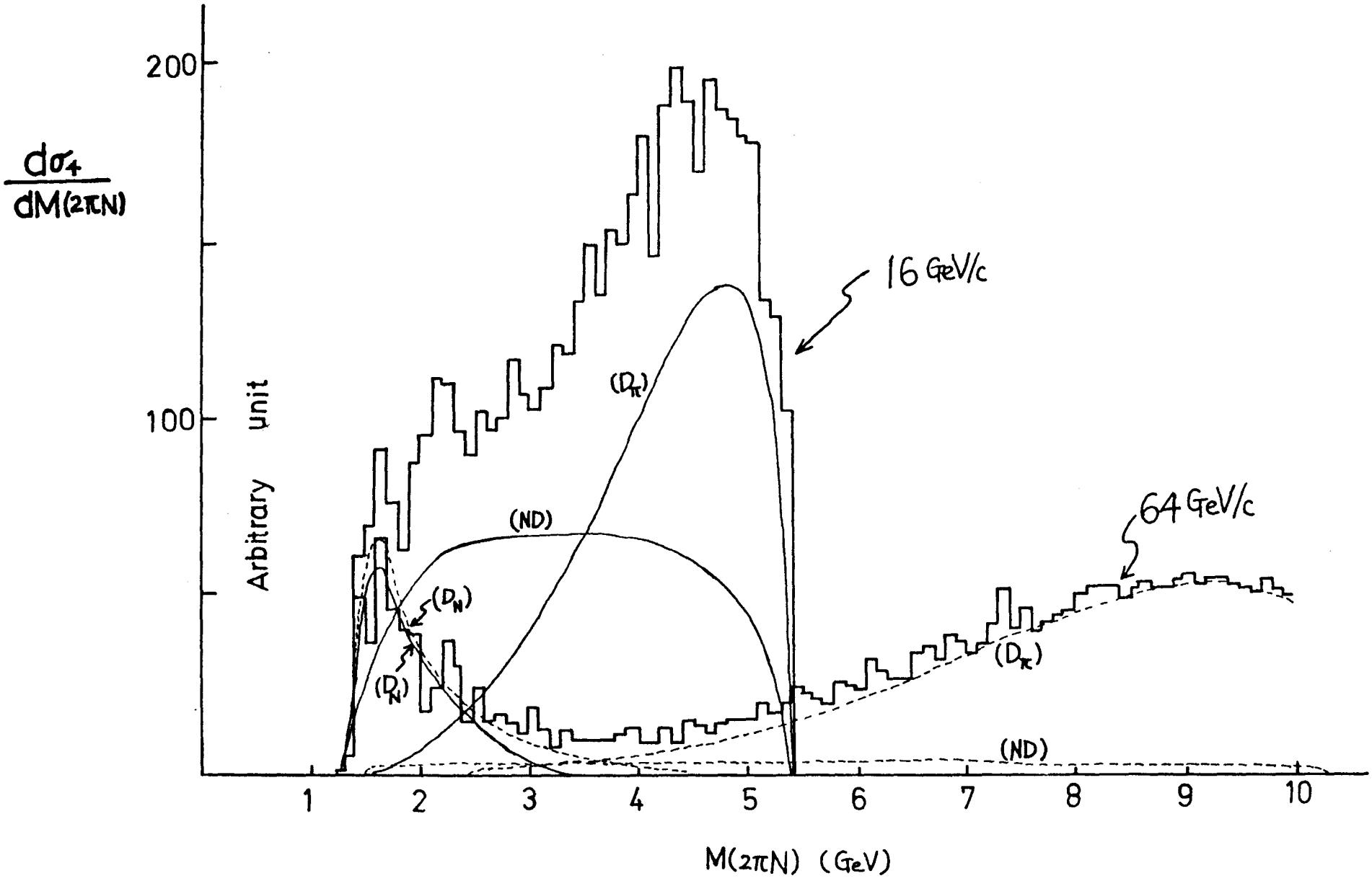
$\frac{d\sigma_4}{dM(2\pi N)}$
200
100
Arbitrary unit
16 GeV/c
64 GeV/c
(D_π)
(ND)
(D_N)
(D_N')
(D_π)
(ND)
1
2
3
4
5
6
7
8
9
10
M(2πN) (GeV)

Fig. 23

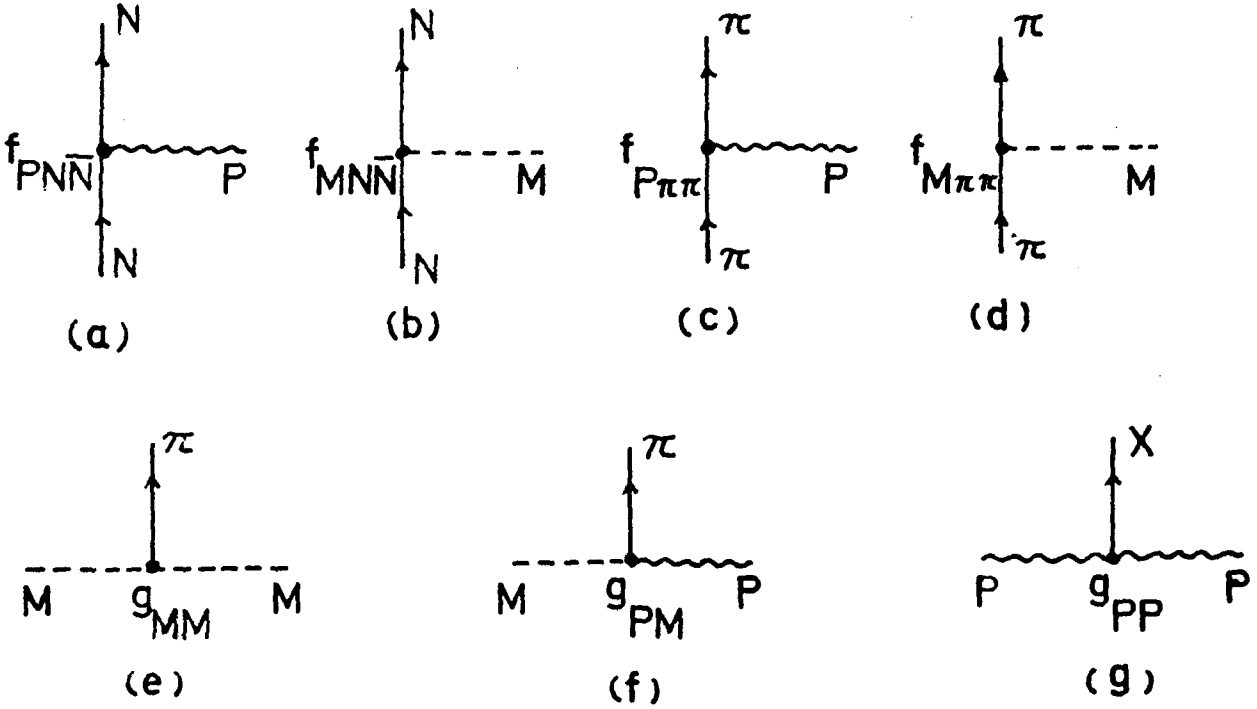
N
N
P
$f_{PN\bar{N}}$
(a)
N
N
M
$f_{MN\bar{N}}$
(b)
π
π
P
$f_{P\pi\pi}$
(c)
π
π
M
$f_{M\pi\pi}$
(d)
π
M
M
g_{MM}
(e)
π
M
P
g_{PM}
(f)
X
P
P
g_{PP}
(g)

Fig. 24

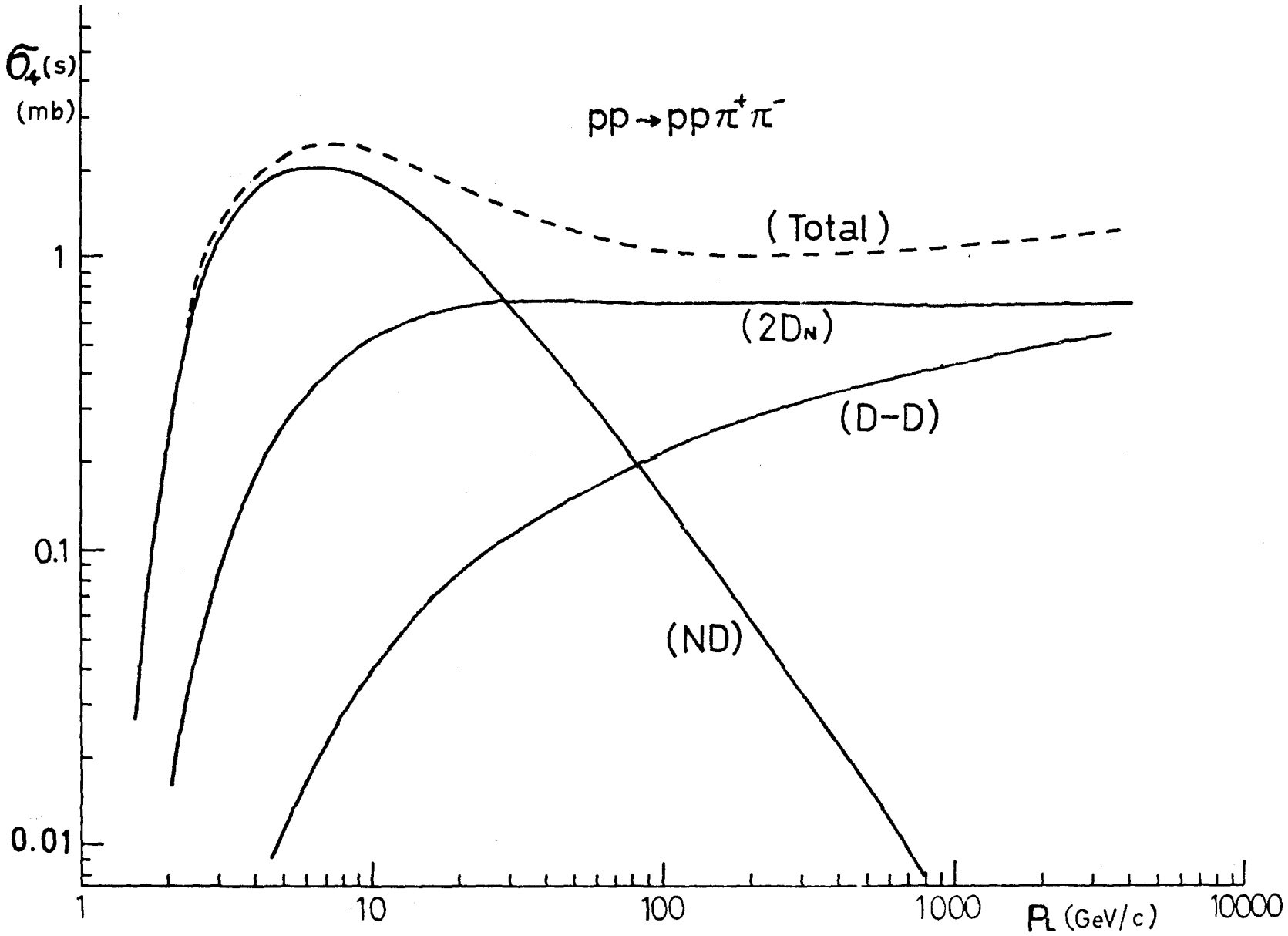
$\sigma_4(s)$
(mb)
$pp \to pp\pi^+\pi^-$
(Total)
$(2D_N)$
(D-D)
(ND)
1
0.1
0.01
1
10
100
1000
P_L (GeV/c)
10000

Fig.25

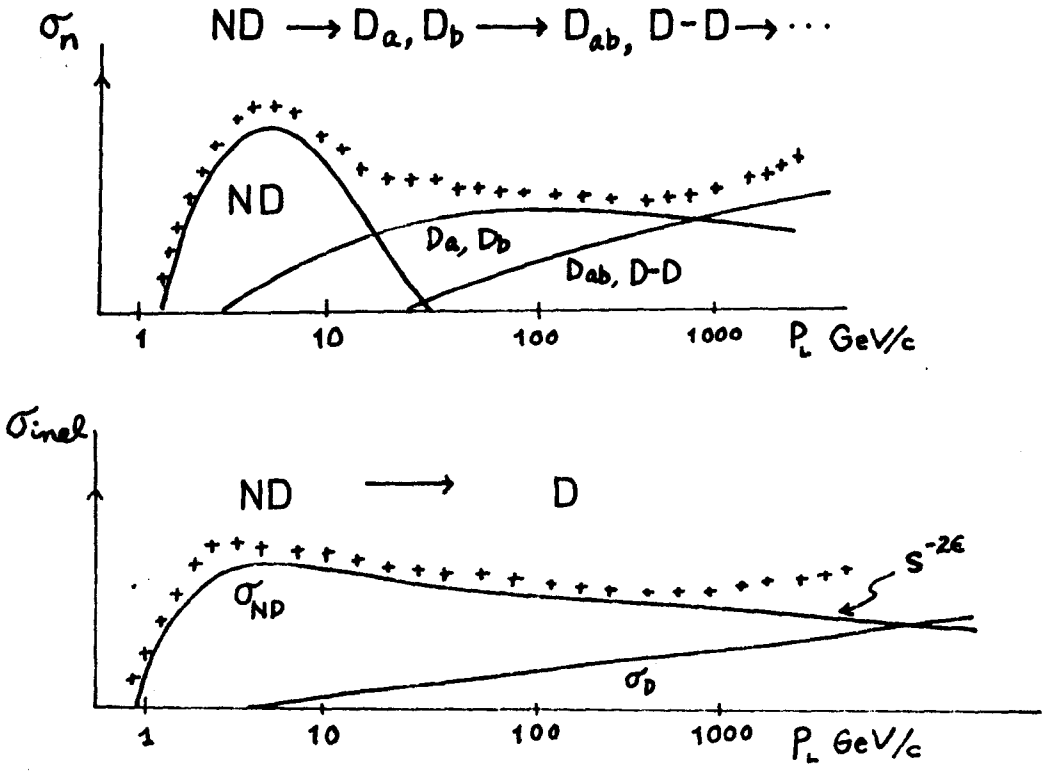
σ_n
ND → D_a, D_b → D_{ab}, D-D → ···
ND
D_a, D_b
D_{ab}, D-D
1
10
100
1000
P_L GeV/c
σ_{inel}
ND → D
σ_{ND}
$s^{-2\epsilon}$
σ_D
1
10
100
1000
P_L GeV/c

Fig. 26

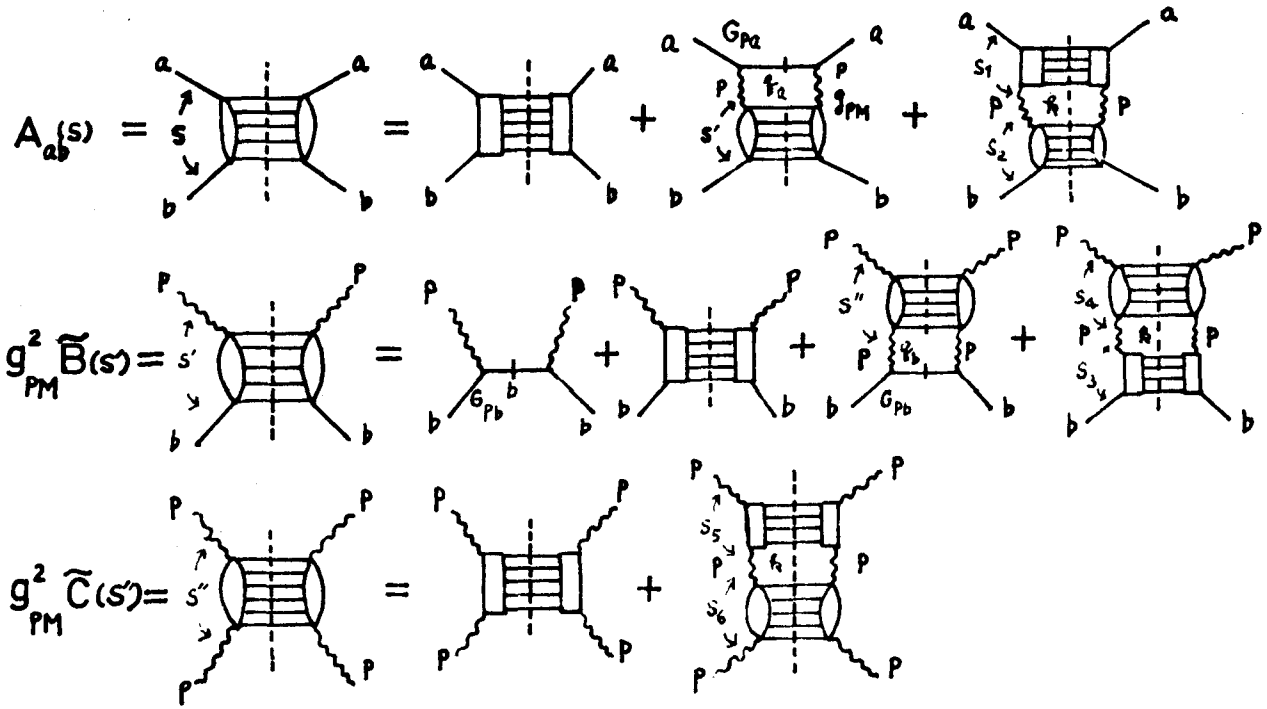

Fig.27

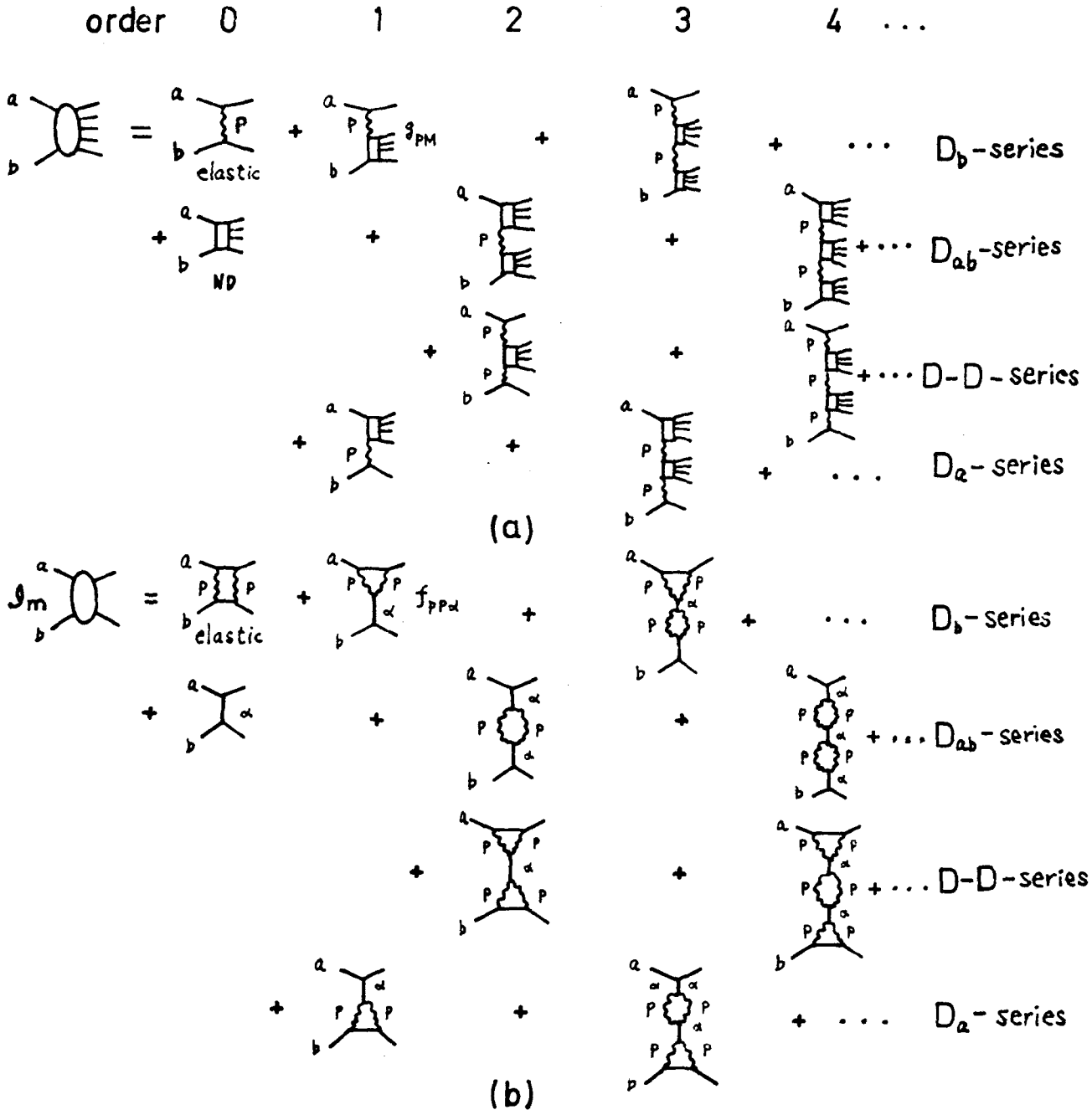
order 0 1 2 3 4 ...
elastic
ND
g_{PM}
D_b-series
D_{ab}-series
D-D-series
D_a-series
(a)
g_m
elastic
$f_{PP\alpha}$
D_b-series
D_{ab}-series
D-D-series
D_a-series
(b)

Fig. 28

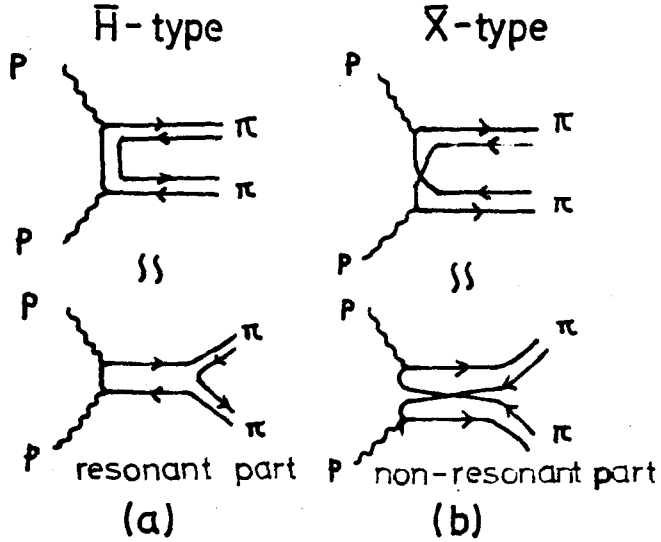
H-type
X-type
P
π
resonant part
non-resonant part
(a)
(b)

Fig. 29

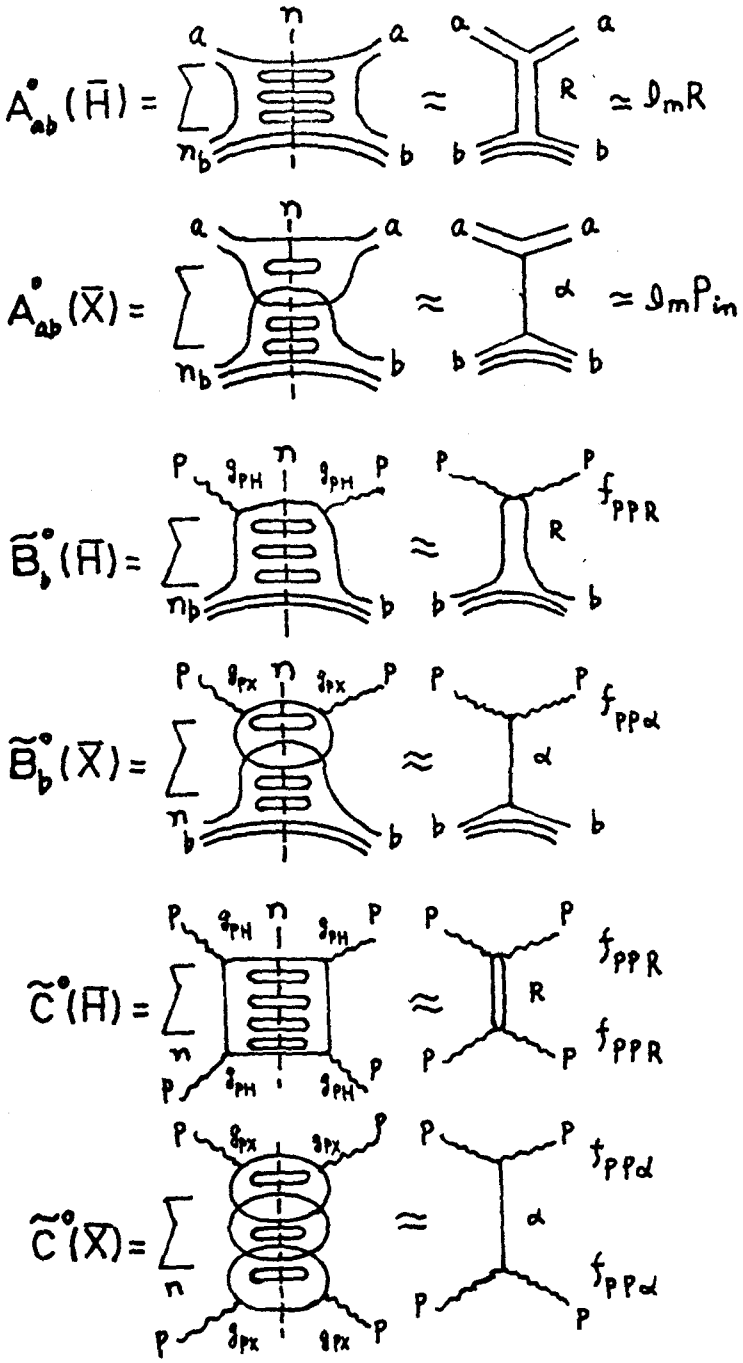
$A^{\circ}_{ab}(\bar{H}) =$
$\approx$
$\simeq \mathrm{Im} R$
$A^{\circ}_{ab}(\bar{X}) =$
$\approx$
$\simeq \mathrm{Im} P_{in}$
$\tilde{B}^{\circ}_{b}(\bar{H}) =$
$\approx$
f_{PPR}
$\tilde{B}^{\circ}_{b}(\bar{X}) =$
$\approx$
$f_{PP\alpha}$
$\tilde{C}^{\circ}(\bar{H}) =$
$\approx$
f_{PPR}
f_{PPR}
$\tilde{C}^{\circ}(\bar{X}) =$
$\approx$
$f_{PP\alpha}$
$f_{PP\alpha}$

Fig. 30

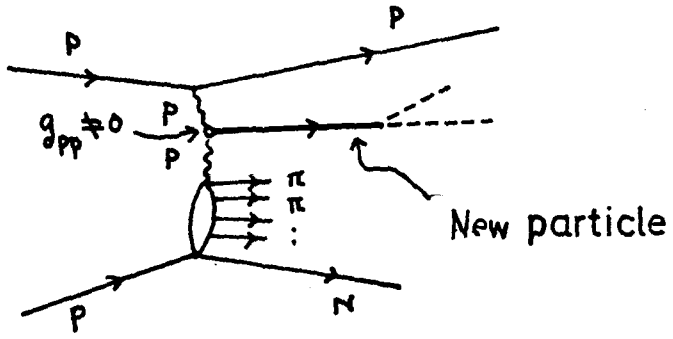
$g_{pp} \neq 0$
New particle

Fig. 31